

T. R.  
VAN YUZUNCU YIL UNIVERSITY  
INSTITUTE OF NATURAL AND APPLIED SCIENCES  
DEPARTMENT OF CHEMISTRY

**SYNTHESIS OF Pd NANOPARTICLES SUPPORTED ON CARBOXYLATED  
GRAPHENE OXIDE FOR ELECTROANALYTICAL DETERMINATION OF  
PARACETAMOLE IN HUMAN SERUM**

M. Sc. THESIS

PREPARED BY: Shaimaa Jameel Saleem SALEEM  
SUPERVISOR: Assist. Prof. Dr. Muhammet GÜLER

VAN-2019



T. R.  
VAN YUZUNCU YIL UNIVERSITY  
INSTITUTE OF NATURAL AND APPLIED SCIENCES  
DEPARTMENT OF CHEMISTRY

**SYNTHESIS OF Pd NANOPARTICLES SUPPORTED ON CARBOXYLATED  
GRAPHENE OXIDE FOR ELECTROANALYTICAL DETERMINATION OF  
PARACETAMOLE IN HUMAN SERUM**

M. Sc. THESIS

PREPARED BY: Shaimaa Jameel Saleem SALEEM

VAN-2019



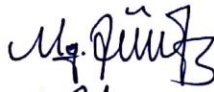
## ACCEPTANCE and APPROVAL PAGE

This thesis entitled “Synthesis of Pd Nanoparticles Supported on Carboxylated Graphene Oxide for Electroanalytical Determination of Paracetamol in Human Serum” presented by Shaimaa Jameel Saleem SALEEM under supervision of Assist. Prof. Dr. Muhammet GÜLER in the department of chemistry has been accepted as a M. Sc. thesis according to Legislations of Graduate Higher Education on 21/11/2019 with unanimity of votes members of jury.


Chair: Prof. Dr. Halit DEMİR

Signature: 

Member: Assist. Prof. Dr. Muhammet GÜLER (supervisor)

Signature: 

Member: Assist. Prof. Dr. Fikret TÜRKAN

Signature: 

This thesis has been approved by the committee of The Institute of Natural and Applied Science on...29.../...11.../...2019... with decision number...2019/62-I.

Signature:   
Prof. Dr. İsmail AKKOÇ  
Director of the Institute  




## **THESIS STATEMENT**

All information presented in the thesis obtained in the frame of ethical behavior and academic rules. In addition, all kinds of information that does not belong to me have been cited appropriately in the thesis prepared by the thesis writing rules.

Signature

Shaimaa Jameel Saleem SALEEM





## ABSTRACT

### SYNTHESIS OF Pd NANOPARTICLES SUPPORTED ON CARBOXYLATED GRAPHENE OXIDE FOR ELECTROANALYTICAL DETERMINATION OF PARACETAMOL IN HUMAN SERUM”

SALEEM, Shaimaa Jameel Saleem  
M. Sc. Thesis, Department of Chemistry  
Supervisor: Assist. Prof. Dr. Muhammet GÜLER  
November 2019, 89 Pages

The study includes a novel paracetamol (PA) sensor depending on Pd nanoparticles (PdNPs) deposited on carboxylated graphene oxide (GO-COOH) modified glassy carbon electrode (GCE). Nafion (Nf) was used as a protective membrane. The as prepared composites were characterized utilizing high resolution transmission electron microscopy (HRTEM), X-ray diffraction (XRD), X-ray photoelectron spectroscopy (XPS), and Fourier transform infrared spectroscopy (FTIR). The experimental results illustrated that Nf/GO-COOPd nanocomposite exhibited excellent electro catalytic response to the oxidation of PA. The linear range of the sensor was found to be 0.04-800  $\mu\text{M}$  for PA with limit of detection (LOD) of 0.012  $\mu\text{M}$  and sensitivity of 232.89  $\mu\text{A mM}^{-1} \text{cm}^{-2}$ . By considering the excellent electrocatalytic performance of Nf/GO-COOPd composite such as a wide linear range, lower detection, better selectivity, repeatability, reproducibility, and storage stability, the GO-COOH support is a promising support for the modification of electrode material in electrochemical sensor and biosensor field.

**Keywords:** Carboxylated grapheme oxide, Pd nanoparticles, Paracetamol, Sensor



## ÖZET

### İNSAN SERUMUNDA PARASETAMOLÜN ELEKTROANALİTİK TAYİNİ İÇİN KARBOKSİLENMİŞ GRAFEN OKSİT DESTEKLİ Pd NANOPARÇACIKLARIN SENTEZLENMESİ

SALEEM, Shaimaa Jameel Saleem  
Yüksek Lisans Tezi, Kimya Bölümü  
Tez Danışmanı: Dr. Öğr. Üyesi Muhammet GÜLER  
Kasım 2019, 89 Sayfa

Çalışma, karboksillenmiş grafen oksit üzerine Pd nanoparçacıkların (PdNPs) biriktirilmesiyle modifiye edilen camı karbon elektrot dayalı yeni bir parasetamol (PA) sensörünü içermektedir. Nafion (Nf) koruyucu membran olarak kullanıldı. Hazırlanan kompozitler, yüksek çözünürlüklü transmisyon elektron mikroskobu (HRTEM), X-ışını difraksiyonu (XRD), X-ışını fotoelektrik spektroskopisi (XPS) ve Fourier transform infrared spektroskopisi (FTIR) kullanılarak karakterize edildi. Deney sonuçları, Nf/GO-COOPd nano kompozitin PA oksidasyonuna mükemmel elektrokatalitik cevap verdiğini göstermiştir. Sensörün doğrusal tayin aralığı, 0.012  $\mu\text{M}$  gözlenebilme sınırı ve 232.89  $\mu\text{A mM}^{-1} \text{cm}^{-2}$  duyarlılık ile 0.04-800  $\mu\text{M}$  olduğu belirlenmiştir. Nf/GO-COOPd kompozitin geniş doğrusal tayin aralığı, düşük gözlenebilme sınırı, daha iyi seçicilik, tekrarlanabilirlik, tekrarolusturulabilirlik ve depolama kararlılığı gibi mükemmel elektrokatalitik performansı dikkate alındığında, GO-COOH desteğinin elektrokimyasal sensor ve biyosensörlerde elektrot materyalin modifikasyonu için umut verici bir destektir.

**Anahtar kelimeler:** Karboksillenmiş grafen oksit, Pd nanoparçacıkları, Parasetamol, Sensör



## **ACKNOWLEDGMENT**

In the name of Allah, Most Gracious, Most Merciful After praising to God, the completion of this thesis would not have been possible without the generous contribution of many remarkable people, also I would like to express my sincer gratitude, first and for most, to my Assist. Prof. Dr. Muhammet GÜLER who provided constrictive guidance, helped, and support throughout the invaluable asset to my education, without his guidance, supports, and good nature, I would have never been able to complete this study. I would like to express my special thanks to my family for their support and help, patience, sacrifice and encouragement. Special thanks to the soul of my father who always encouraged and supported my education. Special thanks go to my close friends and relatives for their endless support and encouragement.

2019

Shaimaa Jameel Saleem SALEEM



## TABLE OF CONTENTS

	<b>Page</b>
ABSTRACT.....	i
ÖZET.....	iii
ACKNOWLEDGMENT.....	v
TABLE OF CONTENTS.....	vii
LIST OF TABLES .....	xi
LIST OF FIGURES .....	xiii
SYMBOLS	AND
	ABBREVIATIONS
.....	xvii
1. INTRODUCTION .....	1
1.1. Graphene Oxide .....	5
1.1.1. Definition of graphene oxide.....	5
1.1.2. Chemical properties of graphene oxide.....	6
1.1.3. Electrical properties of graphen oxide.....	7
1.1.4. Physical properties of graphene oxide.....	8
1.1.5. Mechanical properties of graphene oxide.....	9
1.1.6. Thermal properties.....	10
1.1.7 Catalytic properties .....	11
1.1.8. Synthesis methods for graphene oxide .....	12
1.1.8.1. Brodie method .....	13
1.1.8.2. Staudenmaier method.....	14
1.1.8.3. Hummers method .....	14
1.1.8.4. Tour method .....	15
1.1.8.5. Free-water oxidation method .....	16
1.1.8.6. Sun method .....	16
1.1.8.7. Peng method .....	17
1.1.8.8. 4-steps method .....	18
1.2. Noble Metal Nanoparticle.....	21

	<b>Page</b>
1.3. Palladium .....	22
1.3.1. Catalytic properties.....	24
1.4. Electrochemical Sensors .....	25
1.4.1. Why electrochemical sensing.....	26
1.4.2. Advantages of electrochemical sensors.....	27
1.4.3. Disadvantages of electrochemical sensors.....	29
1.4.4. Using areas of electrochemical sensors .....	29
1.4.5. Performance factors of sensors .....	30
1.5. Paracetamol .....	31
1.5.1. Chemical properties .....	31
1.5.2. Pharmacokinetics Properties .....	32
1.5.2.1. Absorption .....	32
1.5.2.2. Distribution .....	33
1.5.2.3. Metabolism .....	33
1.5.2.4. Elimination .....	33
1.5.2.5. Fetus, neonates, infants, and children .....	34
1.5.2.6. Geriatric .....	34
1.6. Voltammetric methods.....	34
1.6.1. Cyclic voltammetry (CV).....	35
1.6.2. Electrochemical impedance spectroscopy (EIS) .....	36
2. LITERATURE REVIEW.....	39
3. MATERIALS AND METHODS.....	51
3.1 Materials and Apparatus .....	51
3.2. Methods .....	51
3.2.1. Synthesis of graphene oxide (GO) .....	51
3.2.2. Synthesis of carboxyted graphene oxide GO-COOH .....	52
3.2.3. Synthesis of carboxylated graphene oxide palladium nanoparticles (GO-COOPd).....	52



3.2.4. Synthesis of graphene oxide palladium nanoparticles (Pd@GO)..	52
	<b>Page</b>
3.2.5. Preparation of GO-COOH and GO-COOPd modified electrodes	53
3.2.6. Electrochemical studies	53
3.2.7. determination of paracetamol (PA) in human serum samples.....	54
4. RESULTS.....	55
4.1. Characterization of GO—COOH and GO-COOPd	55
4.2. Electrochemical Characterization of GCE and Modified Electrode	58
4.3. Effect of pH and Scan Rate on Nf/GO-COOPd/GCE	60
4.4. Determination of PA on Nf/GO-COOPd/GCE Electrochemical Sensor	63
4.5. Interference Study	64
4.6. Repeatability, Reproducibility, and Storage Stability	64
4.7. Real Sample Analysis	67
5. DISCUSSION AND CONCLUSION.....	69
REFERENCES.....	75
APPENDIX: EXTENDED TURKISH SUMMARY (GENİŞLETİLMİŞ TÜRKÇE ÖZET).....	83
CURRICULUM VITAE.....	89



## LIST OF TABLES

<b>Table</b>	<b>Page</b>
Table 1.1. Summary of the primary synthetic techniques used to prepare GO.....	20
Table 4.1. The comparison of the Nf/GO-COOPd/GCE PA sensor with the previous works.....	66
Table 4.2. Detection of PA in serum samples using Nf/ GO-COOPd/GCE sensor.....	67





## LIST OF FIGURES

<b>Figure</b>		<b>Page</b>
Figure 1.1.	Molecular shape of graphene oxide.....	6
Figure 1.2.	Visible absorption spectra of single-layer graphene (blue circles), single-layer GO (red triangles), and single-layer rGO (black diamonds).....	8
Figure 1.3.	Plots of different components of deformation as a characteristic of Length.....	10
Figure 1.4.	Scheme of GO production beginning from graphite as carbon source. Three paths may be described to get as final product the graphene oxide material.....	13
Figure 1.5.	Procedure scheme for Tour approach. The starting materials is expanded graphite to be used for producing graphene oxide through Tour method in comparison with Hummers method and its modification .....	15
Figure 1.6.	Reaction scheme for Sun technique (left). Right images of a) combination of reagent, b) volumetric enlargement (foam-like), c) hydrolysis and d) concentrated dispersion after purification.....	17
Figure 1.7.	Reaction mechanism proposed by Peng and co-workers for the synthesis of graphene oxide using $K_2FeO_4$ as oxidizing agent. This work is licensed under a Creative Commons Attribution 4.0 worldwide License.....	18
Figure 1.8.	Reaction scheme for the four-Steps technique. The temperature influences the final product according with the “heat” or “bloodless” route. The graphene oxide is only acquired when the warm route is observed, and, by way of contrast, graphite oxide is produced at decrease temperature below $30^\circ C$ .....	19
Figure 1.9.	Block go with the flow diagram of a probable method for the production of	20

	GO.....	
Figure 1.10.	The dimensions of nanotechnology.....	22
Figure 1.11.	The principle stages within the sensor operation.....	26
<b>Figure</b>		<b>Page</b>
Figure 1.12.	Standards for examples of the possibility of the use of Electrochemical sensing.....	30
Figure 1.13.	Acetaminophen (paracetamol) (N-(4-Hydroxyphenyl) ethanamide or N(4-Hydroxyphenyl) acetamide or (N-Acetyl-para aminophenol) chemical structure highlighting energetic components.....	32
Figure 1.14.	Vector representation of the complicated impedance Z.....	37
Figure 1.15.	Schematic representation of a parallel RC circuit's impedance analysis reaction.....	38
Figure 1.16.	Most important electrochemical techniques and their subdivisions	38
Figure 4.1.	GO (a) and GO-COOH (b) FTIR spectra.....	55
Figure 4.2.	XRD graph of GO (a), GO-COOH (b) and GO-COOPd (c).....	55
Figure 4.3.	XPS full spectrum of GO-COOPd composite.....	56
Figure 4.4.	XPS spectra of Pd.....	56
Figure 4.5	TEM pictures of GO-COOH (a) and GO-COOPd (b,c).....	57
Figure 4.6.	Electrochemical impedance Nyquist plot of Nf/GCE (a), Nf/GO/GCE (b), Nf/Pd@GO/GCE (c), Nf/GO-COOH/GCE (d),	

	and Nf/GO-COOPd/GCE (e) in 5 mM $[\text{Fe}(\text{CN})_6]^{3-}/[\text{Fe}(\text{CN})_6]^{4-}$ containing 0.1 M KCl. Applied potential: 0.2 V. Amplitude: 10 mV. Frequency range: 0.02 Hz to 100 kHz.....	58
Figure 4.7.	CVs of GO-COOH/GCE in 5 mM $[\text{Fe}(\text{CN})_6]^{3-}/[\text{Fe}(\text{CN})_6]^{4-}$ containing 0.1 M KCl using different scan rates (from 0.04 to 0.26 V s <sup>-1</sup> ).....	58
Figure 4.8.	CVs of GO-COOPd/GCE in 5 mM $[\text{Fe}(\text{CN})_6]^{3-}/[\text{Fe}(\text{CN})_6]^{4-}$ containing 0.1 M KCl using different scan rates (from 0.04 to 0.26 V s <sup>-1</sup> ).....	59
Figure 4.9.	Plot of oxidation peak current of 5 mM $[\text{Fe}(\text{CN})_6]^{3-}/[\text{Fe}(\text{CN})_6]^{4-}$ (1:1) at Nf/GCE (a), Nf/GO/GCE (b), Nf/Pd@GO/GCE (c), Nf/GO-COOH/GCE (d), and Nf/GO-COOPd/GCE vs. the square root of scan rate (Scan rate: 0.04–0.26 V/s).....	59
<b>Figure</b>		<b>Page</b>
Figure 4.10.	CVs of Nf/GCE, Nf/GO/GCE, Nf/Pd@GO/GCE, Nf/GO-COOH/GCE, and Nf/GO-COOPd/GCE in 0.1M PBS (pH 7.5) containing 0.5 mM PA. Scan rate: 0.05 V/s.....	60
Figure 4.11.	CV response of Nf/GO-COOPd/GCE to 0.2 mM PA in 0.1 M PBS with different pH values (4.5 to 9.0).....	60
Figure 4.12.	The plot of E/V vs. various pH values (from 4.5 to 9.0).....	61
Figure 4.13.	The effect of pH on the oxidation peak current response of Nf/GO-COOPd/GCE to 0.2 mM PA.....	61
Figure 4.14.	CVs of Nf/GO-COOPd/GCE to 0.2 mM PA in 0.1 M PBS at various scan rates (from 0.005 to 0.16 V/s). Inset: plot of oxidation and reduction peak current response of Nf/GO COOPd/GCE versus square root of scan rate.....	62
Figure 4.15.	Plot to E/V versus logv/V s <sup>-1</sup> .....	62

Figure 4.16.	Amperometric graph obtained on the Nf/GO-COOPd/GCE with different PA concentrations at 0.48 V.....	63
Figure 4.17.	PA oxidation current vs. PA concentration.....	63
Figure 4.18.	Amperometric response of Nf/GO-COOPd/GCE to PA with 80 $\mu$ M AA, UA, DA, Glu, Fruc, Man, His, and FA in 0.1 M PBS (pH 7.5) at 0.48 V.....	64
Figure 4.19.	Repeatability graph of 0.05 mM PA measurements using the same Nf/GO-COOPd/GCE sensor.....	64
Figure 4.20.	Reproducibility graph of 0.05 mM PA measurements using eight different Nf/GO-COOPd GCE sensor.....	65
Figure 5.1.	The electro-oxidation mechanism of PA at Nf/GO COOPd/GCE..	72





## **SYMBOLS AND ABBREVIATIONS**

Some symbols and abbreviations used in the study are presented below, along with description.

### **Symbols**

### **Description**

**GO-COOPd**

Carboxylated graphene oxide palladium nanoparticles

<b>GO-COOH</b>	Carboxylated graphene oxide
<b>Pd@GO</b>	Palladium nanoparticles@Graphene oxide
<b>Ag/AgCl</b>	Silver/Silver chloride
<b>PBS</b>	Phosphate buffer solution
<b>Glu</b>	Glucose
<b>Fruc</b>	Fructose
<b>Man</b>	Mannose
<b>His</b>	Histidine
<b>GO</b>	Graphene oxide
<b>PA</b>	Paracetamol
<b>AC</b>	Acetaminophen
<b>Nf</b>	Nafion
<b>AA</b>	Ascorbic acid
<b>UA</b>	Uric acid
<b>DA</b>	Dopamine
<b>FA</b>	Folic acid

**Abbreviation**

**Description**

<b>HRTEM</b>	High resolution transmission electron microscopy
<b>FTIR</b>	Fourier Transform Infrared Spectroscopy
<b>XRD</b>	X-ray Diffraction

**Abbreviation**

**Description**

<b>SEM</b>	Scanning electron microscopy
<b>TEM</b>	Transmission Electron Microscopy
<b>XPS</b>	X-ray photoelectron spectroscopy
<b>EDX</b>	Energy-dispersive X-ray spectroscopy
<b>DPV</b>	Differential pulse voltammetry

<b>EIS</b>	Electrochemical impedance spectroscopy
<b>RSD</b>	Relative standard deviation
<b>GCE</b>	Glassy carbon electrode
<b>LOD</b>	Limit of detection
<b>LOQ</b>	Limit of quantification
<b>CV</b>	Cyclic voltammetry
<b>Pt</b>	Platinum
<b>SD</b>	Standard deviation
<b>DP-ASV</b>	Differential pulse-anodic stripping voltammetry

## 1. INTRODUCTION

Paracetamol (N-acetyl-p-aminophenol or acetaminophen) is a treasured non-steroidal anti-inflammatory drug in the prevalent utilize of pain remedy and fever decrease in a diversity of patients, containing kids, pregnant ladies, the old and those with osteoarthritis, simple headaches, and non-inflammatory musculoskeletal illnesses. Its popularity as an analgesic and antipyretic medicine steadily increased. On the other hand, paracetamol is the favored alternative to aspirin, especially for patients who cannot tolerate aspirin and its usage is one of the most common causes of poisoning in the world. At the suggested prescription, there are no side effects. But, overdoses reason to liver and kidney injury. It is supposed that a metabolite of paracetamol is the definite hepatotoxic agent (Asghari et al., 2015). It is usually utilized for the relief of headaches and other minor pains and cares. Paracetamol is also the main component in a great number of cold and flu treatments. While it is combined with opioid analgesics, paracetamol ability to be employed to develop more severe ache for example post-surgical pain, as well as offering palliative care in progressive cancer patients. It is not usually kinds as a non-steroidal anti-inflammatory drug (NSAID) although paracetamol is employed to treat inflammatory pain, as shows only weak anti-inflammatory activity. It is usually safe for utilize at proposed doses, while compared to other over-the-counter ache relievers, acetaminophen is considerably more poisonous. In overdose the gathering could cause kidney and liver damage (Fernandez et al., 2015).

Electrochemical Sensors have advantages in request of a cheap and basic technique to identify biomolecules. They usually are sensitive and have a quick reply time. A basic electrode for electrochemical dimensioning is a fine metal wire or a fiber that is fully insulated excluding for the exposed tip of the electrode. An insulator is essentially a film of a polymeric material. The metal utilized as an electrode material should be electrically conductive. Common electrochemical sensor materials are solid metals for example gold, platinum, tungsten and aluminum with different formula of carbon-based materials and

semiconductors for example silicon. Electrochemical sensor ability is coated with diverse protective layers or deposited with nanoparticles (NP). Protective layers facilitate to reduce electrode fouling and can enhance selectivity. For example, Neon, phenyl acetate, conducting polymers such as polyprole and its derivatives are utilized as protective layer (Wahlström, 2016).

Nano-materials have been the focus of excessive interest in the developing world. To date, they have been utilized in several research fields for example medicine (diagnostics, drug supply, and tissue engineering), situation (filtration and discovery of pesticide), energy, information and communication (memory storage, semiconductor and optoelectrical devices, and so on), heavy manufacturing (catalysis and construction), and customer's goods (diet, optics, cosmetics). Among these research areas, nano-materials have been widely utilized for fabrication of electrochemical sensors so as to detect biologically significant substances for example glucose, hydrogen peroxide, dopamine, uric acid, and folic acid since nanomaterial's own high conductivity, excellent sensitivity and selectivity, repeatability, reproducibility, relatively low cost, and easy preparation (Guler, et al., 2018). NPs can be synthesized using metals (Au, Ag, Pt.), oxides ( $\text{SiO}_2$ ,  $\text{TiO}_2$ ,  $\text{ZrO}_2$ ,  $\text{MnO}_2$ ), or semiconductors (Cods, Pubs). NPs are utilized in increasing the surface zone of the electrode that enhance the sensor current. NPs are also utilized in improving the electrochemical reaction by reducing the potential obligatory for the redox reaction of the molecule of interest. NPs increase the electron transfer rate between the electrode and the solution. NPs are typically charged particles so they able to absorb other charged biomolecules from the solution. NPs are generally 1-100 nm in diameter and biocompatible materials (Wahlström, 2016).

Palladium (Pd) named after the asteroid Pallas, is arguably the most flexible and ubiquitous metal in different applications like catalytic hydrogenation-dehydrogenation reactions, petroleum breaking, modern organic synthesis and electro catalysis. Palladium is a noble metal with high catalytic activity, and is utilized in numerous industrial processes. The capacity of palladium to absorb significant amounts of hydrogen at room temperature makes it a perfect candidate for effective and safe storage of hydrogen gas. Palladium metal is generally utilized in catalytic convertors, where it changes damaging gases like hydrocarbons, CO and NO from automobile exhaust into less destructive compounds like

CO<sub>2</sub>, N<sub>2</sub> and H<sub>2</sub>O (Kumar, 2016). Palladium nanoparticles have immersed considerable consciousness in the field of biomedical requests because of their enormous catalytic and sensor activities. The size and shape-controlled production of palladium nanoparticles is crucial for facile selective catalytic and detecting properties towards several chemical and biological analytes. The moderately large amount of palladium over other noble metals for example gold and platinum makes it a cheaper element for application in different electrochemical sensing and biosensing platforms. Because of unique electronic properties, progressed catalytic and selective sensing performance, a variety of palladium nanomaterials for example nano composites, bimetallic nanoparticles, metal oxide nanomaterial's, and carbon nanomaterials with variable composition have been inspected for the finding of several biomarkers over the last decade (Maduraiveeran et al., 2018a).

Nafion (Nf) conducting polymers known as intrinsically conducting polymers (ICPs) are a modern class of polymers that has a high electron affinity and high electronic conductivity by numerous orders of magnitude of doping (while keeping mechanical flexibility and high warm air stability). These abilities to be related to the  $\pi$ -electron spine owned by ICPs. One of the ICPs groups that are often utilized in sensors application, Nf is one of the most widely utilized ICPs in the fabrication of bioanalytical sensors. Nf is a suffocated tetrafluoroethylene-based fluoropolymer-copolymer with a conductive asset. Because of existence of perfluoroalkyl backbones in Nf, it has high hydrophobicity assets consequently making it an effective matrix to scatter graphene in an aqueous solution as graphene tends to agglomerate or indeed restack to make graphite through strong  $\pi$ - $\pi$  stacking and van der Waal's interaction. In sensor application, Nf was utilized as an electrode changer for sensor electrode fabrication because of its antifouling capability, chemical inertness and great porousness for captions. Besides that, Nafion also supports to improve the constancy of graphene adjusted electrodes because of its excellent film founding capacity. As an activity exchange polymer, Nf supports to blocks the anionic species from getting the electrode surfaces and permits the activity conduction to permit through, hence leads to good selectivity. Fascinatingly, the hydrophilic negatively charged sulfonate group in Nf film empowers choosy pre-concentration of positively charged biomolecules through electrostatic interaction, while the hydrophobic fluorocarbon network of the polymer offers a choosiness for the hydrophobic portion of the molecule.

These advantages make Nf a perfect choice for the manufacture of electrochemical sensors (Norazriena, 2017).

Graphene oxide (GO), a layered atomic thin graphene sheet functionalized with numerous oxygen-containing functional groups (including epoxide, hydroxyl, and carboxylic groups), has fascinated substantial attention because of its excellent physical and chemical properties (i.e. high surface zone, great thermal conductivity, and mechanical stiffness) (Wu et al., 2013). The GO with a big variety of oxygen-comprising chemical groups, is properly simple to conjugate biomolecules when no additional activation is required. Because of the brilliant hydrophobicity of GO, the sol designed by suspending GO sheets in water or low ionic buffers may be constant at room temperature for years without any surfactants. GO may be simply synthesized in the labs at very low cost (Yu et al., 2017). Currently, the projected chemical reactions concentrating on the epoxy groups of GO have been inspected in the model blend system with high concentration of GO. However, the anticipated covalent interactions via other reactive hydroxyl and carboxyl groups of GO must be further confirmed. Consequently, it is essential to clarify the effects of functional groups of GO. To prepare the carboxylated graphene oxide (GO-COOH) hydroxyl groups of GO convert into carboxylic acid (-COOH) moieties. It is projected that carboxylation of GO not only reduces suggested catalytic effects but also offers reactive locations for further covalent and monovalent interactions (Wu et al., 2013). GO sample was treated with chloroacetic acid under strongly plain conditions in order to stimulate the epoxide and ester groups and to modification hydroxyl groups into -COOH moieties (Park., 2014).

To the best of our information, there is no study associated to the manufacture of Nf/GO-COOPd/GCE nano composite-based electrochemical sensor for determination of PA. Herein, we have built an electrochemical sensor utilizing Pd deposited on GO-COOH support modified GCE for the electroanalytical analysis of PA. The carboxylated GO had better solubility, constancy, higher active surface zone, and more carboxylic groups, that Pd nanoparticles may be simply deposited on the support. Owing to the synergistic possessions between GO-COOH and Pd, the sensor showed brilliant sensitivity, selectivity, stability, repeatability, reproducibility, and quick reply towards the oxidation of PA. The morphology and characterization of GO-COOH and GO-COOPd were examined by means

of FTIR, HRTEM, XPS, and XRD. The electrochemical properties of bare GCE, GO-COOH, and GO-COOPd were assessed utilizing cyclic voltammetry (CV), electrochemical impedance spectroscopy (EIS), and aerometry.

## **1.1. Graphene Oxide**

### **1.1.1. Definition of graphene oxide**

GO is a single-atomic-layered material including carbon, hydrogen, and oxygen molecules by the oxidation of graphite crystals that are cheap and plentiful. It is dispersible in water and easy to procedure. Most significantly, the GO may be (partly) reduced to graphene-like sheets by eliminating the oxygen-containing groups and with the recovery of a conjugated structure (Ray, 2015). GO has two significant features, (i) it can be produced utilizing cheap graphite as the raw material then by utilizing cost-effective chemical methods with a high yield and (ii) It is highly hydrophilic and can form steady aqueous colloids toward simplify the gathering of macroscopic structures by simple and cheap solution processes. According to Ray (2015), the surface of GO was researched with detected very defective areas, possibly because of the existence of oxygen, and other zones are almost intact. Therefore, GO can be designated as a random scattering of oxidized zones with oxygen-containing functional groups joint with no oxidized areas where most of the carbon atoms protect  $sp^2$  hybridization.

GO is one of the utmost studied graphene derivatives with layers of graphite containing hydrophilic oxygenated useful groups on the ends and basal planes. The preparation of GO may be achieved by the addition of oxygen frame into the structures through an oxidation procedure, therefore distorts the carbon lattices. The alteration of carbon lattices is identified to be as defects. The distorted molecular structure of monolayer GO with the existence of oxygenated lattice is shown in Figure 1.1. The existence of the oxygen functionalities on the graphene surface offers an improved layer separation and developed hydrophilicity. Therefore, GO can separate very simply in different medium including aqueous solvents and organic solvents. Due to the expansion of oxygenated lattice, the thickness layer of GO is found to be 1.1 nm, which is thicker than graphene that is 0.345 nm. GO has a band gap energy related to the stoichiometric ratio between carbon



and oxygen, resulting in 3.1 eV band gap energy. The appearance of functional groups such as carboxyl, carbonyl, and hydroxyl groups can be identified by FTIR spectra. The presence of different CO bonds, namely, C—O (286.2 eV), C = O (287.8 eV), and O—C=O (289.0 eV), can be identified by XPS spectra. The defects also can be recognized by the appearance of the D band at  $1300\text{ cm}^{-1}$  of the Raman spectrum that is attributed to the formation of  $\text{sp}^3$  bond. Compared with graphene, GO is known as a good electric insulator as it shows low electric conductivity. This is due to expansion of oxygen lattice that disturb the  $\text{sp}^2$  bonding network. Due to the drawbacks in electric properties of GO, the oxygen content can be removed by a reduction process utilizing different reduction reagents. Reduced graphene oxide (rGO) is commonly discussed as the removal of oxygen content from GO by the reduction process. The conductivity of this kind of material is improved as the  $\text{sp}^2$  bond is restored (Zobir et al., 2019).

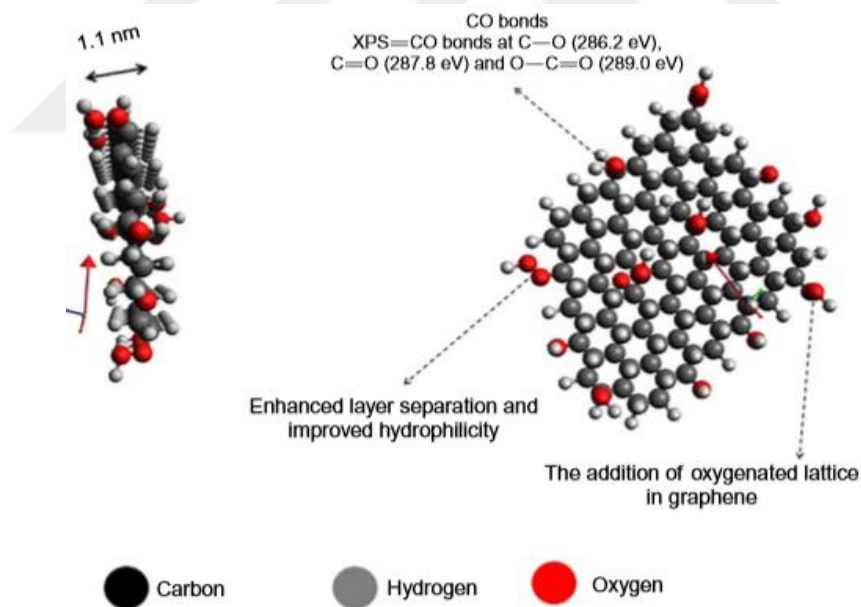


Figure 1.1. Molecular shape of graphene oxide (Zobir et al., 2019).

### 1.1.2. Chemical properties of graphene oxide

GO and GO multilayers should be prepared by the oxidation of graphene with fuming nitric acid and potassium chlorate under cooling, as reported for the first time by the British chemist Boride. Other procedures were also developed by Staudenmaier, Hummers, and

Foeman. The product compound, named as GO, has a composition of around  $C_8O_2(OH)_2$ , and nearly none of the carbon in graphite is lost throughout the formation of GO (Boehm, 2010). Numerous molecular models have been reported for GO. In 2010, Boehm suggested a structure found on experimental data, where epoxy groups bind to graphene with a composition of  $C_2O$  (Hofmann and Holst, 1939). With the evidence that hydrogen is found in GO, Rues presented hydroxyl groups into the model, which leads to  $sp^3$  hybridization and no planar distortion of the basal plane (Boehm, 2010). GO is a metastable material whose structure and chemistry were developed even at room temperature with a characteristic relaxation time of about one month. Under thermal annealing, GO structures should also undergo a stage change into prominent oxidized and graphitic spaces by temperature-driven oxygen diffusion (Kumar et al., 2014). At the quasi-equilibrium, GO reaches about constant reduced O/C ratio, and shows a structure deprived of epoxide groups and enriched in hydroxyl groups (Hofmann and Holst, 1938).

### 1.1.3. Electrical properties of graphene oxide

Since GO is heavily oxidized, it is not electrically conductive. Reduction of GO results in the removal of the main of the useful groups, increases the size of graphitic regions and as a result, partially restores the conductivity of the material. According to the theoretical research by Boukhvalov and Katsnelson, GO sheets become conducting if their coverage with functional groups does not surpass 25%, then they are insulators (Murali, 2012). GO's optical properties are important different from those of graphene. Graphene is a zero-gap semiconductor, which possesses a significant, near-constant absorption across the visible ( $\sim 2.3$  % absorption, %A, first panel, Figure 1.2). On the other hand, GO's optical absorption is approximately an order of magnitude smaller ( $\sim 0.3$  %A, second panel). Also, GO's absorption spectrum is wavelength dependent; it peaks in the UV/blue edge of the visible spectrum and falls towards the close infrared (NIR). Discernible  $\pi-\pi^*$  and  $n-\pi^*$  moves are also present in its UV absorption (200–320 nm) and arise from the existence of oxygen-containing functionalities. GO's optical response is thus beautifully sensitive to its degree of oxidation. As a diagram, the last two panels in Figure. 1.2 show

that GO's absorption dramatically rises across the visible upon the removal of these functionalities and approaches graphene's 2.3 % A (Gao, 2015).

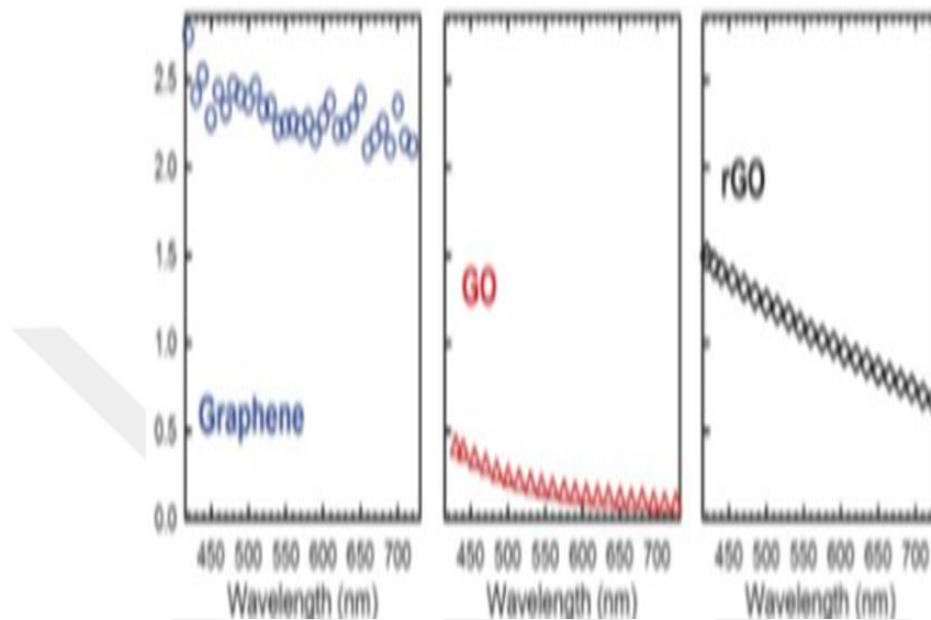


Figure 1.2. Visible absorption spectra of single-layer graphene (blue circles), single-layer GO (red triangles), and single-layer rGO (black diamonds) (Gao, 2015).

#### 1.1.4. Physical properties of graphene oxide

Physically, graphene oxide is an atomically thin, semi-aromatic network of  $sp^2/sp^3$  bonded carbon atoms intermittently decorated with oxygen-containing functionalities. These functional groups comprise hydroxyl (OH), epoxy (C–O–C), carbonyl (C=O), and carboxyl (COOH) species, with OH and C–O–C being the dominant groups across GO's basal plane. Their subsequent removal through disproportionation reactions results in rGO, a chemical analogue of graphene. GO reduction provides a scalable, low-cost approach for getting a graphene-like material. In this regard, reduction can be attained through many means. They include chemical, thermal, photo thermal, and laser- induced reduction methods, all remove GO's oxygen-containing functionalities and simultaneously change basal plane of carbon atoms from  $sp^3$  to  $sp^2$  hybridization, restoring the system's aromaticity to a convinced extent. To better explain the mechanism behind GO to rGO inter-conversion for possible large-scale production, important structural characterization

has been conducted on these materials at the microscopic level. Electron and tunneling microscopies, in specific, have provided detailed vision into GO's chemical and physical structure. These TEM measurements along with scanning tunneling microscopy (STM) experiments also design sizable oxygen functionality and  $sp^2$  size distribution heterogeneities within GO. Oxygen-containing functionalities of GO are moreover identified to be dynamic. Exactly, under electron beam irradiation, they migrate across GO basal plane (Gao, 2015).

### **1.1.5. Mechanical properties of graphene oxide**

Mechanical properties of one to three layers of GO sheets were explored by AFM. The measured Young's modulus of a monolayer GO sheet was 207.6 GA, which is much lower than the pristine graphene, due to the oxygenated functional groups which unfavorably change the "perfect" 2D structure of monolayer graphene. The discovery of the researcher was an effective approach to develop the mechanical properties of GO papers. The mechanical properties of GO papers relied on the size of the precursor GO sheets. The GO papers made from large-size GO sheets had higher Young's modulus, fracture toughness, and tearing strength than those made from smaller GO. The reliance of mechanical properties of GO papers on the size of GO sheets is recognized to two interrelated characteristics, namely, the compactness of GO papers and the existence of defects in GO sheets. Figure 1.3 shows the contributions of two different components to the total deformation of GO papers as a function of GO size, viewing that more than 90 % of the deformation originated from the inter sheet deformation regardless of the GO size on the nano scale whereas the deformation arising from the expansion of GO sheets themselves were moderately small. This observation implies that for developed mechanical properties of GO papers, tensile strength must be reduced by cross-linking them utilizing metal ions or functionalization (Zheng and Kim, 2015).

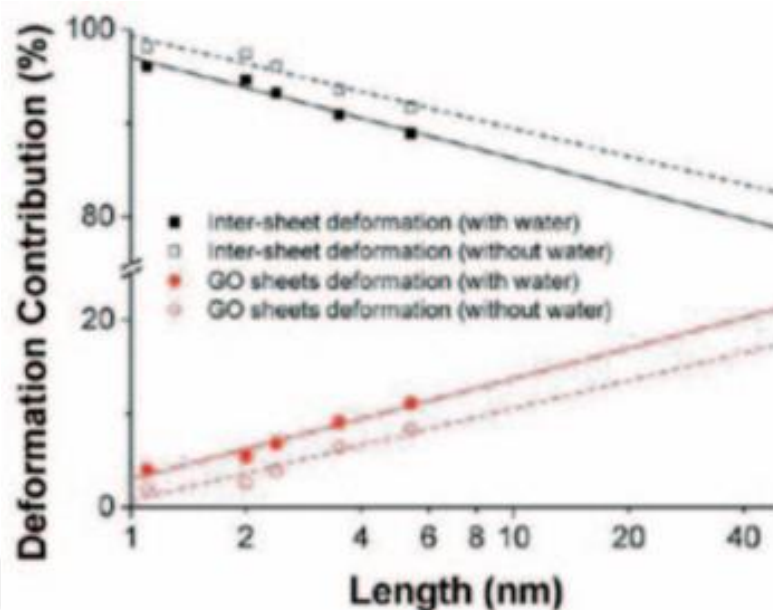


Figure 1.3. Plots of different components of deformation as a characteristic of GO length. (Zheng and Kim, 2015).

### 1.1.6. Thermal properties

Similar to the mechanical properties and electrical conductivities, the thermal conductivities of GO are much lower than that of pristine graphene due to the disorders arising from the residual oxygenated groups and the presence of defects. It is also worth noting that GO revealed an increasing thermal conductivity in response to an external tensile stress, an entirely opposite trend to those revealed by other nano-structured materials, including pristine graphene. The thermal conductivities of multilayer graphene and GO sheets were measured utilizing the thermal flash technique. It was revealed that the multilayer graphene including 30 – 45 layers had a thermal conductivity similar to bulk graphite, while that of 3-layer GO was higher than that of bulk graphite. The enhancement in thermal conductivity of multilayer GO than graphite is credited to the intercalating oxygen atoms that introduced covalent bridges between the interlayers for interaction (Zheng and Kim, 2015).

### 1.1.7. Catalytic properties

When GO is used as a catalyst the most important properties for the catalytic activity are the following. Carbon to oxygen ratio the plenty of oxygen atoms in the material reflects the number of functional groups that were implanted on the carbon grid upon oxidation of the main material. As mentioned in the description of the structure, there is a significant variation, in terms of functional groups, in addition to their localization. The C-O ratio can differ between 2:1 and 3:1 relying on the manufacturing method whereas, additional thermal and/or chemical treatment can increase the ratio to 14:1, by decreasing the oxygen concentration due to reduction (Eigler and Hirsch, 2014; Krishnan et al., 2012). The strict reproducibility of the C- O ratio, as well as the quality of the functional groups combined, is of utmost importance, as in most cases these functional groups are the ones responsible for the catalytic activity of GO.

High surface area is one of the main benefits of nanomaterials, which makes them so interesting not only for catalysis but also for other applications, is their high particular surface area, as typically determined by the Bruner-Emmett-Teller (BET) method. This provides a high interaction area, when compared to bulk materials, and – in combination with the abundance of functional groups on the surface of GO – a high proportion of catalytically active moieties per unit weight of material. The hypothetical surface area of monolayer graphene is  $2630 \text{ m}^2\text{g}^{-1}$ . At the same time, the one calculated for GO is  $890 \text{ m}^2\text{g}^{-1}$ , when the experimentally determined value in aqueous solution is  $736.6 \text{ m}^2\text{g}^{-1}$ . The apparent value is in line with the theoretical one, once the agglomeration level is taken into account. The surface area can be expanded again by reduction of the material, at the expense of the oxygen functionalities. For instance, activated reduced GO (RGO) films have a much higher particular area, of about  $2400 \text{ m}^2 \text{ g}^{-1}$ , quite close to the theoretical value for monolayer graphene. Extremely high surface zones of up to  $3100 \text{ m}^2\text{g}^{-1}$  were reported for microwave exfoliated graphite oxide, activated after treatment with KOH. The researchers recommend that the fine-tuning of the surface area depends on the proportion of KOH to graphite oxide. Although it seems a paradox, higher surface areas when compared to graphene are probable, by introducing heptagons and octagons into the carbon

lattice, therefore disrupting the typical six membered rings - the sheet gets a negative curvature and adopts a saddle shape (Eigler and Hirsch, 2014; Krishnan et al., 2012).

The conductivity of its derivatives is one of the properties that are easily tunable. The fine-tuning of these properties is highly needed for applications such as the design of super capacitors and fuel cells. The high electrical conductivity and electron mobility of graphene results from a very small effective mass. The electrons behave as massless particles in the graphene lattice, traveling with a speed of about  $10^6 \text{ ms}^{-1}$ , granting an exceptional in-plane conductivity of about  $20000 \text{ S cm}^{-1}$  and an intrinsic mobility limit of  $2 \times 10^5 \text{ cm}^2 \text{ V}^{-1} \text{ s}^{-1}$ , considerably higher compared to any silicon conductor. Because of the disruption of the  $\text{sp}^2$  bonding network, the conductivity of GO (of C/O ratio 2:1) is quite low, at the level of some  $\mu\text{Scm}^{-1}$ ; thus, GO is frequently described as an insulator. The removal of the oxygen atoms via reduction can regain an important portion of the conductivity, up to  $5880 \text{ Sm}^{-1}$ . The removal of the oxygen functionalities of GO can dramatically increase its capacitance, to levels comparable to those for pristine graphite or graphene (about  $100\text{--}300 \text{ Fg}^{-1}$ ). As a result of the fine tuning of the C/O ratio, in addition to the functionalization, GO and its derivatives are attractive materials for energy storage or super-capacitor fabrication (Eigler and Hirsch, 2014; Krishnan et al., 2012).

### 1.1.8. Synthesis Methods for Graphene Oxide

Graphene oxide can be synthesized in a dry or wet medium. The dry synthesis approach contains an oxidation reaction of graphene through atomic oxygen in ultrahigh vacuum conditions, to exposure to molecular oxygen and treating with ozone under ultraviolet light. By contrast, appropriate approach comprises of wet synthesis in which graphite is usually utilized as graphene source, because of its natural abundance and cost-effective (Figure.1.4), the three major reaction routes are shown. The first approach begins with utilizing graphene, produced with mechanical method, followed by advance oxidation, whereas the second one is based on exfoliation in aqueous medium by means of ultrasonic treatment (Pendolino and Armata, 2017).

The final route takes in a concurrent of oxidation and exfoliation process in strong acidic medium as found in Boride-Staudenmaier-Hummers method. Generally, these paths

bring to the formation of graphene oxide, but the structural properties of each kind of GO are diverse, such as the structure or the reactivity sites. In the following paragraphs, in chronological order, the preparing approaches for GO are reported. During the final century, numerous methods were suggested and the three main methods are Brodie, Staudenmaier and Hummers. From these basic methods number of differences were derived to develop the overall field and quality of the product, for example the Tour method. Recently, a “primitive” approach was approved by a number of researchers which contains in a free-water exfoliation and oxidation of graphite through strong oxidizing agent in a strong acidic medium often ( $\text{H}_2\text{SO}_4$ ).

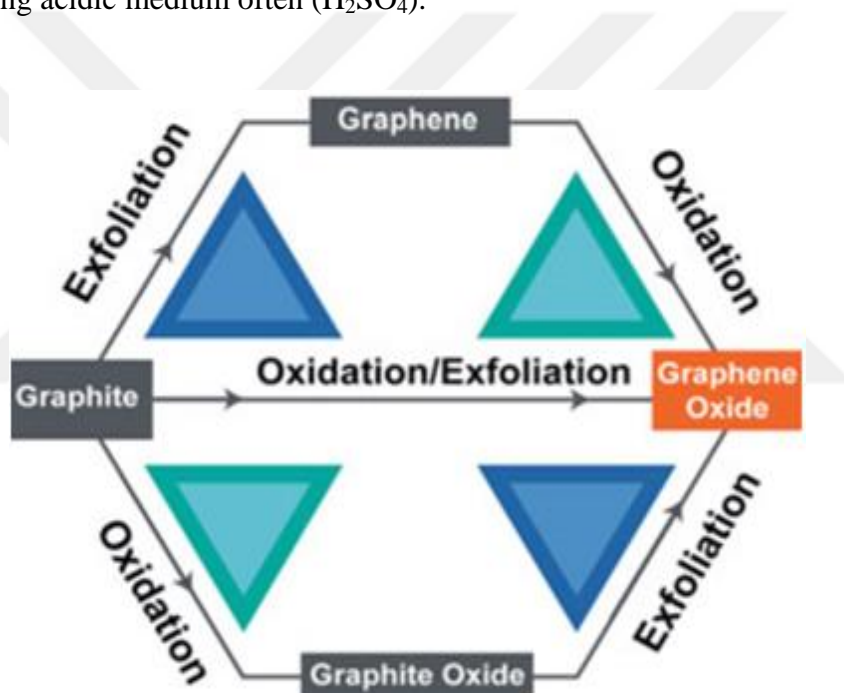


Figure 1.4. Scheme of GO production beginning from graphite as carbon source. Three paths may be described to get as final product the graphene oxide material (Pendolino and Armata, 2017).

### 1.1.8.1. Brodie method

The first documented synthesis of graphitic oxide material is accredited to Brodie in 1859. His research was focused on finding the weight of graphite and, as common at that time, a chain of chemical reactions was explored to elucidate the properties of a novel material. Therefore, graphite was mixed with potassium chlorate ( $\text{KClO}_3$ ) and solubilized in fumes nitric acid to oxidize the sample and inferring the molecular weight. Additional



oxidation processes were carried out on the sample up to any changes were obvious. The elemental analysis showed a composition of circa 60% C, 2% H and 38% O. The resulting product, a mixture of graphene and graphite oxide, was soluble in pure water (Pendolino and Armata, 2017).

### **1.1.8.2. Staudenmaier method**

In 1898, Staudenmaier developed the Boride's reaction by adding sulfuric acid to increase the acidity of the mixture, and many aliquots of solid  $\text{KClO}_3$  over the course of reaction. Although that, Brodie and Staudenmaier method generates  $\text{ClO}_2$  toxic gas which quickly decomposes in air giving explosions. These modifications led to a more oxidized graphitic material and a simplification of the reaction (Pendolino and Armata, 2017).

### **1.1.8.3. Hummers method**

In 1958, Hummers and Offeman projected an alternative way for developing oxide graphite in the safe operational conditions with an extreme reducing time, from 10 to 2 days. They mixed graphite with concentrated sulfuric acid ( $\text{H}_2\text{SO}_4$ ), sodium nitrate ( $\text{NaNO}_3$ ) and potassium permanganate ( $\text{KMnO}_4$ ) to get a brownish grey pasty. The suspension was diluted with water and hydrogen peroxide ( $\text{H}_2\text{O}_2$ ) was added to achieve a higher oxidation degree and to remove manganese from the dispersion (yellow-brown mixture). Finally, the sample was filtered and washed with warm water. They got the same degree of oxidation reported by Staudenmaier, however, the amount of GO results are very little. The weakness of this method contains a time-consuming of the separation and purification process. From Hummers method an enormous number of variation/optimization approaches has been improved and a typical GO product is made by flakes of about 1nm and a lateral size of  $1\mu\text{m}$  (Pendolino and Armata, 2017).

### 1.1.8.4. Tour method

A modified Hummers Method was suggested by Tour's group at Rice University in 2010. They have substituted the sodium nitride with phosphoric acid in a mixture of  $\text{H}_2\text{SO}_4/\text{H}_3\text{PO}_4$  (9:1) and increasing the amount of  $\text{KMnO}_4$ . The benefit of this method contains no generation of poisonous gases, such as  $\text{NO}_2$ ,  $\text{N}_2\text{O}_4$  or  $\text{ClO}_2$ , in the reaction and an easy temperature control. The authors claim that the existence of phosphoric acid makes a more intact graphitic basal plane. A comparison of the improved method with the conventional and modified Hummers' procedures can be seen in Figure.1.5. The benefit of the Tour method contains a production of graphene oxide having a higher hydrophilic degree, in contrast with GO produced by Hummers method (Table 1.1). Therefore, this graphene oxide results more oxidized and soluble (Pendolino and Armata, 2017).

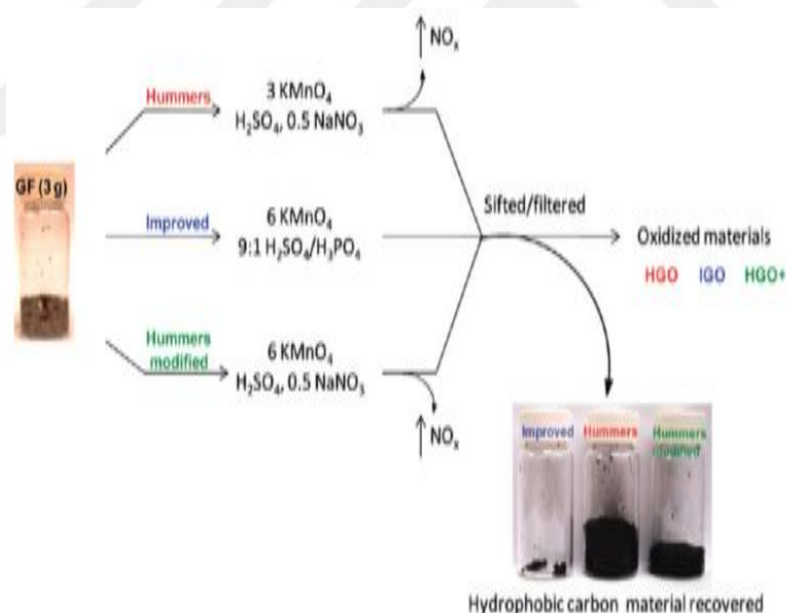


Figure 1.5. Procedure scheme for Tour approach. The starting materials is expanded graphite to be used for producing graphene oxide through Tour method in comparison with Hummers method and its modification (Pendolino and Armata, 2017).

#### **1.1.8.5. Free-water oxidation method**

The Free-Water Oxidation method takes benefit of a reaction between extended graphite and oxidizing agent in a free-water medium. Since inorganic carbon is necessary inert at room temperature, its solubilization dispersion in a solvent requires strong protic acid or mixture of warm acids, for example sulphuric or nitric acid. Furthermore, a strong oxidizing agent, as potassium permanganate ( $\text{KMnO}_4$ ), makes sure the bonds of oxygen functionalities to organic carbons from historical reason. The free-water oxidation methods derived from a modification of the Hummers method in which some limitations, such as dangerous reagents, were developed (Pendolino and Armata 2017).

#### **1.1.8.6. Sun method**

In 2013, Sun and Fugetsu at Hokkaido University presented a more direct method to produce graphene oxide. They utilized extended graphite as carbon precursor. The potassium permanganate had two-fold impacts: inter collating agent and oxidizing agent. The inter collation of  $\text{KMnO}_4$  between graphitic layers produced a further spontaneous expansion which looks like a foam of graphitic material, as shown in Figure.1.6b. The reaction occurs in acidic medium of sulfuric acid. The proportion of graphite and  $\text{H}_2\text{SO}_4$  was reduced to 1:20 and the added reagents were removed from the reaction procedure. For this reason, Sun protocol can be considered as one of the first green procedure of among the wet synthetic methods (Pendolino and Armata 2017).

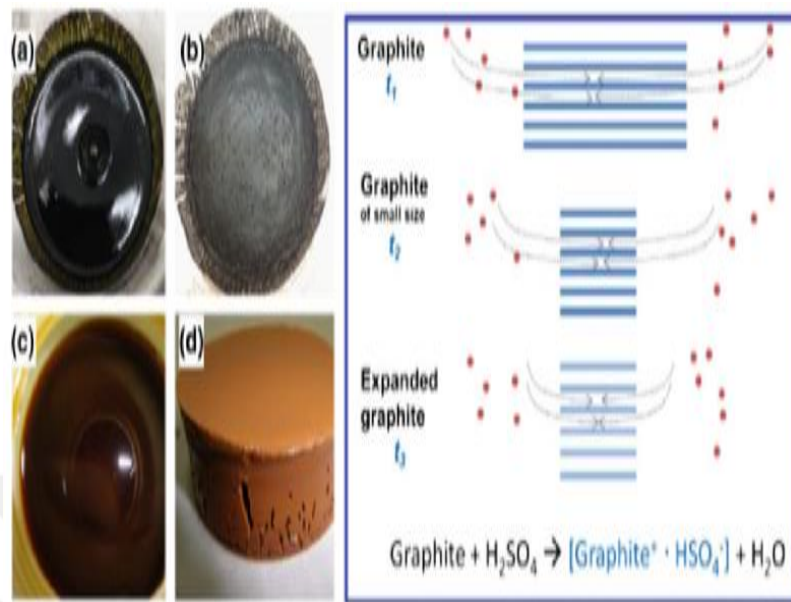


Figure 1.6. Reaction scheme for Sun technique (left). Right images of a) combination of reagent, b) volumetric enlargement (foam-like), c) hydrolysis and d) concentrated dispersion after purification (Pendolino and Armata, 2017).

#### 1.1.8.7. Peng method

Very recently in 2015 year, Peng and co-workers proposed a scalable and green method (Figure 1.7) to produce graphene oxide using potassium ferrate ( $K_2FeO_4$ ) as strong oxidant. This compound avoids the introduction of heavy metals or the formation of toxic gases during the preparation. In this method, a mixture of graphitic flakes and  $K_2FeO_4$  dispersed in concentrated sulphuric acid were loaded into a reactor and stirred for 1h at room temperature. The product was water-washing by repeated centrifugation to obtain highly water-soluble graphene oxide (Pendolino and Armata, 2017).

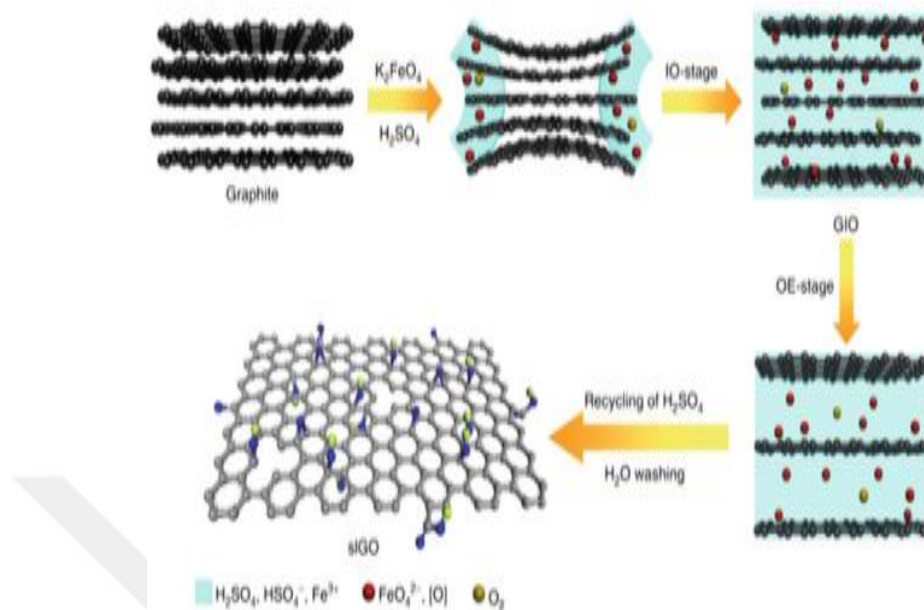


Figure 1.7. Reaction mechanism proposed by Peng and co-workers for the synthesis of graphene oxide using  $K_2FeO_4$  as oxidizing agent. This work is licensed under a Creative Commons Attribution 4.0 worldwide License (Pendolino and Armata, 2017).

#### 1.1.8.8. 4-Steps method

This method derived from the basic exfoliation-oxidation procedure and was improved by Pendolino and co-workers. The method contains of 4 reaction steps controlled by temperature, which affects strongly the final product. A scheme of reactions is shown in Figure 1.8 in which two paths are proposed depending on temperature. In the first phase, the oxidation process for the mixture graphite- $KMnO_4$  dispersed in the concentrated sulfuric acid gets a pasty slurry. The second step (warm) contains the exfoliation of graphite and is the most critical one. In fact, the production of graphene oxide is restricted by temperature and only occurs while the water bath is around  $30^\circ C$ . By contrast, the exfoliation is repressed for lower temperature with a resulting cold graphite oxide. The hydrolysis, at  $90^\circ C$  for 1h, completes the third step. The purification of product is achieved by centrifugation utilizing warm water up to the neutrality of the spreading, at the fourth step. Through the 4-Steps method two different products can be synthesized just controlling the temperature along the reaction. The benefit of this method is related to the improved of

safety operational conditions (limiting explosive reaction due to  $Mn_2O_7$  in concentrated sulfuric acidic for temperature above  $55^\circ C$ ) and the production of a type of GO which comprises an amount of oxygen domains lower (20-30%). This kind of GO can be employed for filter/remediation or biosystems because of the low toxic impact (Pendolino and Armata, 2017).

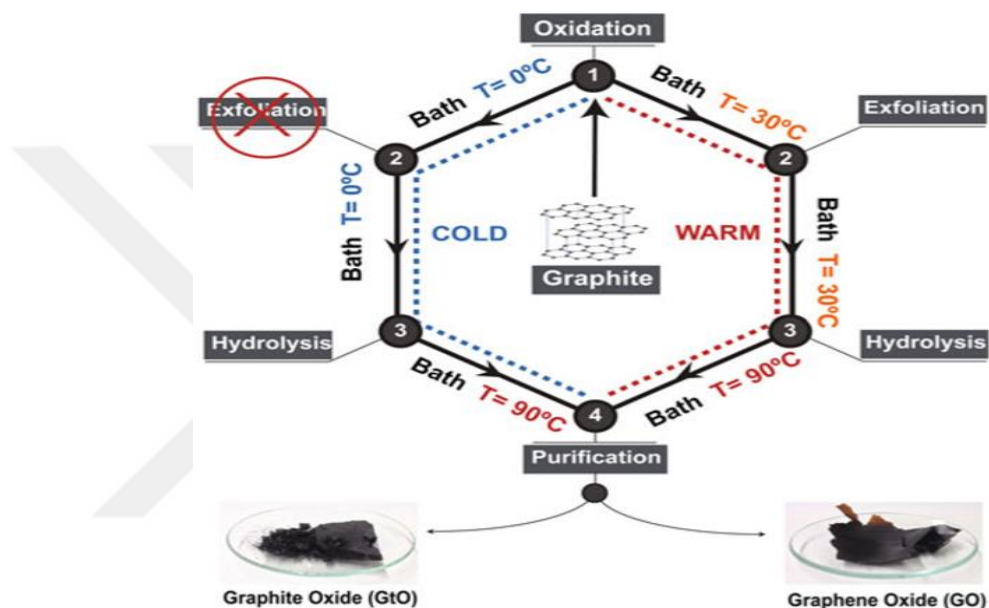


Figure 1.8. Reaction scheme for the four-steps technique. The temperature influences the final product according with the “heat” or “bloodless” route. The graphene oxide is only acquired when the warm route is observed, and, by way of contrast, graphite oxide is produced at decrease temperature below  $30^\circ C$  (Pendolino and Armata, 2017).

Table 1.1. Summary of the primary synthetic techniques used to prepare GO (Pendolino and Armata, 2017).

Method	Oxidant	Solvent	Additive	C/O	Resistivity
<b>Brodie</b>	KClO <sub>3</sub>	HNO <sub>3</sub>	-	2.4- 2.9	0.15-60
<b>Staudenmaier</b>	KClO <sub>3</sub>	Fuming HNO <sub>3</sub>	-	2.2	120
<b>Hummers</b>	KMnO <sub>4</sub>	H <sub>2</sub> SO <sub>4</sub>	NaNO <sub>3</sub>	1.8-2.5	0.005-0.01
<b>Tour</b>	KMnO <sub>4</sub>	H <sub>2</sub> SO <sub>4</sub>	H <sub>3</sub> PO <sub>4</sub>	0.7 – 1.3	0.2 – 1000
<b>Sun</b>	KMnO <sub>4</sub>	H <sub>2</sub> SO <sub>4</sub>	-	2.5	0.18
<b>Peng</b>	K <sub>2</sub> FeMO <sub>4</sub>	H <sub>2</sub> SO <sub>4</sub>	-	2.2	2.7
<b>4-Steps</b>	KMnO <sub>4</sub>	H <sub>2</sub> SO <sub>4</sub>	-	3.5	23

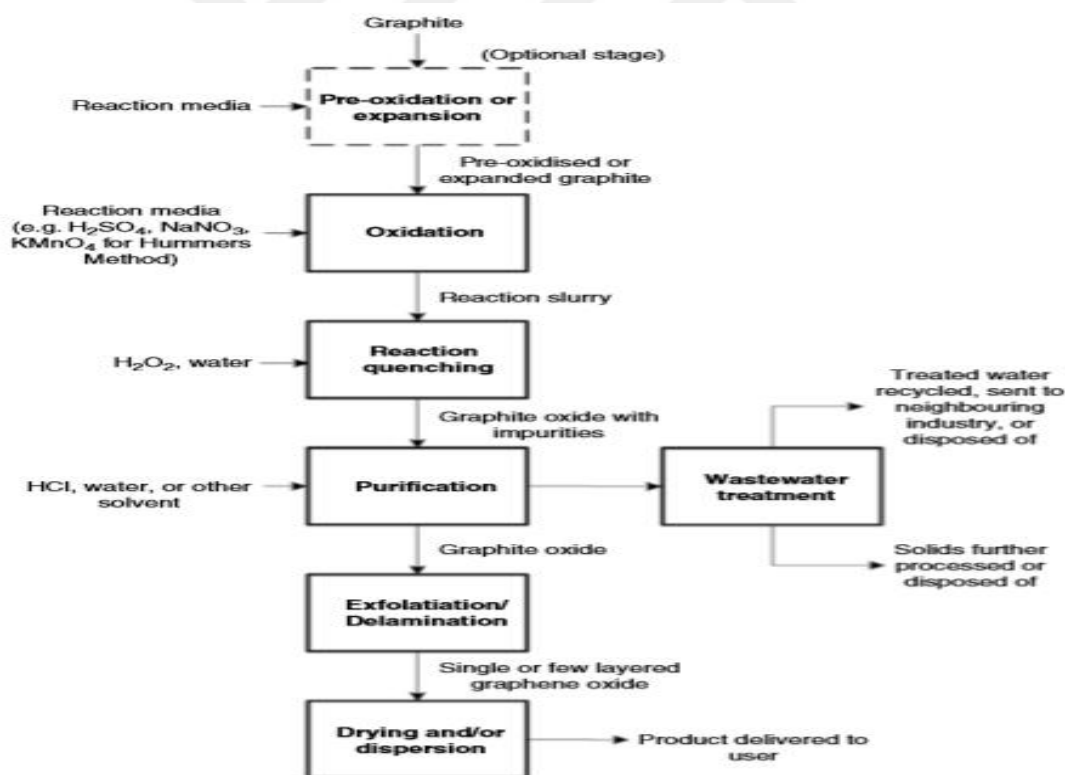


Figure 1.9. Block go with the flow diagram of a probable method for the production of GO (Dimiev and Egle, 2016).

## 1.2. Noble Metal Nanoparticles

Nanomaterials are materials with particle size between 1 and 100 nm shown in Figure 1.10. The primary aim of synthesis of metal nanoparticles can be followed back to 1850's. Faraday synthesized the first pure gold colloids by reducing gold chloride with phosphorus in water and requested the chemicals he made were in the nano-scale. Size, shape and composition of metal nanoparticles are of great significance to their functions and applications. The final two decades have witnessed a blossom of publications on the preparation of metal nano-crystals. Noble metal catalysts play main roles in the different organic reactions. Due to the deficiency of fossil fuels, new sources of energy, such as lithium ion batteries, solar cells and fuel cells, have been paid great attention. As interest in energy increases, the request for noble metals (catalysts for energy production) gradually goes up (Gao, 2012).

Noble metal nanoparticles have been reported for the modification of the active surface of electrodes because of their unusual electronic, optical, catalytic properties, good electron transfer rate, large surface area, and remarkable stabilities. The electrochemical communication between the analyte and these nano-materials have been developed utilizing silica, graphene, carbon nanotubes, and titanium dioxide as supporting materials. But, the sensitivity and selectivity of these nanoparticles are not very satisfactory. Thus, it is necessary to improve the sensitivity and selectivity of the working electrode utilizing reasonable nano-composite materials. Furthermore, the fabrication of new nano-composite materials for making low-cost, exact, and dependable electrochemical sensors is especially significant. To this conclusion, numerous noble metal nanoparticles have been the center of interest because of their excellent electrochemical properties (Guler et al., 2018).



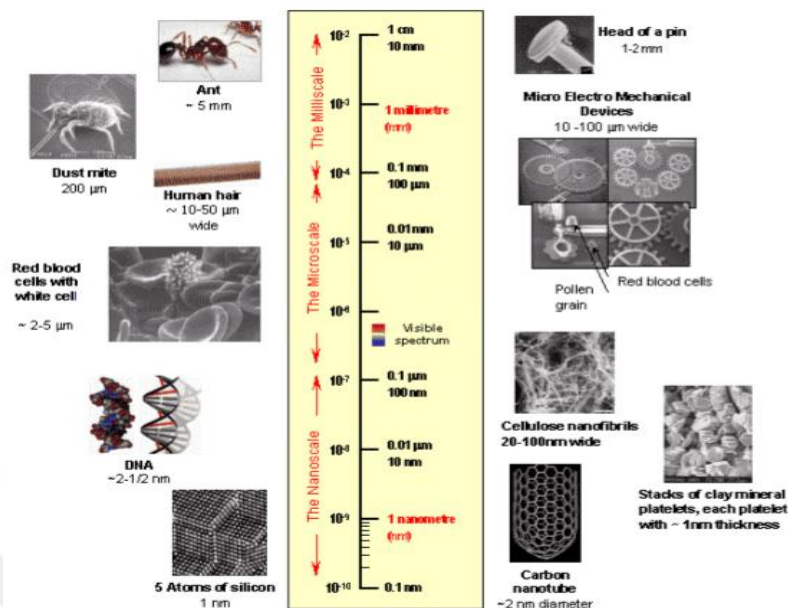


Figure 1.10. The dimensions of nanotechnology (Gao, 2012).

### 1.3. Palladium

In recent years, there has been significant interest in the synthesis and application of palladium, denoted as Pd, a rare silver white metal belonging to the platinum group along with platinum, rhodium, ruthenium, osmium and iridium. The industrial request for Pd is high and was ~316 metric tons in 2016 (Balamurugan et al., 2018). Pd is in automobile catalytic converters for reduction in toxin emissions (nitrogen oxide, carbon monoxide and hydrocarbons) from automobile exhausts and is also utilized in the electric and electronic instrument industry for the production of diodes, industrial circuits and semiconductors (Umemura et al., 2015).

Through three different oxidation states ( $\text{Pd}^0$ ,  $\text{Pd}^{2+}$  and  $\text{Pd}^{4+}$ ), Pd shows highly catalytic effects in hydrogenation, dehydrogenation, oxygenation and hydrogenolysis reactions. Therefore, Pd is widely utilized as a catalyst in chemical and petroleum industries, such as the oxidative conversion of alcohols to aldehydes, synthesis of drugs like rofecoxib and cefprozil, C-H functionalization, the Makarov-type cyclisation reaction, the Suzuki-Maura reaction, the Buchwald-Hartwig amination reaction and the Sonogashira reaction (Balamurugan et al., 2018).

Pd catalysts are also employed in carbon–carbon bond formation and plays an essential role in the synthesis of complex structures, such as natural products, pharmaceuticals, functional materials, polymers and super molecules .Because Pd can absorb enormous quantities of hydrogen, almost 900 times its own volume at ambient temperature and pressure, this opens up the possibilities of utilizing Pd for the purification and storage of hydrogen and its utilize in fuel cells (Adams and Chen, 2011).

In the healthcare and medicine sector, Pd is being utilized in dental alloys and in surgical tools. Such widespread utilize has increased Pd pollution in medicines caused by process containment and the environment because of the release from wastes, thus resulting in increased health risks. Pd is known to have high mobility among the platinum group metals and its transfer coefficient into plants is over 0.1. It is also highly soluble in rain water from dust when compared to platinum (Kielhorn et al., 2002).

The concentration of Pd in contaminated soil has been reported to be 440 ng/g. Pd in contaminated soils and aquatic ecosystems can be transferred to biological systems and undergoes biogeochemical transformations, which increases its bioavailability and causes severe health threats (Gao, 2012). The Pd byproducts achieved during organic molecule synthesis are transported into living organisms via a divalent metal transporter (DMT1), and are dangerous to human health and the environment. For example, Pd could destroy DNA, organize with thiol containing amino acids, bind to vitamin B6, trigger protein denaturation and harm several cellular processes (Yusop et al., 2011). Due to strong bonding with organic ligands, Pd can associated with macromolecules like proteins and DNA, intensify hydroxyl radical damage, interfere with mitochondrial functions and prevent the activities of numerous enzymes, which disturb cellular functions and equilibrium in cellular environments. Therefore, Pd is believed to be cyto-poisonous, causing cellular harm which could be sometimes fatal to the cell itself. Pd is a known pain and sensitizier, and continuous exposure can cause contact dermatitis. It is also known to cause stomatitis and periodontal gum infection (Faurshou et al., 2011). Pd can also leach from dental alloys and collect, specifically in the liver and kidneys in humans. The final threshold for Pd in end products is severely limited, with set governmental limitations (no more than 5-10 ppm) and there is a proposed maximum dietary admission of palladium (as a rough assess) of less than 2 µg per person per day. As a result, information of how to

identify the concentration and distribution of Pd inside biological systems is an important issue (Balamurugan et al., 2018).

### 1.3.1. Catalytic properties

The high material cost of palladium naturally limits the application of palladium nanoparticles. Catalysis is the most important application for palladium or its alloy clusters, and has been widely examined. Transition metal nanoparticles are known to be effective catalysts because of their large surface area arising from the extreme reduction of size. For the past decades, palladium nanoparticles have played a significant role in organic catalysis. In general, the catalysis of organic reactions can be grouped as structure sensitive, such as Suzuki coupling reactions and Heck coupling reactions or structure-insensitive, including hydrogenation reactions. Pd nanoparticles show outstanding performance in reactivity and selectivity for catalyzing these organic reactions. Besides catalyzing these organic reactions, pure palladium clusters can work as activators for electroless copper deposition (Yang et al., 2005). Palladium also serves as a main catalyst in the automobile industry. Over half of palladium supplies are utilized in catalytic converters, which convert up to 90% of harmful gases from auto exhaust into less-harmful substances. Palladium has shown a very large capability for hydrogen absorption. Nanostructured palladium thin films perform well as micro sensors, which have been connected in hydrogen detection. Palladium also plays a key role in the fuel cells technology, which combines hydrogen and oxygen to produce electricity, heat and water (Gao, 2012).

Palladium as an important noble metal, its properties significantly differ from those of catalysts containing (Rh, Pt, Ru, Ni or Cu). Palladium is one of the most active metals in the hydrogenation of double bonds conjugated with an aromatic ring, such as (Ar-C=C, Ar-C=O, or Ar-C=NR) (Pikna et al., 2018). Furthermore, Pd is one of the most selective metal catalysts in the hydrogenation of triple and conjugated double bonds and the most active metal in hydrogenolysis including reductive cleavage of C-X bonds (Belykh et al., 2006). There are several different materials utilized as support for Pd loading. An active catalyst separating on a convenient support should stabilize the catalytic nanoparticles,

bring optimum catalyst utilization, and reduce the amount of utilized valuable metal, thus reducing catalyst cost (Chai et al., 2004). Most frequently, activated carbon is utilized as a support, but recently carbon nanotubes (CNTs) have been considered as a promising catalyst support material. The tubular structure of CNTs makes them unique among different forms of carbon. High surface area, low resistance, and high stability propose that CNTs are suitable materials as catalyst supports (Tang et al., 2004). Excellent nanomaterial supports not only maximize the availability of the nano sized catalyst surface area for electron transfer but also provide better transport of reactants to the catalyst (Zhao and Zhao, 2013). It was reported that the catalytic activity of Pd-based catalysts depends strongly on the size, shape, and size distribution of the particles, in addition to their dispersion on the support (Pandey and Lakshminarayanan, 2009). Electrochemistry is an instrument well suited for quick and simple characterization of catalysts. Electrochemical methods show advantageous properties for example superior sensitivity, fast analysis, easy to handle, cost effective, high selectivity, and exceptional long-term calibration stability (Pikna et al., 2018).

#### **1.4. Electrochemical Sensors**

A sensor is a device that responds to a physical stimulus, such as heat, light, sound, pressure, magnetism, or movement, and transmits a resulting electrical motivation as a means of measuring the change of any intrinsic property of the constituent material. The source of the word sensor comes from the Latin stem sentient-sensing, to feel. Semantically, sensors have the feature of feeling into their surrounding environment to describe a coupling relationship (Simões and Xavier, 2016). A sensor (also called detector) is a converter that measures a physical quantity and changes it into a signal which can be read by a spectator or by an instrument (today generally electronic). The sensor contains an acknowledgment element that enables the choosy response to a specific analyte or a group of analytes, thus minimizing interferences from other sample components (Raj and John, 2019).

A chemical sensor is a self-contained device that is able to providing real time analytical information in a test sample. By chemical information we understand here the

concentration of one or more chemical species in the sample. A target species is generally termed as the analyte or determined. Besides chemical species, micro-organisms and viruses can be followed by means of specific bio compounds such their nucleic acid or membrane components (Banica, 2012).

Electrochemical sensors, in specific, are a class of chemical sensors in which an electrode is utilized as a transducer element in the presence of an analyte (Simões and Xavier, 2016). Electrochemical sensors change the information related to electrochemical reactions (the reaction between an electrode and analyte) into an applicable qualitative or quantitative signal. The electrochemical sensors are mostly divided into three kinds: potentiometric, conductometric, amperometric or voltammetry. Electrochemical sensors can produce electronic outputs in digital signals for assist analysis as per the steps as shown in Figure 1.11. Generally, the reactions found in these sensors are due to the chemical and electrical interactions, which are eventually based upon the conductometric, amperometric, and potentiometry dimensions. Electrochemical determination is superior to other measurement systems due to its speed and simple features (Wang, 1999).

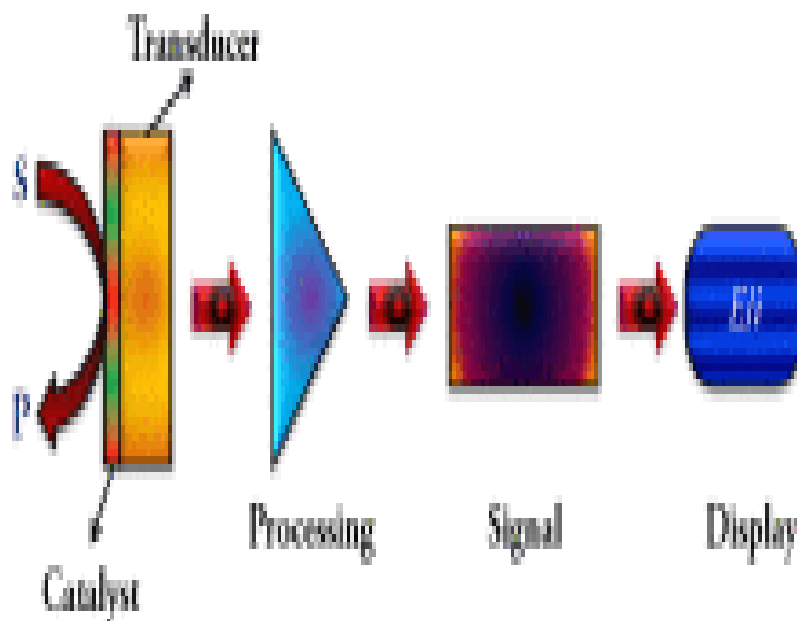


Figure 1.11. The principle stages within the sensor operation (Shetti et al., 2019)

#### 1.4.1. Why electrochemical sensing

The general characteristics of electrochemical sensors and these criteria allow the advantages of electrochemical detecting to be put forward. Most of this uses voltammetry or amperometric sensing. The choice of electrode material can lead to selectivity in potentiometric and in voltammetry sensors. In potentiometric sensing, ion-selective electrodes are selected for analyte determination. In voltammetric sensors, the electrode material can impact the over potential of some species in mixtures (Brett and Oliveira-Brett, 2011).

Each electro active species experiences reaction (oxidation or reduction) at a specific potential. Thus, an applied potential in voltammetric or amperometric sensors can lead to high selectivity and specificity, and enable probing of speciation (including different species in the same oxidation state). Few other analytical techniques have this possibility.

Since the signal achieved at an electrochemical sensor is electrical in nature (a voltage or a current), no assist signal transduction is required. Thus, with modern electronic circuitry for voltammetric sensing, instrumentation can simply be adjusted to apply complex potential waveforms and analyses the response utilizing a variety of signal treatment software program and chemometric instruments, leading to sensors with high sensitivity and low detection limits. Surface-modified electrode characteristics can be tuned through suitable plans and architectures so that the electrode is itself both a reagent and a detector for electrochemical sensing detection (Brett and Oliveira-Brett, 2011).

Small, portable sensor systems combining the sensor itself and committed battery-powered instrumentation, can be utilized outside the laboratory, particularly in situations where no pretreatment of sample is required.

Sensors can be simply miniaturized and joined in flow systems for online monitoring (Brett and Oliveira-Brett, 2011).

#### **1.4.2. Advantages of electrochemical sensors**

Electrochemical sensors and detectors are interesting to track down onsite pollution as well as to meet environmental requirements. They are utilized to control at various points of the dimension, which can provide relevant information at different steps in the

decision-making process. This is particularly important for biological samples, which are usually small in size and the injury of tissue should be reduced especially when required for in vivo observation (Moretto and Kalcher, 2014). The possibility of automation and manufacturing of small sensors is of great advantage for scientific purposes. Electrochemical sensors have several benefits over the conventional analytes that will lead to positive utilization in the near future. They are a fascinating scientific device due to the excellent selectivity and sensitivity towards electroactive analyte, occasionally due to the accuracy and specificity; they are less time expanding, have flexibility and are simple to set up. They are lightweight and transferrable devices, easy to utilize and compact; resulting in quickness in research data arrangement. The choice of suitable functional principles, the plan, and the material for detection of analyte is based on the aspects such as portability, selectivity, sensitivity, the require for single or multivariate discovery, and any suitable field applications (Wang, 1999).

The electrodes can sense the materials that are situated in the host without doing any harm to the host system with low detection limit and high specificity. These devices contain important information that selectively produces an electrical signal that is connected to the concentration of the analyte studied. The active sensing material on the electrode should act as a catalyst and catalyze the reaction of the chemical and biochemical compounds to get the output signals (Raj and John, 2019). An electrochemical sensor also has appeared a great capacity to decide the concentration of an analyte within a complex sample at the point-of-care and in near-real time. Consequently, this sensor has fascinated a great interest particularly for medical diagnosis, observing of existing conditions, and environmental monitoring. It is important to note that the sensitivity of the electrochemical sensor will be influenced based on: (i) the surface modification techniques, (ii) electrochemical transduction mechanisms, and (iii) the choice of the recognition receptor molecules. The most common technique utilized by most of the researchers to improve the sensor performance is to chemically change the surface of working electrode. The surface architectures that connects the sensing element with the biological samples play an important role in the detection performance of electrochemical sensor. Metals, metal oxides, carbon nanotubes, and polymers are some examples of active materials that have frequently been utilized to modify the sensor electrodes (Yusoff, 2019).

Electrochemical sensors present several advantages as follows: very good sensitivity which allows low LODs and LOQs; quick analytical response making them useful for flow analysis and alert systems; simplicity offering practically an unlimited selectivity of electrode materials, geometries, and configurations; simplicity of utilize (simple and low-cost tools, possibility to be combined as detection module in various analytical systems, few analytical steps, it does not request specialized personnel); miniaturization and automation (useful in environmental and biomedical applications); and mass fabrication, meaning low cost and improvement of single-utilize disposable sensors, very significant especially in the medical field where contamination is a major issue (Moretto and Kalcher, 2014).

#### **1.4.3. Disadvantages of electrochemical sensors**

The main disadvantages of electrochemical sensors have been discussed: low or deficiency of selectivity, low reproducibility, and difficult validation of the analytical method. In contrast with disadvantages of electrochemical sensor and biosensor, the high quick analysis and the ability of detecting very small volumes and low concentrations without significantly perturbing the sample stay highly attractive features of electrochemical sensors (Moretto and Kalcher, 2014).

#### **1.4.4. Using areas of electrochemical sensors**

Several properties of modern electrochemical sensors such as physical, chemical, or biological parameters were utilized to identify different parameters in our everyday lives. Some examples are environmental monitoring, health and instrumentation sensors, and sensors related to machines, such as automobiles, airplanes, mobile phones, and technology media. In last decades, modern sensing systems have benefited from progresses in microelectronic and micro-engineering, generally through the manufacturing of even smaller sensors with more sensitivity and more selectivity, and with lower production and maintenance costs (Simões and Xavier, 2016).



In deciding whether or not to utilize electrochemical detecting, a number of significant criteria must be evaluated (Figure 1.12). This will permit the choice to be made as to whether pursuing electrochemical sensing is practical and a good alternative to the others (Brett and Oliveira-Brett, 2011). Electrochemical sensor technology is an essential part of modern analytical chemistry and has gained great attention. Understanding the fundamentals of sensors requires a strong information of different academic areas connected to every aspect of science. This results in a multidisciplinary field filled with chemists, physicists, electrical engineers, and biologists. The potential applications of sensors can be found in different fields such as science, pharmaceuticals, medicine, analysis, chemistry, materials engineering, synthesis, molecular engineering, and biotechnology (Wang, 1999).

Electrochemical sensing devices have a main affect upon the observing of priority pollutants by permitting the instrument to be taken to the sampling site (instead of the conventional way of bringing the sample to the laboratory). Such devices can perform automated chemical analyses in complex matrices and provide quick, dependable, and cheap dimensions of a variety of inorganic and organic pollutants (Moretto and Kalcher, 2014).

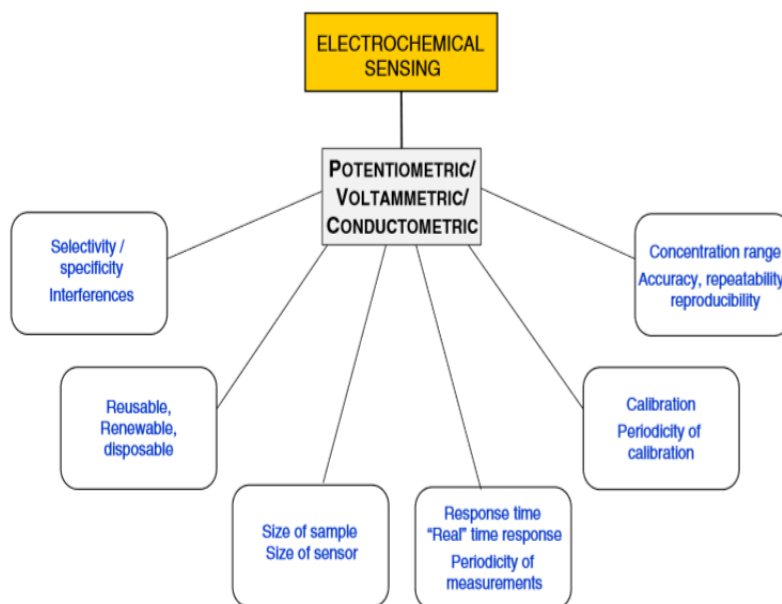


Figure 1.12. Standards for example of the possibility of the use of electrochemical sensing (Brett and Oliveira-Brett, 2011).

#### 1.4.5. Performance factors of sensor

One of the performance factors, selectivity is very important for electrochemical sensors and biosensors. It is rare to find a sensor which will respond to only one analyte, although some do exist. It is difficult to find a sensor that will respond mainly to one analyte, with a limited response to another similar analyte. Alternatively, the response may be to a group of analytes of similar chemical structure, such as carbonyl compounds. Sensitivity range usually needs to be sub-mill molar, but in special cases can go down to the femtomolar accuracy. This needs to be better than 5%. Nature of solution such as pH, temperature and ionic strength must be considered. Response time is usually much longer (30 s or more) with biosensors than with chemical sensors. Recovery time is the time that elapses before the sensor is ready to analytes the next sample - it must not be more than a few minutes. The working lifetime is usually determined by the stability of the selective material. For biological materials this can be as short as a few days, although it is often several months or more range (Eggins, 2008).

#### 1.5. Paracetamol

Acetaminophen (N- (4-Hydroxyphenyl) ethanamide or N- (4Hydroxyphenyl) acetamide), as well as called paracetamol (para-Acetylaminophenol) or APAP (NAcetyl - para-aminophenol) is a manufactured nonopioid analgesic and antipyretic. Because it is not significantly anti-inflammatory, it is not an NSAID (non-steroidal anti-inflammatory drug), even though in general it's analgesic and antipyretic viability are equivalent to those of NSAIDs. Acetaminophen has a generally long history. Acetanilide (N-Phenylacetamide) was fortunately found to have antipyretic properties in the final half of the 1800s and it was promoted beneath the name of antifebrin. However, concerns over toxicity provoked a search for a safer compound. An aniline derivative of acetanilide, phenacetin (N-(4-Ethoxyphenyl) acetamide) it was chosen and promoted, but it also had unsatisfactory harmfulness. It was consequently found that the poisonous of acetanilide and phenacetin were attributable to a metabolite and that pain relieving and antipyretic activities were held in a different, but common, metabolite – acetaminophen. Acetaminophen was reintroduced

in 1955 beneath the brand name Tylenol™ and in 1956 as Panadol™. It is presently one of the most commonly- and broadly-utilized no opioid analgesics global (Taylor et al., 2012).

### 1.5.1. Chemical properties

The chemical structure of acetaminophen is seen in Figure 1.13 where it is displayed to demonstrate its different components as described. Acetaminophen has a center aromatic (benzene) ring substituted in para orientation by two groups: a hydroxyl and an acetamide (ethanamide). Multiple portions of the molecule are conjugated, comprising the benzene ring, the hydroxyl oxygen, the amide nitrogen, and the carbonyl carbon and oxygen. As a result, the benzene ring is highly reactive toward electrophilic aromatic substitution (all positions being around similarly actuated both oxygens and the nitrogen much less fundamental and the hydroxyl acidic (Taylor et al., 2012).

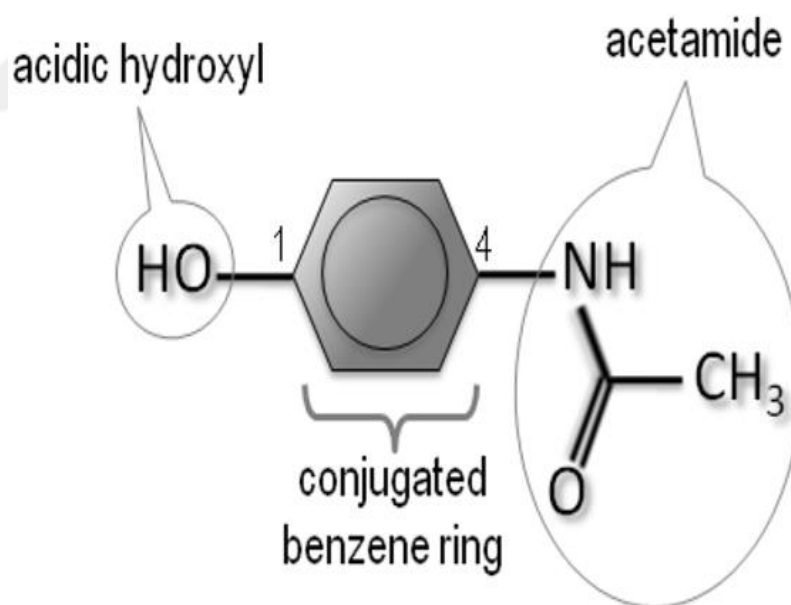


Figure 1.13. Acetaminophen (paracetamol) (N-(4-Hydroxyphenyl) ethanamide or N(4-Hydroxyphenyl) acetamide or (N-Acetyl-para aminophenol) chemical structure highlighting energetic components (Taylor et al., 2012).

### 1.5.2. Pharmacokinetics properties

#### 1.5.2.1. Absorption

Immediate release rapid absorption of orally managed acetaminophen mainly happens through the small intestine of the gastrointestinal tract, with minimal uptake by the stomach. This absorption route permits acetaminophen to get a relative bioavailability of 85% to 98% (Taylor et al., 2012).

### **1.5.2.2. Distribution**

Plasma protein binding of acetaminophen is relatively low (10 - 25%) and disperses broadly during the body with a volume of distribution of 0.7 - 1.0 L/kg in both adults and children. Acetaminophen metabolites do not bind to plasma proteins (Taylor et al., 2012).

### **1.5.2.3. Metabolism**

Metabolism of acetaminophen can happen by three fundamental pathways, all of which mainly participate in the liver. These pathways consist of conjugation with glucuronide; conjugation with sulfate; and oxidation by the cytochrome P450 (CYP450) enzyme pathway. In addition, acetaminophen can experience hydroxylation to form 3-hydroxy-acetaminophen and methoxylation to form 3-methoxy-acetaminophen, which may be assist to conjugated glucuronide or sulfate. The major CYP450 isoenzymes complicated in the oxidation of acetaminophen is CYP2E1 with CYP1A2 and CYP3A4 having minimal involvement. The major reactive metabolite of the oxidation process, N-acetyl-p-benzoquinone imine (NAPQI) is hepatotoxic, nevertheless is usually quickly changed to an inert cysteine and/or mercapturic acid metabolite by conjugation with glutathione. However, the increase of the poisonous metabolite can happen if this pathway is saturated or glutathione are depleted for any reason. The result is severe hepatic toxicity, perhaps resulting in liver failure (Taylor et al., 2012).

### **1.5.2.4. Elimination**

The elimination half-lives are similar with age (>2 years) and may vary slightly with diverse ethnic and medical backgrounds. The elimination  $t_{1/2}$  for healthy adults is around 2 to 3 hours and approximately 1.5 to 3 hours in children. In neonates, cirrhotic patients the half-life is roughly 4 hours. Acetaminophen is fundamentally excreted in the urine, with a common eliminated in the glucuronide form (40 - 65%), sulfate form (25 - 35%), and as unaltered acetaminophen (3.5%) (Taylor et al., 2012).

#### **1.5.2.5. Fetus, neonates, infants, and children**

The usage of acetaminophen in this patient population is considered to be secure and efficacious while managed at suggested dosages. Just as in youths and adults, there is a hazard of hepatotoxicity and proper precautions need to be taken. Pharmacokinetic parameters for kids more than 2 years of age and adults are similar, however change with decreasing age from < 2 years to newborns. Oxidation of acetaminophen to the reactive hepatotoxic metabolite is about ten times slower in the fetal liver than adult and rises with fetal age. Fetal livers mainly utilize sulfate conjugation to detoxify acetaminophen and not glucuronic acid. However, the fetus is able to detoxify acetaminophen; the generation of the hepatotoxic metabolite still is a danger if mothers are uncovered to an excess amount (Taylor et al., 2012).

#### **1.5.2.6. Geriatric**

Management of acetaminophen does not need special dosage alteration in the aging. It is the favored pain-relieving by the American Geriatrics Society as the first line treatment for mild to reasonable musculoskeletal pain. In general, acetaminophen is usually considered a safe and tolerable pain-relieving in the elderly (Taylor et al., 2012).

### **1.6. Voltammetry methods**

The common characteristic of all voltammetry methods is that they include the application of a potential (E) on an electrode and the detection of the resulting current (I)

flowing through the electrochemical cell. In numerous cases, the applied potential is varied or the current is controlled for a period of time ( $t$ ). Consequently, all voltammetry methods can be described as a function of potential, current, and time ( $E$ ,  $I$ , and  $t$ ). The analytical benefits of the many voltammetry methods include the following: excellent sensitivity with the detectable concentration range of organic and inorganic species; a large number of beneficial solvents and electrolytes; a broad range of temperatures; fast analysis times (seconds); simultaneous determination of several analyses; the ability to decide kinetic parameters and evaluation unknown parameters; the ease with which different potential wavelength shapes can be produced; and the measurement of small currents (Simões and Xavier, 2016).

The potential sweep methods, also known as voltammetry methods, consist of the application of a potential changing always with time on a working electrode, which leads to the occurrence of oxidation or reduction reactions of electroactive species in the solution (faradaic reactions) in agreement with the adsorption of species with the potential and a capacitive current owing to the electrical double layer. The identified current is therefore different from the current in the steady state. These methods are usually utilized for the research of processes occurring in the working electrode and can be utilized with linear, pulse, and cyclic sweep, in addition to cyclic voltammetry (CV). Their main usage has been for the diagnosis of electrochemical reaction mechanisms for the identification of species present in solution, and for semi quantitative analysis of reaction speeds, and in addition to these applications, these methods are also widely utilized for the determination of kinetic and constant rates, the determination of adsorption processes in surfaces, the study of electron transfers and reaction mechanisms, the determination of thermodynamic properties of solvated species, necessary researches of oxidation and reduction processes in numerous ways, and the determination of complexation values and coordination (Simões and Xavier, 2016).

### **1.6.1. Cyclic voltammetry (CV).**

CV is utilized to understand and describe the redox characteristics, stability, and effective surface area of an electrode for biosensing. The active surface area of the

electrodes can be modified using conducting materials such as PEDOT: PSS and graphene, function as a transducer to change ions into measurable electrons. CV usually contains a three-electrode setup of a working electrode (WE), a reference electrode (RE), and a counter electrode (CE). In CV, a potential applied to the WE is swept back and forth for a defined number of cycles over a given range of voltage and speed of voltage sweep. As the potential is scanned across a specified potential range, the resulting current at the WE is measured. The current created is then plotted against potential to produce a CV graph that provides insights on the transducer material founded on the anodic peak current ( $I_{pa}$ ) from oxidation process and cathodic peak current ( $I_{pc}$ ) from reduction process which happen on the WE. The potentials at which the peak currents happen are known as peak potentials ( $E_p$ ). These top potentials help us to analyze the electrochemical reversibility of the reaction at the electrode surface by increasing the scan rates during experiments. Electrochemically reversible reactions frequently establish fast electron transfer between species and electrode when the electron transfer in irreversible reaction is slower (Ramli et al., 2018).

In a cyclic voltammogram, the most analyzed parameters are the following, Initial potential,  $E_i$  initial sweep direction, sweeping speed,  $v$  maximum potential,  $E_{max}$  minimum potential,  $E_{min}$  and final potential,  $E_f$ . CV can be utilized for quantitative determinations; owing to its limitations, however, it is more generally utilized for exploratory purposes, that is, to determine the redox process of different analytes. To minimize the contribution of the capacitive current and therefore increase the sensitivity of voltammetry methods, potential impulse (or pulse) methods were developed including pulse voltammetry and square wave voltammetry (SWV) (Simões and Xavier, 2016).

### **1.6.2. Electrochemical impedance spectroscopy (EIS)**

Electrochemical impedance spectroscopy (EIS) is a technique used in the analysis of electrochemical processes that occur in the electrode/electrolyte solution interface. This is a method of identification and determination of parameters from a model developed based on the frequency response of the electrochemical system under study. A frequency response analyzer coupled with an electrochemical interface is used in such experiments,

which measures the current response of the system as it changes the frequency of an input sinusoidal signal,  $E = E_0 \sin(\omega t = 2\pi f t)$ , that is applied to an unknown sample; the response is analyzed through a correlation with the resulting current  $I = I_0 \sin(\omega t + \varphi)$ , where  $\varphi$  is the phase angle displacement. The impedance ( $Z$ ) is the vector sum given by

$$Z = R - jX_c$$

Where  $j$  is equal to  $\sqrt{-1}$ , (Fourier)  $R$  is resistance,  $X_c$  is the capacitive reactance and equal to  $1/\omega C$  (measured in ohms) with  $\omega = 2\pi f$ , and  $C$  is the capacitance of the electric double layer. Therefore, it is noted that  $R$  is the real part ( $Z'$ ) and  $-jX_c$  is the imaginary part ( $Z''$ ) of the impedance. The complex impedance, represented by the displacement vector  $Z(\omega)$ , is obtained by changing the alternating signal  $\omega$ ; with these parameters, the modulus  $Z_0 = E_0/I_0$  and the phase angle  $\varphi$  can be calculated to determine the real and imaginary impedance values, as shown in Figure 1.14. An example of a simple equivalent circuit of an electrochemical cell, a resistor in parallel with a capacitor ( $R_c$ ), is depicted in Figure 1.15. The typical resulting spectrum is shown, consisting of a semicircle in the complex impedance plane, with the corresponding imaginary opposite  $Z'' = -\text{Im} = Z_0 \sin(\omega)$  conventionally represented on the y axis and the real component  $Z' = R$  and  $Z = Z_0 \cos(\omega)$  on the x axis. The frequency at the top of the semicircle indicates the resonance condition of the circuit, given by the expression  $2\pi f_0 RC = 1$ . Impedance spectroscopy is often used to study films deposited on electrodes because it can distinguish the different conductivity processes that occur in the material. The results are often associated with an electrical circuit, in which it is possible to distinguish and calculate parameters, such as the electrolyte resistance, ionic conductivity, capacitance of the electrical double layer, and electron transfer resistance (Simões and Xavier, 2016).

EIS has the ability to study any intrinsic material property or specific processes that could influence the conductivity/resistivity or capacitance of an electrochemical system. Therefore, EIS is a useful tool in the development and analysis of materials for biosensor transduction, such as the study of polymer degradation. A recent example of electrochemical EIS was its use to characterize the fabrication process of a hydrogen peroxide (HRP) biosensor (Grieshaber et al., 2008).



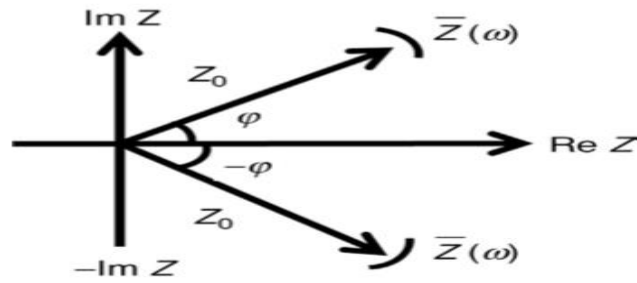


Figure 1.14. Vector representation of the complicated impedance  $Z$  (Simões and Xavier, 2016).

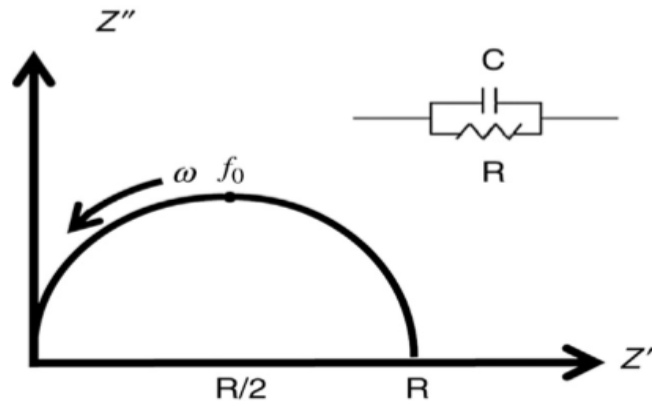


Figure 1.15. Schematic representation of a parallel RC circuit's impedance analysis reaction (Simões and Xavier, 2016)

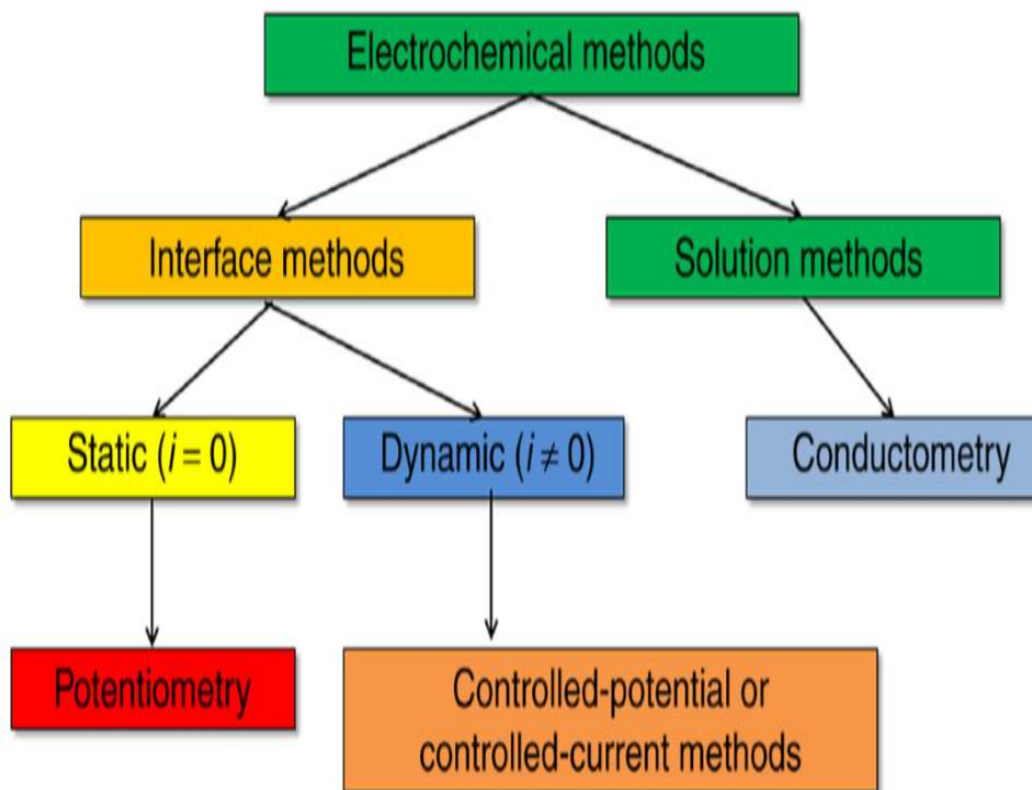


Figure 1.16. Most important electrochemical techniques and their subdivisions. (Simões and Xavier, 2016).

## 2. LITERATURE REVIEW

In recent years, promising results have been obtained with the use of metal and semiconductor nanoparticles for the construction of electrochemical sensors. Single or multilayered layouts of conductive nanoparticles distributed on the electrode surface can be measured as clusters of controllable active regions of nanostructures. The catalytic activity of metal and semiconductor nanoparticles can reduce the extreme potential of some significant reactions in electrochemical analysis and may even offer the electrochemical

transformation of redox reactions that are irreversible in conventional bulk electrodes and occasionally improve electrochemical responses.

Graphene has been a favorable material due to its 2-dimensional layered structure. The two-dimensional stratified structure of graphene ensures a wide surface area. Also, there are carboxyl, hydroxyl and epoxy groups on the graphene oxide. These groups facilitate the binding of functional groups to the graphene. In addition, these groups help to bind biomolecules such as enzymes on the electrode. So far, many nano composites with graphene oxide and reduced graphene oxide have been obtained. Here are some of the studies on electrochemical paracetamol sensor.

So far, many components have been used for the determination of paracetamol by electrochemical methods. For example, Pt nanoparticles nitrogen doped graphene (Pt / NGr) was synthesized. Electrochemical impedance spectroscopy (EIS), cyclic voltammetry (CV) and square-wave voltammetry (SWV) were utilized to evaluate the electrochemical behavior of Pt/NGr on the modified working electrode. According to the results, Pt/NGr modified electrode determined paracetamol linearly between 0.05-90  $\mu\text{mol L}^{-1}$  and the observable limit (LOD) value was determined as 0.008  $\mu\text{mol L}^{-1}$ . In addition, it was determined that the sensor had acceptable repeatability, stability and selectivity (Anuar et al., 2018).

In another study, a composite containing  $\text{Cu}_2\text{O}$  and graphene (GR) was synthesized to modify the glassy carbon electrode (GCE) with the  $\text{Cu}_2\text{O}$ -GR component to prepare a working electrode and use it for the electroanalytical determination of paracetamol. XPS, EIS and SEM were used for the characterization of the composite. In order to investigate the electrochemical oxidation of paracetamol on  $\text{Cu}_2\text{O}$ -GR/GCE, cyclic voltammetry and square-wave voltammetry were utilized. Paracetamol on the  $\text{Cu}_2\text{O}$ -GR / GCE working electrode was determined linearly between  $2.0 \times 10^{-8}$  and  $1.3 \times 10^{-6}$  M and the LOD of paracetamol was  $6.67 \times 10^{-9}$  M. The sensitivity of the sensor was  $14,397.7 \mu\text{A mM}^{-1} \text{cm}^{-2}$ . Stability of the sensor was determined to be satisfactory under the optimum conditions (Yang et al., 2015).

Yu and his colleagues have synthesized reduced graphene oxide (RGO) Au dendrite composite. The structure of the composite is illuminated by scanning electron microscope, energy dispersive x-ray spectroscopy, UV visible region spectroscopy, X-ray diffraction,

Raman spectroscopy, and X-ray photoelectron spectroscopy. It has been discovered that the RGO-Au dendrite composite increases its stability, catalytic activity and stability for the electrocatalytic oxidation and determination of paracetamol. The sensor obtained using the RGO-Au dendrite composite was able to determine the paracetamol linearly between 0.07-3000  $\mu\text{M}$  and the sensor's limit of detection being able to observe the paracetamol was found to be 0.005  $\mu\text{M}$ . In addition, using the RGO-Au dendrite, the selectivity of paracetamol in tablets and urine was investigated (Yu et al., 2018).

In another study, a working electrode was prepared for the electrochemical determination of paracetamol and 4-aminophenol utilizing the Au/Pd/RGO composite. Scanning electron microscopy, X-ray photoelectron spectroscopy and Fourier transform infrared spectroscopy were utilized for description of Au/Pd/RGO composite. Experimental studies have shown an acceptable electrocatalytic activity against redox reactions of paracetamol and 4-aminophenol on the Au/Pd/RGO composite. The linear detection interval for paracetamol was determined as 1.00-250.00  $\mu\text{M}$ , and 4-aminophenol linear determination range was 1.00-300.00  $\mu\text{M}$ . The limit of detection for paracetamol was 0.3  $\mu\text{M}$  and the limit of detection for 4-aminophenol was 0.12  $\mu\text{M}$ . Bimetallic nanocomposites generally increase the sensitivity of the sensor to the analyte because of the synergistic impact between metal nanoparticles (Wang et al., 2018).

Bimetallic Pd-Ag/RGO nanocomposite is a satisfactory composite in sensor preparation due to its wide electroactive surface area, rapid electron transfer and numerous action regions. Due to its strong synergistic effect, Pd-Ag/RGO nanocomposite has shown good electrocatalytic activity for the determination of etilefrine and paracetamol. After the optimization studies, the linear determination range of the sensor for paracetamol was  $9.9 \times 10^{-6}$  -  $4.3 \times 10^{-5}$   $\text{mol dm}^{-3}$  and the linear determination range for ethylphrine was  $2.7 \times 10^{-4}$  -  $5.6 \times 10^{-4}$   $\text{mol dm}^{-3}$ . In addition, these drugs were tested in the blood serum using a sensor based on Pd-Ag/RGO (Reddy et al., 2018).

In a study by Armada and colleagues, the working electrode was modified using Pt nanoparticles and ferrocene functional third generation dendrimers to obtain amperometric paracetamol sensor. The catalytic synergy between ferrocene groups and Pt nanoparticles is ascribed to the formation and properties of ferrocenyl dendrimers. It has been found that the modified electrodes response to the electrocatalytic oxidation of paracetamol was

excellent. Excessive potential for oxidation of paracetamol at pH 7 has been reduced and flow response has been significantly increased. The working electrode obtained under optimum conditions showed 5 linear ranges in the oxidation of paracetamol. The first one was found to be 0-100  $\mu\text{M}$ , the second one was 0.1-1.0 mM, the third was 1.0-4.0 mM, the fourth was 4.0-10.0 mM and the fifth was 10.0-17.0 mM (Armada et al., 2016).

The electrode based on GA@O-CQDs was synthesized in a study by Ruiyi and his colleagues, and the electrode was utilized to evaluate the differential pulse voltammetry of acetaminophen, the best peak potential was 0.15 V (vs. Ag / AgCl). Merit figures consists of a wide linear reply range (0.001–10 $\mu\text{M}$ ) and a limit of detection of 0.38 nM (S / N=3). The sensor was utilized to determine acetaminophen in tablets (Ruiyi et al., 2018).

Acetaminophen's electrochemistry in phosphate buffer solution (pH 8) was studied using cyclic voltammetry, hydrodynamic voltammetry, and amperometric flow injection on a thin film electrode with boron-doped diamond (BDD). Cyclic voltammetry has been utilized as a function of analyte concentration to study the reaction. A polished glassy carbon (GC) electrode was used to perform the comparison of the experimental results. At both of these electrodes, acetaminophen undergoes a quasi-reversible reaction. The BDD and GC electrodes provided well-resolved cyclic voltammograms, but the voltammetric signal-to-background ratios of the diamond electrode were higher than those of the GC electrode. The diamond electrode provided a linear dynamic range of 0.1 to 8 mM and a voltammetric measurement determined LOD of 10  $\mu\text{M}$  (S/B = 3). The results of the diamond electrode flow injection analysis detected a linear dynamic range from 0.5 to 50 M and a 10 nM detection limit based on S/N $\approx$ 4. Acetaminophen was also investigated in syrup specimens. Results from the recovery study (24,68  $\pm$  0.26 mg/mL) were similar to those labeled (24 mg/mL) (Wangfuengkanagul Chailapakul, 2002).

In another study, the electrode modified with the Pd/GO and its electrochemical sensing performance to paracetamol were assessed utilizing electrochemical impedance spectroscopy (EIS), cyclic voltammetry (CV) and differential pulse voltammetry (DPV). The experimental results indicate that the as-synthesized Pd nanoparticles are relatively uniform in size (5–10 nm) without large collection and uniformly dispersed in the carbon matrix with the overall Pd content of 28.77 wt percent in Pd/GO. Compared with the GO-modified electrode, the modified Pd/GO electrode reveals better electrocatalytic activity for

paracetamol oxidation with lower oxidation potential and higher peak current, so that the Pd/GO nanocomposite can be used as an enhanced sensing platform for paracetamol electrochemical determination. The paracetamol electro-oxidation kinetic parameters at the Pd/GO electrode were studied in detail after optimizing the determination conditions. The oxidation peak current is linear in the ranges of 0.005-0.5  $\mu\text{M}$  and 0.5-80.0  $\mu\text{M}$  with a detection limit of 2.2 nM under optimal conditions. Based on the high sensitivity and good selectivity of the modified Pd/GO electrode, the proposed method has been successfully applied to the determination of paracetamol in commercial tablets and human urine, and the satisfactory results confirm the practical applicability of this sensor (Li et al., 2014).

In one study, the fabricated Ti/AuNi NPs modified electrode showed exceptional direct-electrochemical oxidation of acetaminophen through developed load carrier mobility and easy electron transfer interface. The Ti/AuNi NPs electrode has an electrocatalytic activity of  $\sim 2.5$  and  $\sim 1.9$  times higher than that of Ti/Ni NPs and Ti/Au NPs electrodes. The amperometric acetaminophen sensor planned in this research shows a high sensitivity ( $0.2 \mu\text{A nM}^{-1} \text{cm}^{-2}$ ) with a 0.99 correlation coefficient ( $R^2$ ) and a wide linear range (0.0 - 1.75  $\mu\text{M}$ ) with the lowest calculated sensor limit (0.51 nM (S / N=3)). The electrode of Ti/AuNi NPs exhibits a negligible reply from common interferences like glucose, lactose, and glycine. The practical ability of the developed acetaminophen sensing system in human serum samples revealed that the AuNi NPs-based acetaminophen sensor has big potential in the pharmaceutical, quality control, and clinical laboratory fields (Maduraiveeran et al., 2018b).

In a study carried out by Adhikari and his colleagues, a high-role electrochemical sensor for sensitive determination of acetaminophen based on graphene was simultaneously electrochemically reduced and deposited on a glassy carbon electrode (GCE). The electrocatalytic properties of electrochemically reduced graphene (ERG) analyzed for oxidation of acetaminophen were analyzed via cyclic voltammetry (CV), differential pulse voltammetry (DPV) and chronoamperometry. For comparison, various ERG/GCEs were prepared with different electrodeposition cycles to optimize the amount of the ERG. Our experimental outcomes indicated that the optimized ERG/GCE had robust activity in the detection of acetaminophen's electrochemical oxidation, leading to the development of highly sensitive electrochemical sensors. By combining amperometric technique and DPV,

an extremely low detection limit of 2,13 nM and a broad linear determine range of 5,0 nM to 800  $\mu\text{M}$  were obtained. The developed electrochemical sensor was also utilized to determine acetaminophen in human serum, with excellent recovery from 96.08% to 103.2%. The Fabricated electrochemical sensor also showed high selectivity, stability and reproducibility. The broad linear detection range achieved in this research for the detection of acetaminophen showed strong potential as a promising sensing technique for pharmaceuticals, in terms of quality control and in acetaminophen clinical laboratories as it associates to hepatotoxicity determination (Adhikari et al., 2015).

In another study, an easy and new preparation strategy was developed based on electrochemical methods for the manufacture of nanocomposite electrodeposited graphene (EGR) and zinc oxide (ZnO). In the meantime, nanocomposite electrochemical performance with cyclic voltammetry (CV) and electrochemical impedance spectroscopy (EIS) has been performed. An ultrasensitive electrochemical sensor for acetaminophen (AC) and phenacetin (PCT) was successfully manufactured following the synergistic impact of EGR and ZnO nanoparticles. Linearity ranged from 0.02 to 10  $\mu\text{M}$  with high sensitivity of 54295.82  $\mu\text{A mM}^{-1} \text{cm}^{-2}$  for AC. In addition, the practical applicability in pharmaceutical detections has been validated to be dependable and desirable (Jiang et al., 2014).

Phosphorus-doped graphene (P-RGO) has been synthesized and utilized to fabricate electrochemical sensors for acetaminophen (AP) as active electrode material. The P-RGO coated glassy carbon electrode (P-RGO / GCE) exhibited excellent electrocatalytic activity for AP oxidation, resulting from highly advanced electrochemical conductivity and accelerated transfer of electron. The experimental conditions for AP determination were optimized and a linear relationship between current intensity and AP concentration with a detection limit of 0.36  $\mu\text{M}$  (S/N= 3) was achieved under the optimal condition. In the presence of different common species, the developed sensor exhibited high selectivity for AP, excellent reproducibility and stability. In pharmaceutical tablet samples, the current sensor has also been successfully applied for AP detection (Zhang et al., 2018).

In an article, the preparation of  $\text{Fe}_3\text{O}_4/\text{rGO}$ -based electrode and some factors influencing voltammetric responses were examined. The outcomes revealed that  $\text{Fe}_3\text{O}_4/\text{rGO}$  is a potential electrode material for paracetamol detection by differential pulse-

anodic stripping voltammetry (DP-ASV) with a low limit of detection. The interfering impact of uric acid, ascorbic acid, and dopamine on the current reply of paracetamol has been reported. The repeatability, reproducibility, linear range, and limit of detection were also addressed. The proposed sensor was applied to the real samples with satisfactory outcomes. (Thu et al., 2018).

In another study, cobalt hexacyanoferrate (CoHCF) stable electro-active thin film was deposited on the surface of an amine-adsorbed graphite wax compound electrode utilizing a simple method. Cyclic voltammetric experiments exhibited two pairs of well-defined peaks for this modified CoHCF electrode with excellent electrocatalytic properties for paracetamol oxidation at a reduced overpotential of 100 mV and a concentration range of  $3.33 \times 10^{-6}$  to  $1.0 \times 10^{-3}$  M with a good sensitivity slope of  $0.208 \mu\text{A}/\mu\text{M}$ . The immobilized CoHCF maintained its redox activity showing a surface-controlled electrode reaction with an electron transfer rate constant (Ks) of  $0.94 \text{ s}^{-1}$  and a charge transfer coefficient of 0.42. The usefulness of the modified electrode in dynamic systems was explored by hydrodynamic and chronoamperometric studies. To determine paracetamol in commercially available tablets, differential pulse voltammetry (DPV) were applied utilizing the modified electrode. The results show that the electrode can be used as an effective sensor for paracetamol monitoring (Prabakar and Narayanan, 2007).

In this research, the electrochemical sensor depending on Pd-Ag/rGO demonstrates good electrocatalytic performance in determining etilefrine (ET) and acetaminophen (AC) due to the synergistic impact of the bimetallic Pd-Ag/rGO nanocomposites. The individual peaks of ET and AC could be identified with increased of their concentration. The linear response ranges were  $2.7 \times 10^{-4}$  -  $5.6 \times 10^{-4} \text{ mol dm}^{-3}$  and  $9.9 \times 10^{-6}$  -  $4.3 \times 10^{-5} \text{ mol dm}^{-3}$ , respectively with a detection limit of 0.139 and 0.256  $\text{mol dm}^{-3}$ , the validity of the proposed sensor was assessed through its application in real specimens (Bathinapatla et al., 2018).

In this study, an electroanalytical method was developed for the direct quantitative determination of paracetamol (or acetaminophen) in tablet dosage forms depending on its oxidation behavior. The electrochemical oxidation and determination of paracetamol were simply carried out on glassy carbon electrode (GCE) utilizing a variety of voltammetric techniques. The electrochemical measurements were carried out on GCE in different types



of buffer solutions in the pH range from 0.51 to 12.00 by cyclic voltammetry (CV) and differential pulse voltammetry (DPV) techniques. The dependence of pH on the anodic peak current and peak potential was examined. Acetate buffer (pH 4.51) was determined for analytical purposes. Scan rate researches were also completed. The diffusion-controlled nature of the peak was established. A linear calibration curve for DPV analysis was obtained in the paracetamol concentration range from  $4 \times 10^{-6}$  mol/L to  $1 \times 10^{-4}$  mol/L. Limit of detection (LOD) and limit of quantification (LOQ) were achieved as  $3.69 \times 10^{-7}$  mol/L and  $1.23 \times 10^{-6}$  mol/L, respectively. Validation of applied voltammetric techniques was checked with recovery measurements. (Engin et al., 2015).

A composite of poly (3,4-ethylenedioxythiophene)/graphene oxide (PEDOT/GO) was synthesized by monomer and GO in situ potentiostatic polymerization without additional dopants to alter the surface of the glassy carbon electrode. TEM, Raman spectra and XPS characterized the morphology and structure of PEDOT/GO compound film. The compound prepared exhibited excellent electro-catalytic activity towards the acetaminophen redox. Film construction and operational pH were optimized and the determination of AP was based on easy, sensitive and cyclic voltammetry procedure. With a detection limit of 0.57  $\mu$ M, the calibration curve was obtained. The selectivity and stability of the sensor based on PEDOT/GO modified electrode is satisfactory (Si et al., 2014).

Afkhami and his colleagues synthesized the nanocomposites based on graphene (Gr) and  $\text{CoFe}_2\text{O}_4$  with an easy preparation method in order to produce a modified carbon paste electrode. Scanning electron microscopy (SEM) and X-ray diffraction (XRD) investigated the morphology and structure of Gr/ $\text{CoFe}_2\text{O}_4$  nanocomposite. With electrochemical impedance spectroscopy, electrochemical characterization of the nanocomposite was also investigated. An ultrasensitive electrochemical sensor for acetaminophen and codeine (Cod) was successfully fabricated on the basis of the synergistic effect of nanoparticles Gr and  $\text{CoFe}_2\text{O}_4$ . The linearity for both Ac and Cod ranged from 0.03 to 12.0  $\mu$ M. Based on three times the standard deviation of the blank over sensitivity (3 S/N), low detection limits of 0.025  $\mu$ M for Ac and 0.011  $\mu$ M for Cod were achieved. The method proposed was free of glucose, ascorbic acid, caffeine, naproxen, alanine, phenylalanine, glycine, and other interference effects. During successive scans, no electrode surface fouling was observed. High stability, high sensitivity and low detection limit made the electrode proposed for the

analysis of different real samples application. In addition, its practical applicability in biological fluids and analysis of pharmaceutical samples was reliable and desirable (Afkhani et al., 2014).

For the simultaneous determination of PA and caffeine (CAF), Habibi and his colleagues developed carbon-ceramic electrode (CCE) modified a thin film of single-walled carbon nanotubes (SWCNT). Compared to bare CCE, the SWCNT/CCE showed excellent electrochemical catalytic activity for PA and CAF oxidation. In DPV technique, both PA and CAF give sensitive oxidation peaks at 0.71 and 1.38 V vs. saturated calomel electrode, and in optimized experimental conditions PA and CAF show linear response over concentration ranges of 0.08-200.0  $\mu\text{M}$  ( $R^2 = 0.991$ ) and 0.41-300.0  $\mu\text{M}$  ( $R^2 = 0.990$ ), respectively. The detection limits ( $S/N = 3$ ) for PA and CAF were 0.05 and 0.29  $\mu\text{M}$ , respectively. In some real samples, the investigated method demonstrated good stability, reproducibility, repeatability and high recovery (Habibi et al., 2014).

The layer self-assembly technique was used for preparation an electrochemical sensor of acetaminophen based on poly(diallyldimethylammonium chloride) (PDDA)-functional reduced graphene-loaded  $\text{Al}_2\text{O}_3$  – Au nanoparticles coated on glass carbon electrode ( $\text{Al}_2\text{O}_3$ -Au/PDDA/reduced graphene oxide (rGO)/glass carbon electrode (GCE). Scanning electron microscopy, X-ray powder diffraction, and Fourier transform infrared spectroscopy were used for characterization of the as prepared electrode-modified materials. Cyclic voltammetry and differential pulse voltammetry were utilized to investigate the electrocatalytic performance of  $\text{Al}_2\text{O}_3$ -Au/PDDA/rGO-modified glassy carbon electrode toward acetaminophen. To compare and learn the catalytic mechanism, the modified electrodes of graphene oxide (GO)/GCE, PDDA/rGO/GCE and  $\text{Al}_2\text{O}_3$ -Au/PDDA/rGO/GCE were prepared. The research showed good electrochemical performance of  $\text{Al}_2\text{O}_3$ -Au/PDDA/rGO/GCE, attributing to the synergetic effect of  $\text{Al}_2\text{O}_3$ -Au nanoparticles and graphene's special nanocomposite structure and physicochemical properties. It was obtained a low detection limit of 6 nM ( $S/N=3$ ) and a wide linear detection range of 0.02 to 200 $\mu\text{M}$  ( $R^2 = 0.9970$ ). For the detection of acetaminophen in commercial pharmaceutical pills, the sensor was successfully applied (Li et al., 2016).

An electrochemical sensor based on a glass carbon electrode modified by cadmium pentacyanonitrosylferrate (CdPCNF) was fabricated for electrocatalytic oxidation of PA.

The modified GC electrode's electrocatalytic response was linear over 1.64 - 52.90  $\mu\text{M}$ . By amperometric technique, the detection limit was found to be 2.04  $\mu\text{M}$ . The method was successfully used in various pharmaceutical examples to determine PA and the results were compared statistically with those obtained by the official method. Some pharmaceutical and biological compounds have been investigated for interference. The results of the interference study showed that the Nafion-coated CdPCNF electrode can be used for the determination of acetaminophen in human blood serum as a selective amperometric sensor. In the phosphate buffer solution of pH 7.2, the mean values of the rate constant value of  $k$  and the diffusion coefficient were found to be  $4.27 \times 10^2 \text{ M}^{-1} \text{ s}^{-1}$ , and  $(4.25 \pm 0.33) \times 10^{-6} \text{ cm}^2 \text{ s}^{-1}$ , respectively (Razmi and Harasi, 2008).

In this study, Teradale and his colleagues investigated the electrochemical behavior of paracetamol (PA) with carbamazepine (CBZ) film-coated carbon paste electrode in pH 7.4 0.2 M PBS by cyclic voltammetric technique. The modified electrode exhibited good electrochemical activity towards paracetamol oxidation, resulting in a noticeable improvement in peak currents and feasible oxidation compared to the electrode of bare carbon paste. Under optimal experimental conditions, the electrochemical response to PA was linear with a detection limit of 0.24  $\mu\text{M}$  by cyclic voltammetric technique in the concentration range from  $1.0 \times 10^{-4} \text{ M}$  to  $3.94 \times 10^{-4} \text{ M}$ . The modified electrode demonstrated good sensitivity, long-term stability, reproducibility. Finally, the proposed method for determining PA in pharmaceutical samples has been successfully applied (Teradale et al., 2018).

In another work, the use of multi-walled carbon nanotubes (MWCNTs) and fourth generation poly (amidoamine) dendrimers (G4.0 PAMAM) was reported as an electrochemical sensor for the detection of paracetamol (PA). The strategy of this work is to establish a stable covalent connection between carboxylated MWCNTs and amine-ended G4.0 PAMAM via covalent layer-by-layer (LbL) self-assembly, which provides larger surface areas for efficient adsorption of PA. The prepared electrode was characterized first by Fourier transforming infrared spectroscopy and scanning electron microscopy, and then by cyclic voltammetry, electrochemical impedance spectroscopy and chronocoulometry, the electrochemical behavior of PA on (MWCNTs-G4.0)/GCE was investigated in detail. The experimental results showed that the fabricated sensor had excellent catalytic activity

towards PA under optimal conditions, and a wide linear range of  $3.0 \times 10^{-7}$  to  $2.0 \times 10^{-4}$  M was obtained with a detection limit (LOD) of  $1.0 \times 10^{-7}$  M (S/N= 3). In addition, it could also be applied to the determination of PA in commercial tablets and human serum, and the satisfactory results confirm the practical analysis applicability of this sensor (Zhang et al., 2016).

In another study, an easy and sensitive nanocomposite sensor was developed using glycine (Gly) electro polymerization on the surface of a glassy carbon electrode (GCE) using cyclic voltammetry (CV) followed by multi-walled carbon nanotubes (MWCNTs) drop casting. An electrochemical impedance spectroscopy (EIS) technique was used to characterize the developed nanocomposite sensor (MWCNTs/poly(Gly)/GCE). The developed nanocomposite sensor offered high catalytic activity in the individual and simultaneous sensing of paracetamol (PA) in the presence of dopamine (DA) and folic acid (FA). The detection limit (LOD) and quantification limit (LOQ) were found to be  $5 \times 10^{-7}$  M and  $1.7 \times 10^{-6}$  M with a dynamic range of  $5 \times 10^{-7}$  to  $1 \times 10^{-5}$  M, respectively. With a relative standard deviation of 1.28%, the manufactured sensor showed good precision and accuracy. The proposed sensor has been successfully applied in human blood serum and pharmaceutical samples to determine PA (Narayana et al., 2014).

In this study, two different types of electrodes, boron-doped diamond electrode (BDD) and boron-doped carbon nanowalls (B:CNW) electrode were used for the electrochemical determination of paracetamol using cyclic voltammetry and differential pulse voltammetry in phosphate buffered solution (pH = 7.0). The main benefit of these electrodes is their use without any further modification of the surface of the electrode. The peak current for BDD electrode was linearly related to the concentration of paracetamol in the range of 0.065  $\mu$ M to 32  $\mu$ M and for B: CNW electrode of 0.032  $\mu$ M to 32  $\mu$ M. The detection limit for BDD and B: CNW electrode was 0.430  $\mu$ M and 0.281  $\mu$ M, respectively. In addition, in Britton-Robinson buffer solution, the effect of pH on the redox reaction of paracetamol in the range of pH 3.0–12.0 was investigated. The results indicate that the pH value of 7.0 was the most suitable for the determination of PA. Also, studies present the effect of the scan rate (50–500 mV/s) on the sensor response. The selected B:CNW electrode exhibited the detection limit at 0.08006  $\mu$ M (Niedzialkowski et al., 2019).

The use of unmodified boron-doped diamond electrode for the determination of dopamine (DA) and paracetamol (PA) in biological samples and pharmaceutical preparations using differential pulse voltammetry was also demonstrated in the present work. Wide linear range of calibration graphs: from  $1 \times 10^{-7}$  to  $2 \times 10^{-4}$  mol L<sup>-1</sup> for DA and PA with very low detection limits, equivalent to  $1.87 \times 10^{-8}$  mol L<sup>-1</sup> for DA and  $1.35 \times 10^{-8}$  mol L<sup>-1</sup> for PA, respectively. The proposed sensor was successfully used to determine paracetamol in children's syrups, and to determine paracetamol and dopamine simultaneously in blood and serum samples (Tyszczyk-Rotko et al., 2019).

In this study, Au@graphene (AG) core-shell nanoparticles with high conductivity, catalytic activity and stability were synthesized and doped into PEDOT by an easy method of electrodeposition. The PEDOT/AG composite showed high conductivity and excellent catalytic activity towards paracetamol redox and significantly improved electrochemical signals and paracetamol peak profiles at the modified electrode with PEDOT/AG due to the presence of AG nanoparticles. Under optimum conditions, the modified electrode PEDOT/AG exhibited high paracetamol sensitivity over a wide linear range of concentrations from 0.15  $\mu$ M to 5.88 mM, with a detection limit of 41 nM (S/N= 3). In addition, the manufactured sensor showed high selectivity and long-term stability and was able to detect paracetamol with satisfactory accuracy in real pharmaceutical samples (Li et al., 2018).



### **3. MATERIALS AND METHODS**

#### **3.1. Materials and Apparatus**

Graphite powder, paracetamol, dopamine (DA),  $\text{Pd}(\text{NO}_3)_2 \cdot 2\text{H}_2\text{O}$ , nafion (Nf) solution (5% in a mixture of aliphatic alcohols and water), KCl, glucose, ascorbic acid (AA), uric acid (UA), folic acid (FA), mannose (Man), and histidine (His) were purchased from Sigma-Aldrich<sup>®</sup>. Ethanol,  $\text{ClCH}_2\text{COOH}$ ,  $\text{NaBH}_4$  and all other chemicals were attained from Merck<sup>®</sup>. Autolab PGSTAT128N potentiostat/galvanostat with optional FRA 32M was utilized for electrochemical experiments. Fourier transform infrared spectroscopy (FTIR), high-resolution transmission electron microscopy (TEM, JEOL JEM 2100), and X-ray diffractometer (XRD, Bruker D8 Advance) were utilized for the characterization of the compounds. Glassy carbon electrode (GCE), Ag/AgCl (3 M KCl) electrode, and platinum (Pt) wire electrode were bought from BASi Corporation and utilized as working, reference, and counter electrodes, correspondingly. Deionized water was acquired from GFL 2108 double distillation water still and utilized for all the experimental procedures.

## **3.2. Methods**

### **3.2.1. Synthesis of graphene oxide (GO)**

GO was synthesized utilizing Hummer's method with relatively some changes such as the amount of compounds and reaction time (Dikin et al., 2007; Guler et al., 2018). Firstly, 1 g graphite powder, 1 g  $\text{NaNO}_3$ , and 25 mL of 98%  $\text{H}_2\text{SO}_4$  were placed in a beaker fixed in an ice bath. The combination was blended to 2 hours. Secondly, 3 g  $\text{KMnO}_4$  was gradually added to the combination and blended for 2 days at  $35 \pm 3^\circ\text{C}$ . Formerly, it was diluted utilizing 125 mL of deionized water and stirred for another 30 minutes at  $98^\circ\text{C}$ . Thirdly, to complete the reaction, 2.5 mL of 30% of  $\text{H}_2\text{O}_2$  was added to the reaction. The final blend was filtered and the achieved precipitate was dissolved in 125 mL of 10% HCl. It was stirred ultrasonically for 2 hours and filtered again. Lastly, the precipitate was dissolved in deionized water and centrifuged to 20 minutes at 8000 rpm. The centrifugation process was repeated for few times till the pH of the filtrate was neutral. The gotten GO was dried in a vacuum oven at  $60^\circ\text{C}$ .

### **3.2.2. Synthesis of carboxylated graphene oxide (GO-COOH)**

For synthesis of GO-COOH, 2 g GO and 4g of KOH were put into a round-bottom flask including 25 mL bidistilled water. The blend was refluxed for 2 hours to get a clear suspension. Formerly, 3g ClCH<sub>2</sub>COOH dissolved in 6 mL of bidistilled water was added to the combination. The final mixture was stirred for 24 hours. Formerly, it was filtrated and the precipitate was washed utilizing bidistilled water (3x20 mL) and ethanol absolute (3x20 mL), individually. Lastly, the acquired GO-COOH was dried in the vacuum oven at 70 °C (Zhao and Liu, 2014).

### **3.2.3. Synthesis of carboxylated graphene oxide palladium nanoparticles (GO-COOPd)**

For preparation of GO-COOPd compound, 60 mg of GO-COOH was added to a circular bottom flask containing 5 mL bidistilled water. The blend was ultrasonically stirred for 30 minutes to get a homogeneous dispersion. Subsequently, 26.52 mg (0.1 mmol) of Pd(NO<sub>3</sub>)<sub>2</sub>.2H<sub>2</sub>O was added to the mixture. The subsequent mixture remained stirred for 3 h in laboratory temperature (25 °C), and 56.46 mg (1.49 mmol) of NaBH<sub>4</sub> melted in 1 mL bidistilled water was place into the blend. The final mixture remained stirred for few times to complete the reduction procedure. Lastly, the blend was filtrated and washed with bidistilled water (3x20 mL) and ethanol (3x20 mL), correspondingly, and dried in the vacuum oven at 80 °C for 3h (Guler et al., 2017).

### **3.2.4. Synthesis of graphene oxide palladium nanoparticles (Pd@GO)**

For preparation of Pd@GO composite, the same way selected for carboxylated graphene oxide palladium nanoparticles was used. Thus, 60 mg of GO was added to a circular bottom flask containing 5 mL bidistilled water. The blend was ultrasonically stirred for 30 minutes to get a homogeneous mixture. Subsequently, 26.52 mg (0.1 mmol) of Pd(NO<sub>3</sub>)<sub>2</sub>.2H<sub>2</sub>O was added to the mixture. The consequential mixture was stirred for 3 hours in laboratory temperature (25°C), and 56.46 mg (1.49 mmol) of NaBH<sub>4</sub> dissolved in 1 mL bidistilled water was put into the mixture. The final combination was stirred for some times until the reduction was completed. Lastly, the blend was filtrated and washed with



bidistilled water (3x20 mL) and ethanol (3x20 mL), correspondingly, and dried in the vacuum oven at 80 °C for 3h (Guler et al., 2017).

### 3.2.5. Preparation of GO-COOH and GO-COOPd modified electrodes

Before modification, GCE was cleaned with alumina slurry, sonicated in nitric acid/water (1:1), and ethanol for 5 min, correspondingly, until a mirror similar to surface was achieved, and dried in laboratory conditions for further experiments. 2 mg of GO-COOPd was added to 1 mL ethanol and the mixture was ultrasonically distributed to get a homogeneous suspension. Afterward, 5  $\mu$ L of the distribution was drop-casted on the GCE, and dried in laboratory temperature ( $25 \pm 2$  °C) to get GO-COOPd/GCE working electrode. 3  $\mu$ L of nafion (Nf) solution (0.2% in ethanol) was loaded on the electrode surface to get the desired working electrode of Nf/GO-COOPd/GCE. Nf/GO/GCE, Nf/Pd@GO/GCE, and Nf/GO-COOH/GCE was prepared utilizing the same procedures.

### 3.2.6. Electrochemical studies

After preparing the materials, they were characterized using FTIR, XRD, XPS, SEM, TEM, and EDX. The determined GO-COOH and GO-COOPd composites was utilized to modify the active surface zone of the working electrode. EIS and CV methods were used to determine the conductivity of the prepared electrodes, the response to paracetamol and the active surface areas of the electrodes.  $[\text{Fe}(\text{CN})_6]^{3-/4-}$  and KCl compounds was utilized to determine the active surface areas and the conductivities of the modified electrodes. Phosphate buffers solution (PBS) with different pH values (4.5 - 9.0) was prepared to determine the optimum pH response of the working electrode to paracetamol. Then, using the CV method, the best pH value was determined by which the sensor response was the best to paracetamol. A linear graph for paracetamol was obtained by using amperometry. The sensitivity, limit of detection (LOD) and limit of quantification of the sensor was also determined. For the reproducibility of the sensor, different measurements were made with the same electrode, and the standard deviation (SD) and relative standard deviation (RSD) was obtained. As in repeatability measurements, in the reproducibility studies, the standard deviation (SD) and relative standard deviation (RSD)

was calculated by using different working electrodes. The storage stability of the sensor for the determination of paracetamol was evaluated. As it is known, composites such as ascorbic acid, dopamine, and uric acid are electrochemically active compounds. These compounds may affect the correct determination of the analyte by demonstrating an interference effect at the studied potentials. Therefore, the effects of this type of interfering substances on the paracetamol response of the sensor was investigated in our study.

### **3.2.7. Determination of paracetamol (PA) in human serum samples**

After the necessary optimization parameters were obtained, The Nf/GO-COOPd/GCE modified electrode was utilized for the determination of PA in human serum samples. For this, serum sample was obtained from Faculty of Medicine, Yüzüncü Yil University, Van, Turkey. The sample was centrifugated (4000 rpm, 20 min) and diluted 20 times utilizing 0.1 M PBS (pH 7.5). Then, the sample was divided into six portions. The first portion did not contain PA and the others were spiked with various concentrations of PA (5, 50, 100, 140, and 160  $\mu\text{M}$ ). The PA concentrations in these samples were determined using standard addition method.

## **4. RESULTS**

### **4.1. Characterization of GO-COOH and GO-COOPd**

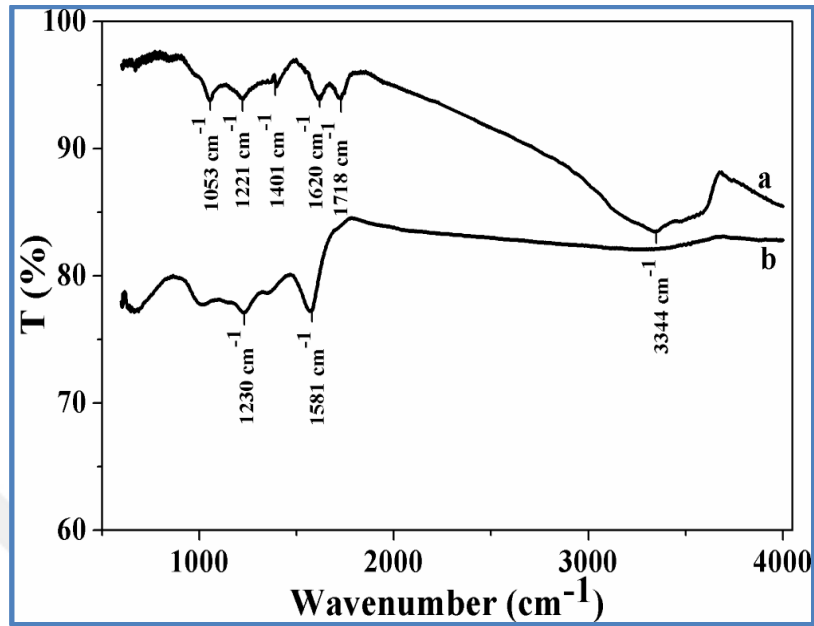


Figure 4.1. GO (a) and GO-COOH (b) FTIR spectra.

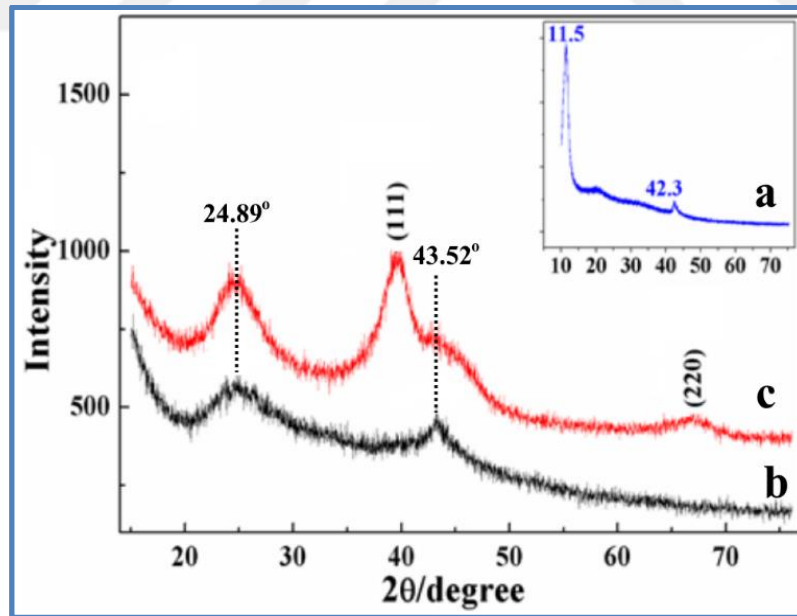


Figure 4.2. XRD graph of GO (a), GO-COOH (b) and GO-COOPd (c).

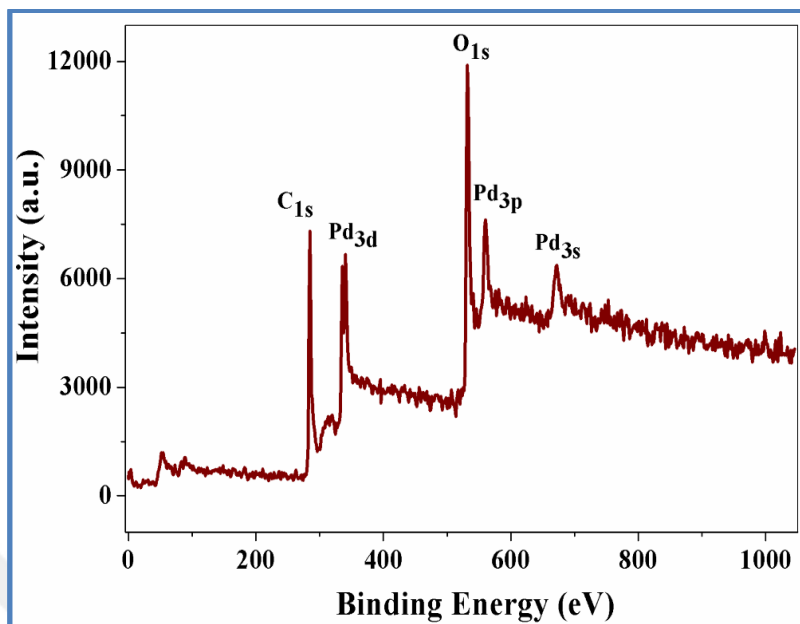


Figure 4.3. XPS full spectrum of GO-COOPd composite.

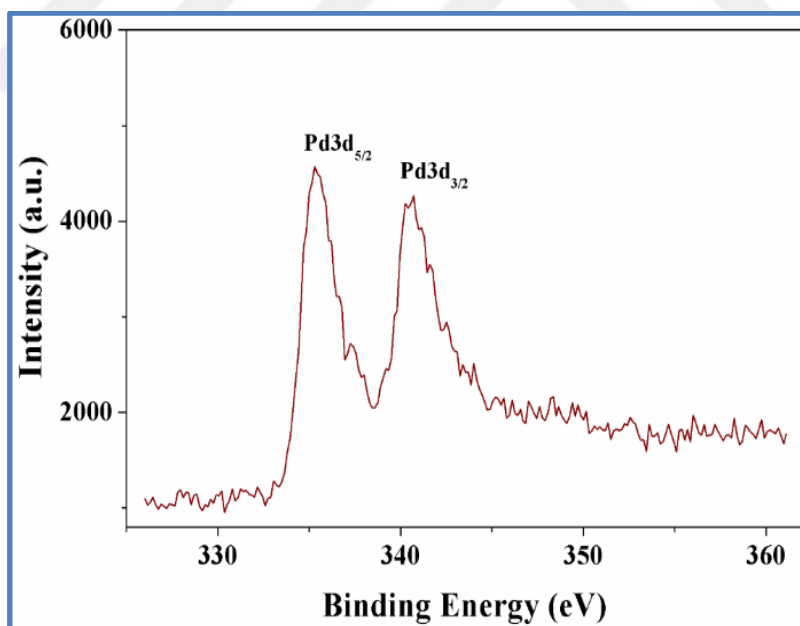


Figure 4.4. XPS spectra of Pd.

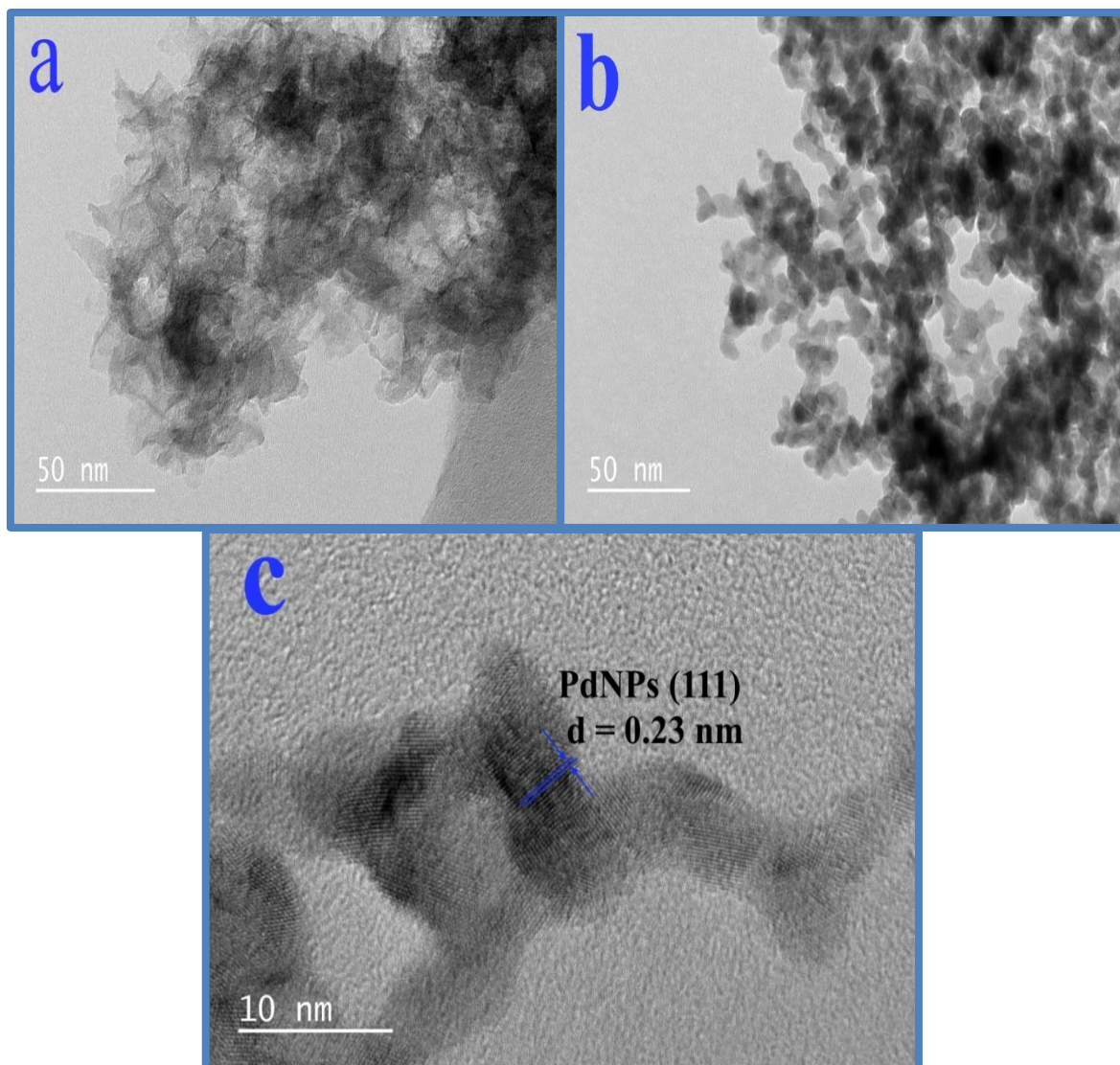


Figure 4.5. TEM pictures of GO-COOH (a) and GO-COOPd (b,c).

## 4.2. Electrochemical Characterization of GCE and Modified Electrode

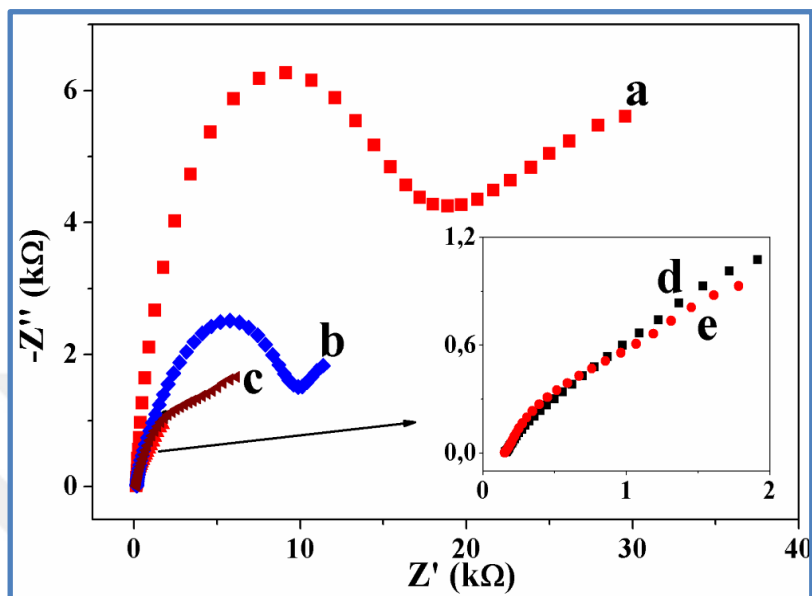


Figure 4.6. Electrochemical impedance Nyquist plot of Nf/GCE (a), Nf/GO/GCE (b), Nf/Pd@GO/GCE (c), Nf/GO-COOH/GCE (d), and Nf/GO-COOPd/GCE (e) in 5 mM  $[\text{Fe}(\text{CN})_6]^{3-}/[\text{Fe}(\text{CN})_6]^{4-}$  containing 0.1 M KCl. Applied potential: 0.2 V. Amplitude: 10 mV. Frequency range: 0.02 Hz to 100 kHz.

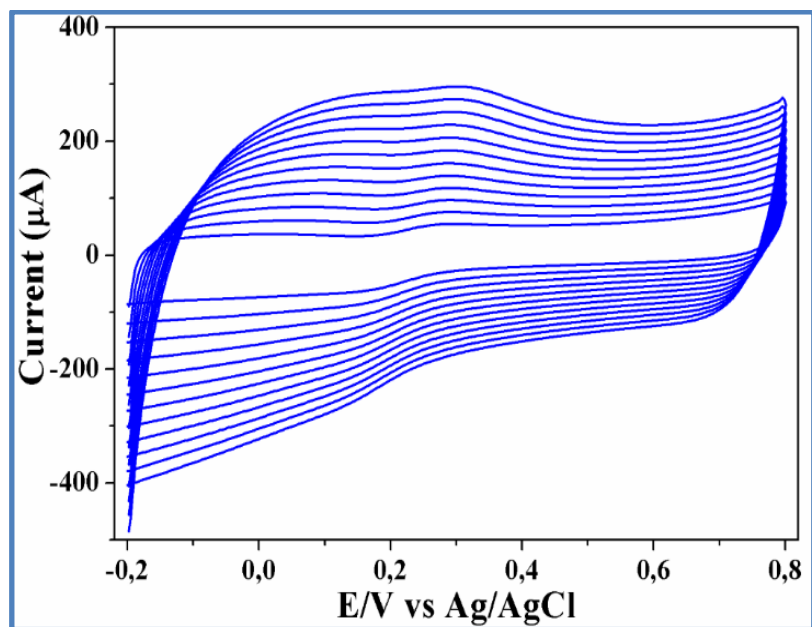


Figure 4.7. CVs of GO-COOH/GCE in 5 mM  $[\text{Fe}(\text{CN})_6]^{3-}/[\text{Fe}(\text{CN})_6]^{4-}$  containing 0.1 M KCl using different scan rates (from 0.04 to 0.26  $\text{V s}^{-1}$ ).

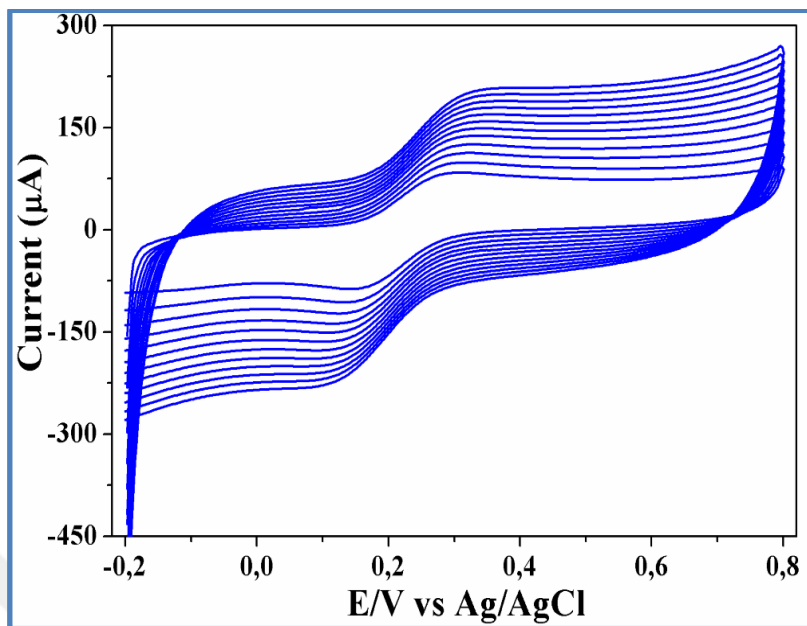


Figure 4.8. CVs of GO-COOPd/GCE in 5 mM  $[\text{Fe}(\text{CN})_6]^{3-}/[\text{Fe}(\text{CN})_6]^{4-}$  containing 0.1 M KCl using different scan rates (from 0.04 to 0.26  $\text{V s}^{-1}$ ).

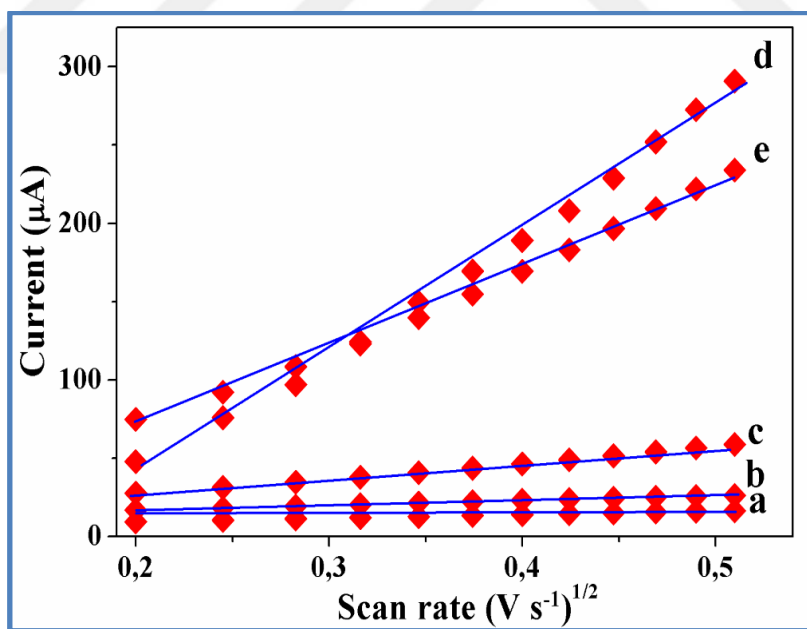


Figure 4.9. Plot of oxidation peak current of 5 mM  $[\text{Fe}(\text{CN})_6]^{3-}/4-$  (1:1) at Nf/GCE (a), Nf/GO/GCE (b), Nf/Pd@GO/GCE (c), Nf/GO-COOH/GCE (d), and Nf/GO-COOPd/GCE vs. the square root of scan rate (Scan rate: 0.04–0.26  $\text{V/s}$ ).

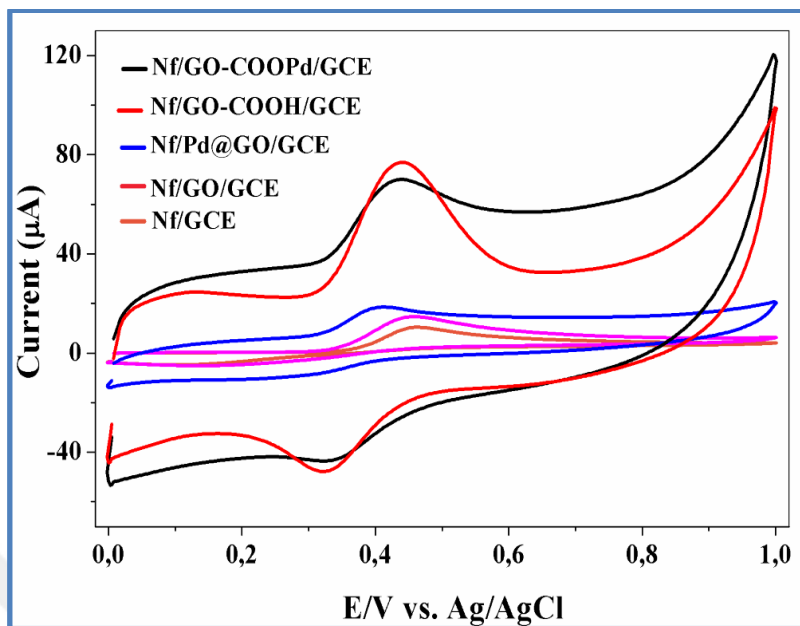


Figure 4.10. CVs of Nf/GCE, Nf/GO/GCE, Nf/Pd@GO/GCE, Nf/GO-COOH/GCE, and Nf/GO-COOPd/GCE in 0.1M PBS (pH 7.5) containing 0.5 mM PA. Scan rate: 0.05 V/s.

#### 4.3. Effect of pH and Scan Rate on Nf/GO-COOPd/GCE

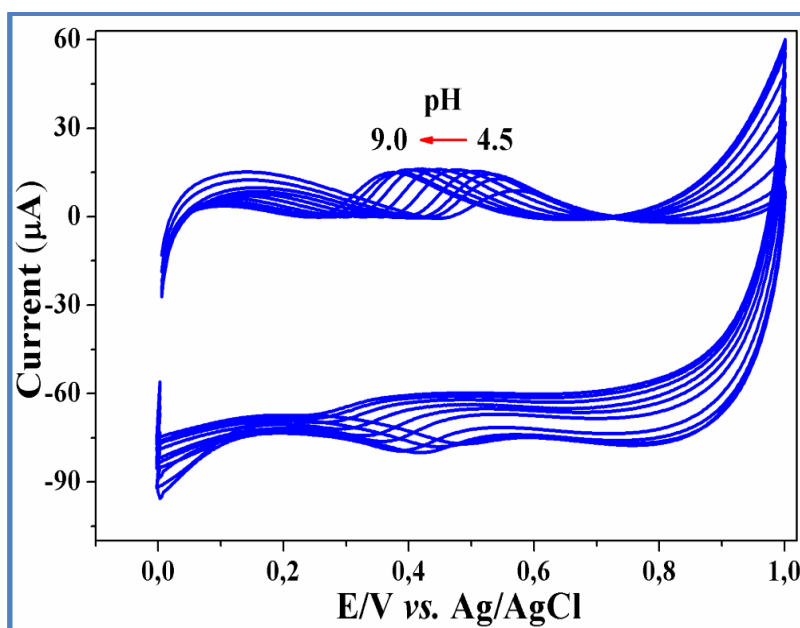


Figure 4.11. CV response of Nf/GO-COOPd/GCE to 0.2 mM PA in 0.1 M PBS with different pH values (4.5 to 9.0).



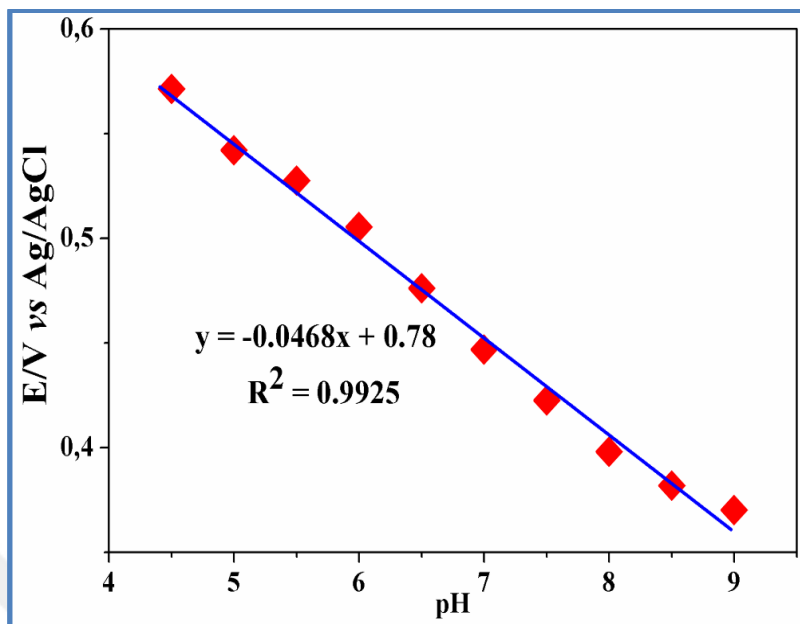


Figure 4.12. The plot of  $E/V$  vs. various pH values (from 4.5 to 9.0).

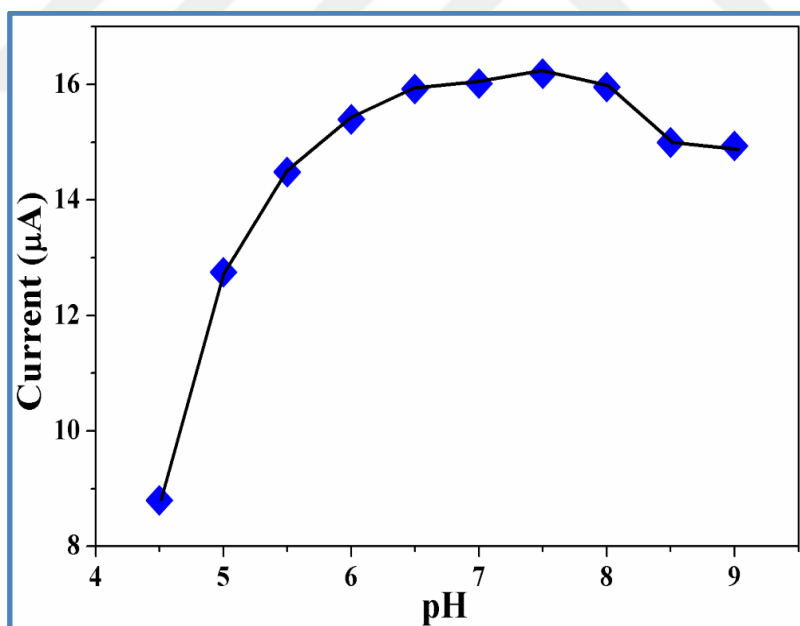


Figure 4.13. The effect of pH on the oxidation peak current response of  $Nf/GO-COOPd/GCE$  to 0.2 mM PA.

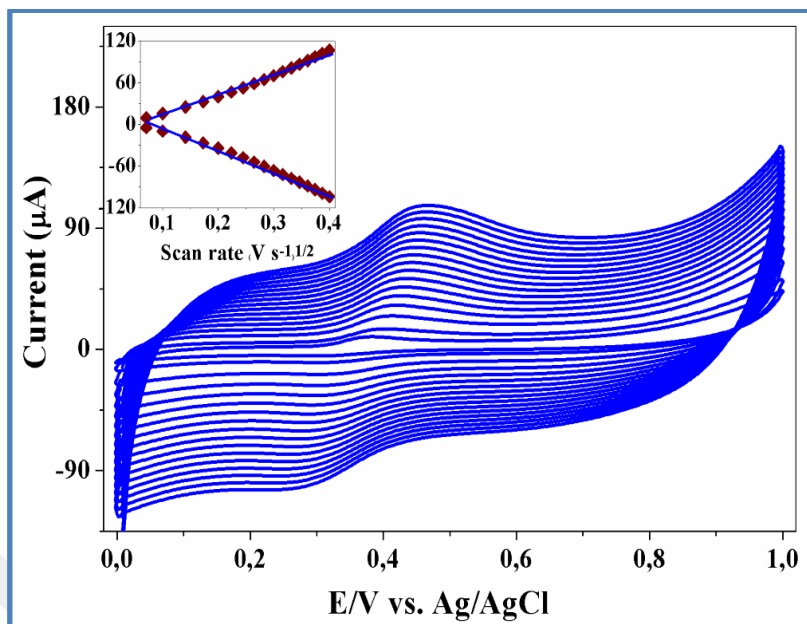


Figure 4.14. CVs of Nf/GO-COOPd/GCE to 0.2 mM PA in 0.1 M PBS at various scan rates (from 0.005 to 0.16 V/s). Inset: plot of oxidation and reduction peak current response of Nf/GO-COOPd/GCE versus square root of scan rate.

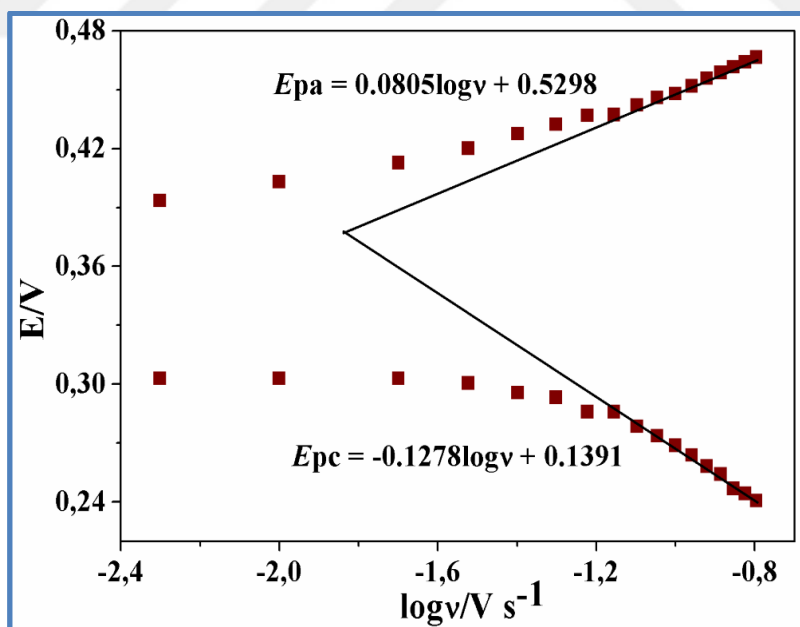


Figure 1.15. Plot to E/V versus  $\log v/V s^{-1}$ .

#### 4.4. Determination of PA on Nf/GO-COOPd/GCE Electrochemical Sensor

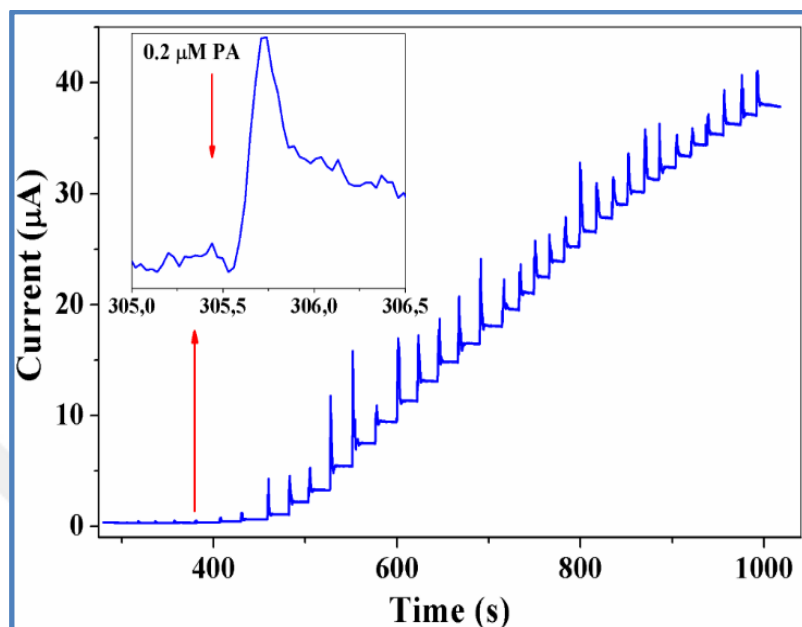


Figure 4.16. Amperometric graph obtained on the Nf/GO-COOPd/GCE with different PA concentrations at 0.48 V.

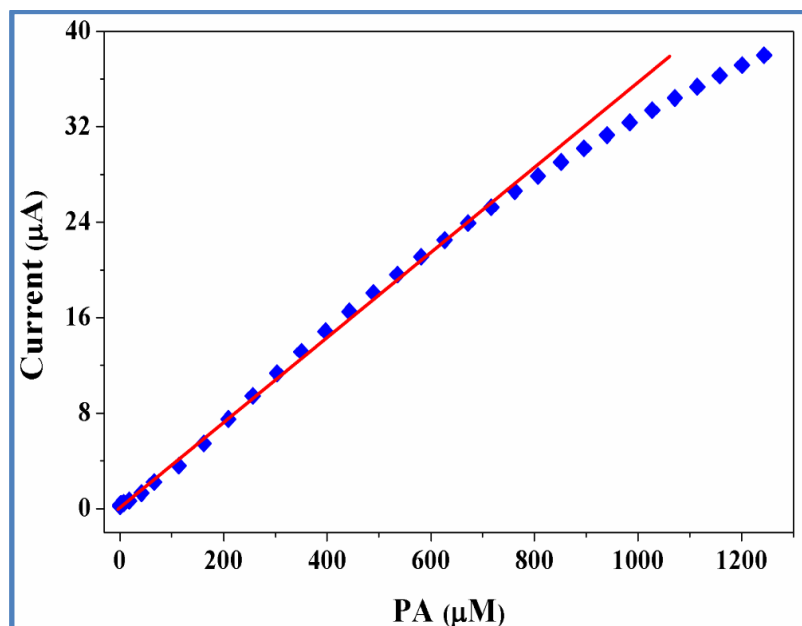


Figure 4.17. PA oxidation current vs. PA concentration.

#### 4.5. Interference Study

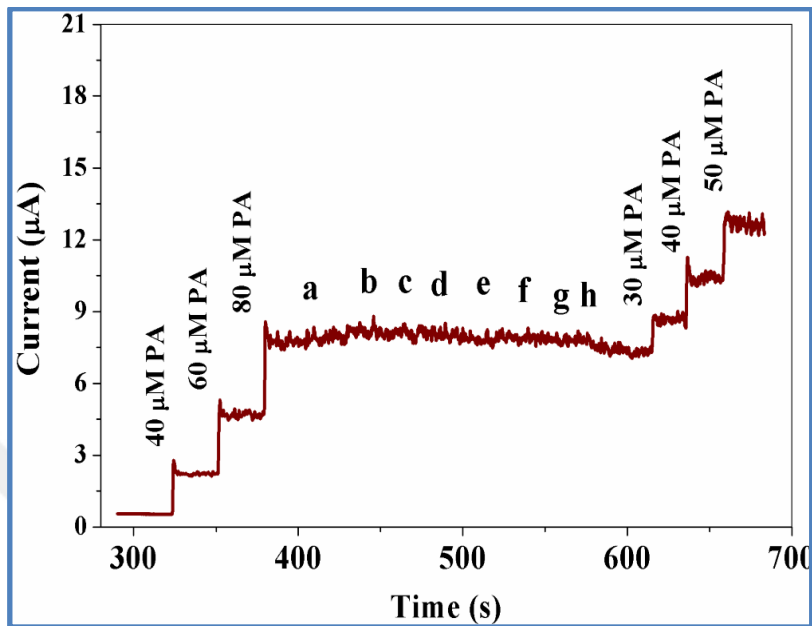


Figure 4.18. Amperometric response of Nf/GO-COOPd/GCE to PA with 80 μM AA, UA, DA, Glu, Fruc, Man, His, and FA in 0.1 M PBS (pH 7.5) at 0.48 V.

#### 4.6. Repeatability, Reproducibility, and Storage Stability

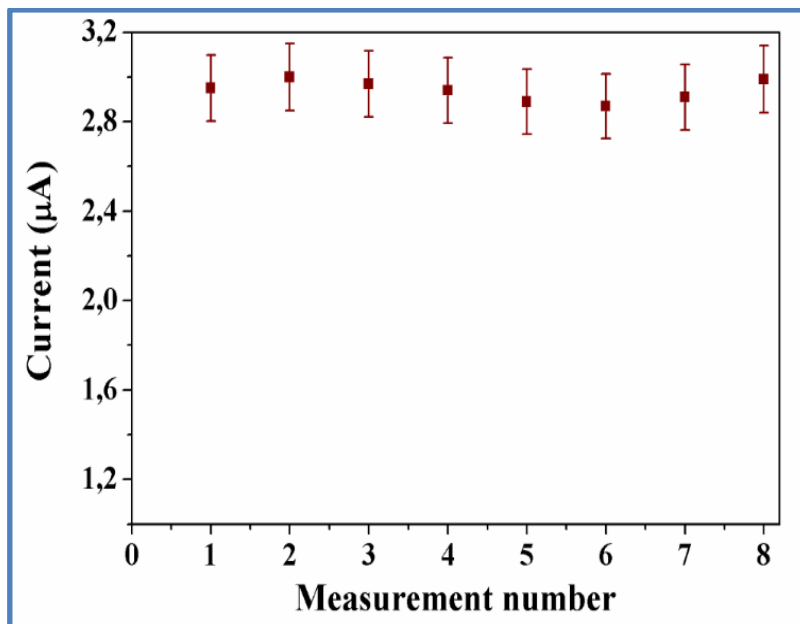


Figure 4.19. Repeatability graph of 0.05 mM PA measurements using the same Nf/GO-COOPd/GCE sensor.

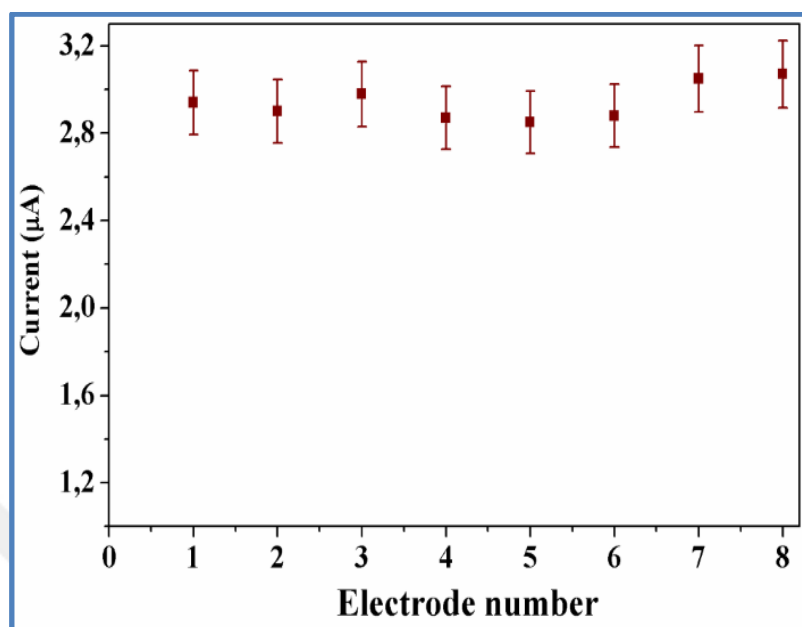


Figure 4.20. Reproducibility graph of 0.05 mM PA measurements using eight different Nf/GO-COOPd GCE sensor.

Table 4.1. The comparison of the Nf/GO-COOPd/GCE PA sensor with the previous works.

Sensor	Sensitivity ( $\mu\text{AmM}^{-1}\text{cm}^{-2}$ )	Linear range ( $\mu\text{M}$ )	LOD ( $\mu\text{M}$ )	Ref.
GAIN/Cu	-	1-700	0.012	(Taleb <i>et al.</i> , 2018)
Graphene/GCE	-	0.1 -20	0.032	(Kang <i>et al.</i> , 2010)
MWCNT/ZnO-Au/GCE	-	0.05-20	0.009	(Kenarkob and Pourghobadi, 2019)
N-CeO <sub>2</sub> @rGO	268	0.05-20	0.0098	(Ponnaiah <i>et al.</i> , 2018)
Cu <sub>2</sub> O/GR/GCE	14,397.7	0.02-1.3	0.00667	(Yang <i>et al.</i> , 2015)
ERG/Ni <sub>2</sub> O <sub>3</sub> -NiO/GCE	-	0.04-100	0.02	(Liu <i>et al.</i> , 2014)
Nf/TiO <sub>2</sub> -graphene/GCE	-	1-100	0.21	(Fan <i>et al.</i> , 2011)
NiONPs-GO-CTS:EPH/GCE	-	0.1- 2.9	0.0067	(Santos <i>et al.</i> , 2017)
RGO-TiN/GCE	-	0.06-660	0.02	(Kong <i>et al.</i> , 2015)
4-ABA/ERGO/GCE	-	0.1-65	0.01	(Zhu <i>et al.</i> , 2014)
Graphene-chitosan/GCE	-	1-100	0.3	(Zheng <i>et al.</i> , 2013)
rGO-PEDOT NT/GCE	-	1-35	0.4	(Huang <i>et al.</i> , 2014).
MoS <sub>2</sub> -Gr/GCE	-	0.1-100	0.02	(Huang <i>et al.</i> , 2013).
Pd/GO/GCE	-	0.005-0.5 0.5-80	0.0022	(Li <i>et al.</i> , 2014)
Nf/GO-COOPd/GCE	232.89	0.04-800	0.012	This study

#### 4.7. Real Sample Analysis

Table 4.2. Detection of PA in serum samples using the Nf/ GO-COOPd/GCE sensor (n=8).

Serum sample	Added ( $\mu\text{M}$ )	Found ( $\mu\text{M}$ )	RSD (%)	Recovery (%)
1	–	not detected	–	–
2	5	5.18	5.33	103.6
3	50	50.08	1.84	100.16
4	100	102.07	2.46	102.07
5	140	144.19	2.77	102.99
6	160	166.47	2.24	104.04





## 5. DISCUSSION AND CONCLUSION

In the present study, the FTIR spectra were achieved for the characterization of oxygen-containing functional groups set on graphene oxides. Figure 4.1a shows the characteristic peaks of GO: the peak at  $3344\text{ cm}^{-1}$  shows the presence of  $\text{—OH}$  groups; the peak at  $1718\text{ cm}^{-1}$  is ascribed to stretching vibrations associated to  $\text{C=O}$  in the carboxylic groups; the band recognized at  $1053\text{ cm}^{-1}$  is identified to stretching vibrations of  $\text{C—O}$  from the ether groups; the bands at  $1221$ ,  $1401$ , and  $1620\text{ cm}^{-1}$  are ascribed to epoxy  $\text{C—O—C}$ ,  $\text{C—OH}$ , and aromatic ring stretching peak of  $\text{C=C}$ , sequentially (Bellamy, 2012). As can be shown from Figure 4.1b, the observed peak at  $1230\text{ cm}^{-1}$  is the stretching band for  $\text{C—O}$  particularly rising from  $\text{O=C—OH}$  groups. The sharp peak at  $1581\text{ cm}^{-1}$  belongs to  $\text{C—O}$  vibration from the carboxylated graphene oxide.

The crystalline structures of GO, GO-COOH, and GO-COO Pd were discovered utilizing XRD. The XRD patterns presented in Figure 4.2a revealing that the interlayer space of GO was  $0.77\text{ nm}$  at  $11.5^\circ$ . This value was bigger than that of graphite ( $0.34\text{ nm}$ ) due to the presence of oxygenated functional groups on the graphene oxide sheets. As seen in Figure 4.2b, after GO was carboxylated, the main peaks for GO-COOH was usually detected at  $24.89^\circ$  and  $43.52^\circ$ , appearing a high edge-increasing degree in solid state (Park, 2014). Figure 4.2c shows the XRD pattern of GO-COOPd. In the figure, the peaks at  $39.52^\circ$   $67.05^\circ$  belong to (111) and (220) face-centered cubic (FCC) PdNPs (JCPDS No. 46-1043), which demonstrates that Pd nanoparticles were deposited on the GO-COOH support surface.

So as to identify the chemical composition and chemical bonds of each element of the as-prepared GO-COOPd composite, X-ray photoelectron spectroscopy (XPS) was utilized. As can be seen in Figure 4.3, the XPS full-spectrum shows only the existence of palladium, oxygen, and carbon. The XPS spectrum revealed in Figure 4.4 displayed the characteristic peaks at  $335.3$  and  $340.7\text{ eV}$ , which are ascribed to  $\text{Pd}^0\text{ }3d_{5/2}$  and  $\text{Pd}^0\text{ }3d_{3/2}$ , correspondingly. These results indicate that the reduction of Pd (II) on the GO-COOH surface to Pd (0) was completed throughout the reduction procedure (Wagner et al., 1979).

To examine the surface morphology of GO-COOH and GO-COOPd, TEM was used. Figure 4.5a, b, and c show TEM images of GO-COOH and GO-COOPd composites. According to the figures, GO-COOH displays layered-structure that enhances the active surface area of the support. As seen in Figure 4.5b and Figure 4.5c, Pd nanoparticles were loaded on the support. Nonetheless, the agglomeration of nanoparticles occurred on the areas of the support because of the multilayered properties of GO-COOH. The lattice spacing of the Nano bars was calculated to be 0.23 nm, displaying the (111) plane of face-centered cubic (FCC) Pd nanoparticles (Figure 4.5c).

In order to examine the electro-active surface area of Nf/GCE, Nf/GO/GCE, Nf/Pd@GO/GCE, Nf/GO-COOH/GCE, and Nf/GO-COOPd/GCE, electrochemical impedance spectroscopy (EIS) and cyclic voltammetry (CV) approaches were performed. EIS offers significant knowledge about the active surface zone of the working electrodes related to the charge transfer resistance ( $R_{ct}$ ) alterations throughout the modification stages. In a Nyquist plot, the diameter of the semicircle is equivalent to the charge transfer resistance of the working electrode (Tan et al., 2010). As can be shown from Figure 4.6, the half circle diameter of the electrodes was in the subsequent order: Nf/GCE (20.55 k $\Omega$ ) > Nf/GO/GCE (10.47 k $\Omega$ ) > Nf/Pd@GO/GCE (5.85 k $\Omega$ ) > Nf/GO-COO Pd/GCE (2.94 k $\Omega$ ) > Nf/GO-COOH/GCE (1.3 k $\Omega$ ). By taking these results into account, the carboxyl groups found on the surface of GO enhances the conductivity of working electrode. The PdNPs deposited on GO-COOH support moderately reduced the conductivity that can be recognized to large nanoparticle size of Pd when compared with multilayered high surface zone of GO-COOH. In addition, although nafion reduced the active surface zone, it improved the stability of the sensor and reduced the interference effect on the sensor response. The active surface zones of the working electrodes were assessed by using CV (Figure 4.7 and Figure 4.8) in 5 mM  $[\text{Fe}(\text{CN})_6]^{3-/4-}$  solution including 0.1 M KCl. In the reversible electrochemical reaction of the probe, the oxidation peak current is proportional to the square root of the scan rate depending on Randles-Sevcik equation (equ. 1) (Bard et al., 1980):

$$I_p = (2.69 \times 10^5) n^{3/2} A D_0^{1/2} C_0 v^{1/2} \dots \dots \dots (5.1)$$

Where  $I_p$  is the peak current as amp (A),  $n$  is the number of electrons participating in the electrochemical reaction,  $A$  is the active surface zone as  $\text{cm}^2$ ,  $C_o$  is the concentration of the probe as  $\text{mol cm}^{-3}$ ,  $D_o$  is the diffusion coefficient, which is  $6.56 \times 10^{-6} \text{ cm}^2 \text{ s}^{-1}$  at  $25^\circ \text{C}$  for  $5 \text{ mM } [\text{Fe}(\text{CN})_6]^{3-/4-}$ , and  $v$  is the scan rate as  $\text{V s}^{-1}$  (Konopka and McDuffie, 1970). Figure 4.9 illustrates the oxidation peak current response of the working electrodes to the probe versus the square root of scan rate. The linear regression equations were  $i (\mu\text{A}) = 22.971v^{1/2} + 4.8481$  ( $R^2 = 0.9998$ ) for Nf/GCE,  $i (\mu\text{A}) = 30.614v^{1/2} + 10.768$  ( $R^2 = 0.9996$ ) for Nf/GO/GCE,  $i (\mu\text{A}) = 101.57v^{1/2} + 6.2463$  ( $R^2 = 0.9967$ ) for Nf/Pd@GO/GCE,  $i (\mu\text{A}) = 790.82v^{1/2} - 121.53$  ( $R^2 = 0.9935$ ) for Nf/GO-COOH/GCE, and  $i (\mu\text{A}) = 523.47v^{1/2} - 37.419$  ( $R^2 = 0.9949$ ) for Nf/GO-COOPd/GCE. According to the linear equations, the active surface areas were  $0.0067 \text{ cm}^2$  for Nf/GCE,  $0.009 \text{ cm}^2$  for Nf/GO/GCE,  $0.03 \text{ cm}^2$  for Nf/Pd@GO/GCE,  $0.229 \text{ cm}^2$  for Nf/GO-COOH/GCE, and  $0.152 \text{ cm}^2$  for Nf/GO-COOPd/GCE. These results were in agreement with the EIS results.

The electrochemical oxidation and reduction of PA at the Nf/GCE, Nf/GO/GCE, Nf/Pd@GO/GCE, Nf/GO-COOH/GCE, and Nf/GO-COOPd/GCE was examined in  $0.1 \text{ M}$  PBS (pH 7.5) utilizing CV technique in the potential range of  $0.0$  to  $1.0 \text{ V}$ . As can be shown in Figure 4.10, the oxidation and reduction peak currents of PA achieved at Nf/GO-COOPd/GCE were the highest while compared with the other working electrodes, which indicates the excellent electro-catalytic reply of Nf/GO-COOPd/GCE to PA. It is obviously seen that PdNPs enhances the electron transfer of PA on the modified electrode. After  $0.5 \text{ mM}$  of PA was added to  $0.1 \text{ M}$  PBS (pH 7.5), a well-defined two pairs of redox peaks were detected at Nf/GO-COOPd/GCE with peak to peak separation potential ( $\Delta E_p$ ) of  $-102 \text{ mV}$  at  $0.05 \text{ V s}^{-1}$  of scan rate.

The results of  $0.1 \text{ M}$  PBS with various pH values ( $4.5$ – $9.0$ ) on the redox reply of Nf/GO-COOPd/GCE to PA was assessed utilizing CV (Figure 4.11). As seen in the figure, the peak potential altered to more negative direction with the increment of pH, signifying that the redox reaction at Nf/GO-COOPd/GCE sensor contains the transfer of protons. The linear regression equation of the pH versus the oxidation peak potential of PA (equ. 2) (Figure 4.12) was achieved as the subsequent equation:

$$E_{pa} = -0.0468 \text{ pH} + 0.78 \text{ (} R^2 = 0.9925 \text{)} \dots \dots \dots (5.2)$$

According to the equation, the achieved slope of 46.8 mV/pH is close to the slope of Nernstian regression equation of 59 mV/pH, which indicates that the equivalent number of electrons and protons takes part in the redox reaction of PA in 0.1 M PBS (pH 7.5) (Mahmoud et al., 2017). Furthermore, the maximum oxidation peak response was detected at pH 7.5 value (Figure 4.13). Hence, pH 7.5 was utilized for further electrochemical measurements.

The effect of scan rates on the redox peak current of PA was shown in Figure 4.14. According to the figure, the redox peak currents increased linearly through the increase of the square root of the scan rate (0.005–0.160 V s<sup>-1</sup>), indicating the electron-transfer kinetics is the typical diffusion-controlled process at Nf/GO-COOPd/GCE in 0.1 M PBS (pH 7.5) (Sharifian and Nezamzadeh-Ejhieh, 2016).

To estimate the charge transfer coefficient ( $\alpha$ ) and the number of electron ( $n$ ) taking part in the electrochemical reaction, Laviron equation was utilized (Laviron, 1979). The following linear regression equations are the anodic and cathodic peak potential of PA versus  $\log v$  (Figure 4.15).

$$E_{pc} = -0.1278\log v + 0.1391 \dots\dots\dots(5.3)$$

$$E_{pa} = 0.0805\log v + 0.5298 \dots\dots\dots(5.4)$$

From the slope of these equations  $\alpha$  and  $n$  were found to be 0.61 and 1.88, correspondingly. These outcomes were in good agreement with those detected for CoOx/CCE (Razmi and Habibi, 2010) and fMWCNT-MGCE (Raouf et al., 2012). From the above outcomes the predictable electrochemical oxidation of PA can be as follows (Scheme 5.1).

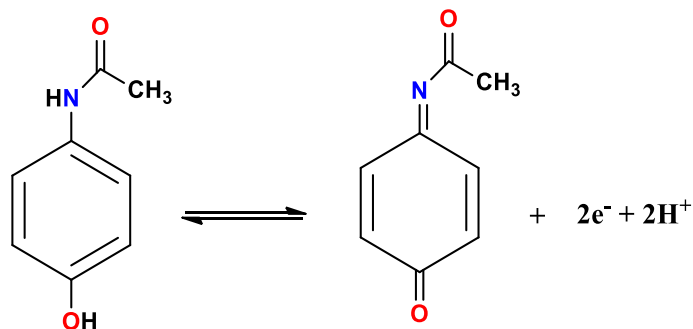


Figure 5.1. The electrochemical oxidation and reduction mechanism of PA at Nf/GO COOPd/GCE.

Amperometric method was utilized to detect the sensitivity of Nf/GO-COOPd/GCE along with the linear determination range, the limit of detection (LOD), and the limit of quantification (LOQ) for PA. Figure 4.16 shows the amperometric response of the fabricated sensor to different concentrations of PA in 0.1 M PBS (pH 7.5) at the potential of 0.48 V. The oxidation peak current reached the steady-state current in the time range between 0.65 s and 2 s from low concentration to high concentration of PA, indicating the sensor showed quick response to low concentration of PA while compared to the high concentration. Figure 4.17 showed the oxidation peak current against the concentration of PA. The linearity was acquired in the concentration range of 0.04–800  $\mu\text{M}$  with a linear regression equation of  $i$  ( $\mu\text{A}$ ) = 0.0354c ( $\mu\text{M}$ ) + 0.2028 ( $R^2=0.998$ ). The LOD was calculated to be 0.012  $\mu\text{M}$  utilizing sign to noise ratio of 3 ( $S/N=3$ ) and the sensitivity was 232.89  $\mu\text{A mM}^{-1} \text{cm}^{-2}$ . The sensing capability of Nf/GO-COOPd/GCE was compared to the studies reported formerly (Table 4.1), According to the table, the fabricated sensor showed excellent linear determination range, sensitivity, and LOD.

Selectivity plays an important role in sensor and biosensor application, so the interference effect of ascorbic acid (AA), uric acid (UA), dopamine (DA), glucose (Glu), fructose (Fruc), Mannose (Man), histidine (His), and folic acid (FA) on the Nf/GO-COOPd/GCE sensor was evaluated utilizing amperometric method. Figure 4.18 depicts the amperometric responses of the as-prepared sensor to PA with interfering substances of 80  $\mu\text{M}$  AA, UA, DA, Glu, Fruc, Man, His, and FA. As can be concluded from the figure, the sensor did not show any recognizable current response to the chosen interfering compounds at the applied potential of 0.48 V, showing perfect selectivity to the determination of PA.

The repeatability of Nf/GO-COOPd/GCE was studied utilizing amperometry in 0.1 M PBS (pH 7.5). The amperometric graph was obtained with successive addition of 50  $\mu$ M PA to PBS. This experiment was repeated for eight measurements using the same modified electrode. The relative standard deviation (RSD) was found to be 1.60% (Figure 4.19). The reproducibility of the sensor was assessed utilizing eight different modified electrodes in 0.1 M PBS (pH 7.5). The amperometric graph was obtained with successive addition of 50  $\mu$ M PA to PBS. RSD was found to be 2.81% (Figure 4.20), which demonstrates that the Nf/GO-COOPd/GCE sensor exhibited well repeatability and reproducibility while compared to the studies described formerly (Karikalan et al., 2016; Anuar et al., 2018).

Moreover, in order to examine the storage stability of the sensor, the amperometric replies were gotten for two weeks. Approximately 97.3% of the beginning response of the sensor to 50  $\mu$ M PA was attained after two weeks, revealing a satisfactory storage stability of the developed sensor.

To further examine the practical application of the fabricated electrochemical sensor, PA was determined in human serum samples using the sensor. For this, various concentrations of PA (5, 50, 100, 140, and 160  $\mu$ M) was selected by taking into account the therapeutic dose of acetaminophen in serum (10–20  $\mu$ g/mL) (White and Wong 1998). All the tests were achieved by standard addition method. As described in Table 4.2, the gotten recoveries for the determination of PA were in the range of 100.16-104.04. These outcomes show that the Nf/GO-COOPd/GCE sensor had high precision and may be utilized for detection of PA in real samples.

In our study, we have fabricated a novel PA sensor depending on PdNPs deposited on carboxylated graphene oxide modified GCE. The functionalization of GO with the carboxyl groups enhanced the hydrophilicity, conductivity, and active surface area of GO and makes the GO-COOH support highly talented material for deposition of PdNPs. Moreover, the -COOH groups improved the electrocatalytic ability of the sensor while compared to bare GCE and Nf/GO/GCE. This support may also be utilized for deposition of different noble metal nanoparticles for fabrication novel electrochemical sensors and biosensors. The synthesized composites were characterized utilizing FTIR, XPS, XRD, and SEM and the electrochemical behaviors of the compound was examined utilizing CV, EIS, and amperometric methods. The sensor showed wide linear detection range for PA from

0.04 to 800  $\mu\text{M}$  with LOD of 0.012  $\mu\text{M}$  and sensitivity of 232.89  $\mu\text{A mM}^{-1} \text{cm}^{-2}$ . Moreover, the sensor showed high sensitivity, excellent selectivity, great repeatability, reproducibility, and acceptable long-term stability. By considering these results, the successful construction of Nf/GO-COOPd/GCE electrochemical sensor may encourage new approaches for the development of electrode materials.

This study was published in *Electroanalysis* journal as “Electroanalytical determination of paracetamol using Pd nanoparticles deposited on carboxylated graphene oxide modified glassy carbon electrode (*Electroanalysis* 2019, 31(11), 2187, 2198)”.

## REFERENCES

- Adams, B. D., Chen, A., 2011. The role of palladium in a hydrogen economy. *Materials Today*, **14**: 282-289.
- Adhikari, B. R., Govindhan, M., Chen, A., 2015. Sensitive detection of acetaminophen with graphene-based electrochemical sensor. *Electrochimica Acta*, **162**: 198-204.
- Afkhami, A., Khoshsafar, H., Bagheri, H., Madrakian, T., 2014. Facile simultaneous electrochemical determination of codeine and acetaminophen in pharmaceutical samples and biological fluids by graphene-COFe<sub>2</sub>O<sub>4</sub> nanocomposite modified carbon paste electrode. *Sensors and Actuators B: Chemical*, **203**: 909-918.
- Anuar, N. S., Basirun, W. J., Ladan, M., Shalauddin, M., Mehmood, M. S., 2018. Fabrication of platinum nitrogen-doped graphene nanocomposite modified electrode for the electrochemical detection of acetaminophen. *Sensors and Actuators B: Chemical*, **266**: 375-383.
- Armada, M. P. G., Vallejo, E., Villena, C., Losada, J., Casado, C. M., Alonso, B., 2016. New acetaminophen amperometric sensor based on ferrocenyl dendrimers deposited onto Pt nanoparticles. *Journal of Solid State Electrochemistry*, **20**(6): 1551-1563.
- Asghari, A., Ameri, M., Ziarati, A.A., Radmannia, S., Amoozadeh, A., Barfi, B. Boutorabi, L., 2015. Electro-oxidation of paracetamol in the presence of malononitrile: Application for green, efficient, none-catalyst, simple and one-pot electro-synthesis of new paracetamols. *Chinese Chemical Letters*, **26**(6), 681-684.
- Balamurugan, R., Liu, J. H., Liu, B. T., 2018. A review of recent developments in fluorescent sensors for the selective detection of palladium ions. *Coordination Chemistry Reviews*, **376**: 196-224.
- Banica, F. G., 2012. *Chemical Sensors and Biosensors: fundamentals and Applications*. John Wiley & Sons.
- Bard, A. J., Faulkner, L. R., Leddy, J., Zoski, C. G., 1980. *Electrochemical Methods: Fundamentals and Applications* (Vol. 2). New York: wiley.
- Bathinapatla, S., Fernandes, D. M., Ch, M., Madhavi, G., 2018. Facile one pot synthesis of bimetallic Pd-Ag/reduced graphene oxide nanocomposite as an electrochemical

- sensor for sensitive detection of anti-hypotensive drug. *Colloids and Surfaces A: Physicochemical and Engineering Aspects*, **546**: 293-300.
- Bellamy, L.J., 2012. *The Infrared Spectra of Complex Molecules: Volume two Advances in Infrared Group Frequencies*. Springer Science & Business Media.
- Belykh, L.B., Titova, Y.Y., Umanets, V.A. Shmidt, F.K., 2006. Palladium hydrogenation catalysts modified with aluminum-and phosphorus-containing compounds and with alcohols: Effect of modifiers. *Russian Journal of Applied Chemistry*, **79**(8): 1271-1277.
- Boehm, H.P., 2010. Graphene — how a laboratory curiosity suddenly became extremely interesting. *Angewandte Chemie International Edition*, **49**(49): 9332-9335.
- Brett, C. M., Oliveira-Brett, A. M., 2011. Electrochemical sensing in solution origins, applications and future perspectives. *Journal of Solid State Electrochemistry*, **15**(7-8): 1487-1494.
- Chai, G. S., Yoon, S. B., Kim, J. H., Yu, J. S., 2004. Spherical carbon capsules with hollow macroporous core and mesoporous shell structures as a highly efficient catalyst support in the direct methanol fuel cell. *Chemical Communications*, (**23**): 2766-2767.
- Dikin, D. A., Stankovich, S., Zimney, E. J., Piner, R. D., Dommett, G. H., Evmenenko, G., Ruoff, R. S., 2007. Preparation and characterization of graphene oxide paper. *Nature*, **448**(7152): 457.
- Dimiev, A.M. and Eigler, S. eds., 2016. *Graphene oxide: Fundamentals and Applications*. John Wiley & Sons.
- Eggins, B. R., 2008. *Chemical Sensors and Biosensors* (Vol. 28). John Wiley & Sons.
- Eigler, S. and Hirsch, A., 2014. Chemistry with graphene and graphene oxide—challenges for synthetic chemists. *Angewandte Chemie International Edition*, **53**(30), pp.7720-7738.
- Engin, C., Yilmaz, S., Saglikoglu, G., Yagmur, S., Sadikoglu, M., 2015. Electroanalytical investigation of paracetamol on glassy carbon electrode by voltammetry. *Int. J. Electrochem. Sci*, **10**: 1916-1925.
- Fan, Y., Liu, J. H., Lu, H. T., Zhang, Q., 2011. Electrochemical behavior and voltammetric determination of paracetamol on Nafion/TiO<sub>2</sub>-graphene modified glassy carbon electrode. *Colloids and Surfaces B: Biointerfaces*, **85**(2): 289-292.
- Faurschou, A., Menné, T., Johansen, J. D., Thyssen, J. P., 2011. Metal allergen of the 21st century—a review on exposure, epidemiology and clinical manifestations of palladium allergy. *Contact Dermatitis*, **64**(4): 185-195.
- Fernandez, C., Heger, Z., Kizek, R., Ramakrishnappa, T., Boruń, A., Faisal, N. A., 2015. Pharmaceutical Electrochemistry: The Electrochemical Oxidation of Paracetamol and Its Voltammetric Sensing in Biological Samples Based on Screen Printed Graphene Electrodes. *Int. J. Electrochem. Sci*, **10**: 7440-7452.
- Gao, H., 2012. **Synthesis of Palladium-Based Electrocatalysis—From Pure Metal to Bimetallic Nanoparticles**. Thesis of Master Degree. University of Tennessee, Knoxville.
- Gao, W. ed., 2015. *Graphene Oxide: Reduction Recipes, Spectroscopy, and Applications*. Springer.
- Grieshaber, D., MacKenzie, R., Voeroes, J., Reimhult, E., 2008. Electrochemical biosensors-sensor principles and architectures. *Sensors*, **8**(3): 1400-1458.



- Guler, M., Turkoglu, V., Basi, Z., 2017. Determination of malation, methidathion, and chlorpyrifos ethyl pesticides using acetylcholinesterase biosensor based on Nafion/Ag@ rGO-NH<sub>2</sub> nanocomposites. *Electrochimica Acta*, **240**: 129-135.
- Guler, M., Turkoglu, V., Bulut, A., Zahmakiran, M., 2018. Electrochemical sensing of hydrogen peroxide using Pd@Ag bimetallic nanoparticles decorated functionalized reduced graphene oxide. *Electrochimica Acta*, **263**: 118-126.
- Habibi, B., Jahanbakhshi, M., Abazari, M., 2014. A modified single-walled carbon nanotubes/carbon-ceramic electrode for simultaneous voltammetric determination of paracetamol and caffeine. *Journal of the Iranian Chemical Society*, **11**(2): 511-521.
- Hofmann, U. and Holst, R., 1939. Über die Säurenatur und die Methylierung von Graphitoxyd. *Berichte der Deutschen Chemischen Gesellschaft (A and B Series)*, **72**(4), pp.754-771.
- Huang, K. J., Wang, L., Li, J., Liu, Y. M., 2013. Electrochemical sensing based on layered MOS<sub>2</sub>-graphene composites. *Sensors and Actuators B: Chemical*, **178**: 671-677.
- Huang, T. Y., Kung, C. W., Wei, H. Y., Boopathi, K. M., Chu, C. W., Ho, K. C., 2014. A high performance electrochemical sensor for acetaminophen based on a rGO-PEDOT nanotube composite modified electrode. *Journal of Materials Chemistry A*, **2**(20): 7229-7237.
- Jiang, L., Gu, S., Ding, Y., Jiang, F., Zhang, Z., 2014. Facile and novel electrochemical preparation of a graphene-transition metal oxide nanocomposite for ultrasensitive electrochemical sensing of acetaminophen and phenacetin. *Nanoscale*, **6**(1): 207-214.
- Kang, X., Wang, J., Wu, H., Liu, J., Aksay, I. A., Lin, Y., 2010. A graphene-based electrochemical sensor for sensitive detection of paracetamol. *Talanta*, **81**(3): 754-759.
- Karikalan, N., Karthik, R., Chen, S. M., Velmurugan, M., Karuppiah, C., 2016. Electrochemical properties of the acetaminophen on the screen printed carbon electrode towards the high performance practical sensor applications. *Journal of Colloid and Interface Science*, **483**: 109-117.
- Kenarkob, M., Pourghobadi, Z., 2019. Electrochemical sensor for acetaminophen based on a glassy carbon electrode modified with ZnO/Au nanoparticles on functionalized multi-walled carbon nano-tubes. *Microchemical Journal*, **146**: 1019-1025.
- Kielhorn, J., Melber, C., Keller, D., Mangelsdorf, I., 2002. Palladium—a review of exposure and effects to human health. *International Journal of Hygiene and Environmental Health*, **205**(6): 417-432.
- Kong, F. Y., Gu, S. X., Wang, J. Y., Fang, H. L., Wang, W., 2015. Facile green synthesis of graphene-titanium nitride hybrid nanostructure for the simultaneous determination of acetaminophen and 4-aminophenol. *Sensors and Actuators B: Chemical*, **213**: 397-403.
- Konopka, S. J., McDuffie, B., 1970. Diffusion coefficients of ferri- and ferrocyanide ions in aqueous media, using twin-electrode thin-layer electrochemistry. *Analytical Chemistry*, **42**(14): 1741-1746.
- Krishnan, D., Kim, F., Luo, J., Cruz-Silva, R., Cote, L.J., Jang, H.D. and Huang, J., 2012. Energetic graphene oxide: challenges and opportunities. *Nano Today*, **7**(2), pp.137-152.

- Kumar, A., 2016. *Electrochemistry of Palladium with Emphasis on Size Dependent Electrochemistry of Water Soluble Palladium Nanoparticles*. Arizona State University.
- Kumar, P.V., Bardhan, N.M., Tongay, S., Wu, J., Belcher, A.M. Grossman, J.C., 2014. Scalable enhancement of graphene oxide properties by thermally driven phase transformation. *Nature Chemistry*, **6**(2): 151.
- Laviron, E., 1979. General expression of the linear potential sweep voltammogram in the case of diffusionless electrochemical systems. *Journal of Electroanalytical Chemistry and Interfacial Electrochemistry*, **101**(1): 19-28.
- Li, J., Liu, J., Tan, G., Jiang, J., Peng, S., Deng, M., Liu, Y., 2014. High-sensitivity paracetamol sensor based on Pd/graphene oxide nanocomposite as an enhanced electrochemical sensing platform. *Biosensors and Bioelectronics*, **54**: 468-475.
- Li, J., Sun, W., Wang, X., Duan, H., Wang, Y., Sun, Y., Luo, C., 2016. Ultra-sensitive film sensor based on Al<sub>2</sub>O<sub>3</sub>-Au nanoparticles supported on PDDA-functionalized graphene for the determination of acetaminophen. *Analytical and Bioanalytical Chemistry*, **408**(20): 5567-5576.
- Li, M., Wang, W., Chen, Z., Song, Z., Luo, X., 2018. Electrochemical determination of paracetamol based on Au@ graphene core-shell nanoparticles doped conducting polymer PEDOT nanocomposite. *Sensors and Actuators B: Chemical*, **260**: 778-785.
- Liu, G. T., Chen, H. F., Lin, G. M., Ye, P. P., Wang, X. P., Jiao, Y. Z., Yang, H. F., 2014. One-step electrodeposition of graphene loaded nickel oxides nanoparticles for acetaminophen detection. *Biosensors and Bioelectronics*, **56**: 26-32.
- Maduraiveeran, G., Rasik, R., Sasidharan, M., Jin, W., 2018b. Bimetallic gold-nickel nanoparticles as a sensitive amperometric sensing platform for acetaminophen in human serum. *Journal of Electroanalytical Chemistry*, **808**: 259-265.
- Maduraiveeran, G., Sasidharan, M., Ganesan, V., 2018a. Electrochemical sensor and biosensor platforms based on advanced nanomaterials for biological and biomedical applications. *Biosensors and Bioelectronics*, **103**: 113-129.
- Mahmoud, B. G., Khairy, M., Rashwan, F. A., Banks, C. E., 2017. Simultaneous voltammetric determination of acetaminophen and isoniazid (hepatotoxicity-related drugs) utilizing bismuth oxide nanorod modified screen-printed electrochemical sensing platforms. *Analytical Chemistry*, **89**(3): 2170-2178.
- Moretto, L.M. Kalcher, K. eds., 2014. *Environmental Analysis by Electrochemical Sensors and Biosensors*. New York: Springer.
- Murali, R. 2012. *Graphene Nanoelectronics: From Materials to Circuits*. Springer Science & Business Media.
- Narayana, P. V., Reddy, T. M., Gopal, P., Naidu, G. R., 2014. Electrochemical sensing of paracetamol and its simultaneous resolution in the presence of dopamine and folic acid at a multi-walled carbon nanotubes/poly (glycine) composite modified electrode. *Analytical Methods*, **6**(23): 9459-9468.
- Niedziałkowski, P., Cebula, Z., Malinowska, N., Białobrzaska, W., Sobaszek, M., Ficek, M., Ossowski, T., 2019. Comparison of the paracetamol electrochemical determination using boron-doped diamond electrode and boron-doped carbon nanowalls. *Biosensors and Bioelectronics*, **126**: 308-314.

- Norazriena, Y., 2017. *Electroanalytical Applications of Reduced-Graphene Oxide for Sensing of Bioanalytes/Norazriena Yusoff*. Doctoral dissertation, University of Malaya.
- Pandey, R.K., Lakshminarayanan, V., 2009. Electro-oxidation of formic acid, methanol, and ethanol on electrodeposited Pd-polyaniline nanofiber films in acidic and alkaline medium. *The Journal of Physical Chemistry C*, **113**(52): 21596-21603.
- Park, K. W., 2014. Carboxylated graphene oxide–Mn<sub>2</sub>O<sub>3</sub> nanorod composites for their electrochemical characteristics. *Journal of Materials Chemistry A*, **2**(12): 4292-4298.
- Pendolino, F., Armata, N., 2017. *Graphene Oxide in Environmental Remediation Process, Switzerland: Springer*: pp 5-21.
- Pikna, L., Heželová, M., Milkovič, O., Smrčová, M., 2018. Study on electrochemical properties of Pd-C and Pd-CNT catalysts. *Particulate Science and Technology*, **1**-9.
- Ponnaiah, S. K., Prakash, P., Vellaichamy, B., 2018. A new analytical device incorporating a nitrogen doped lanthanum metal oxide with reduced graphene oxide sheets for paracetamol sensing. *Ultrasonics Sonochemistry*, **44**: 196-203.
- Prabakar, S. R., Narayanan, S. S., 2007. Amperometric determination of paracetamol by a surface modified cobalt hexacyanoferrate graphite wax composite electrode. *Talanta*, **72**(5): 1818-1827.
- Raj, M. A., John, S. A., 2019. Graphene-Modified Electrochemical Sensors. *In Graphene-Based Electrochemical Sensors for Biomolecules, Elsevier*: 1-41.
- Ramli, N. I., Ismail, N. A. B., Abd-Wahab, F., Salim, W. W. A. W., 2018. Cyclic Voltammetry and Electrical Impedance Spectroscopy of Electrodes Modified with PEDOT: PSS-Reduced Graphene Oxide Composite. *In Transparent Conducting Films. IntechOpen*.
- Raoof, J. B., Ojani, R., Baghayeri, M., Amiri-Aref, M., 2012. Application of a glassy carbon electrode modified with functionalized multi-walled carbon nanotubes as a sensor device for simultaneous determination of acetaminophen and tyramine. *Analytical Methods*, **4**(6): 1579-1587.
- Ray, S., 2015. *Applications of Graphene and Graphene-Oxide Based Nanomaterials*. William Andrew.
- Razmi, H., Habibi, E., 2010. Amperometric detection of acetaminophen by an electrochemical sensor based on cobalt oxide nanoparticles in a flow injection system. *Electrochimica Acta*, **55**(28): 8731-8737.
- Razmi, H., Harasi, M., 2008. Rapid and accurate amperometric determination of acetaminophen in pharmaceutical preparations and spiked human blood serum samples at cadmium pentacyanonitrosylferrate modified glassy carbon electrode. *Journal of the Iranian Chemical Society*, **5**(2): 296-305.
- Reddy, Y. V. M., Bathinapatla, S., Łuczak, T., Osińska, M., Maseed, H., Ragavendra, P., Madhavi, G., 2018. An ultra-sensitive electrochemical sensor for the detection of acetaminophen in the presence of etilefrine using bimetallic Pd–Ag/reduced graphene oxide nanocomposites. *New Journal of Chemistry*, **42**(4): 3137-3146.
- Ruiyi, L., Haiyan, Z., Zaijun, L., Junkang, L., 2018. Electrochemical determination of acetaminophen using a glassy carbon electrode modified with a hybrid material

- consisting of graphene aerogel and octadecylamine-functionalized carbon quantum dots. *Microchimica Acta*, **185**(2): 145.
- Santos, A. M., Wong, A., Almeida, A. A., Fatibello-Filho, O., 2017. Simultaneous determination of paracetamol and ciprofloxacin in biological fluid samples using a glassy carbon electrode modified with graphene oxide and nickel oxide nanoparticles. *Talanta*, **174**: 610-618.
- Sharifian, S., Nezamzadeh-Ejhi, A., 2016. Modification of carbon paste electrode with Fe (III)-clinoptilolite nano-particles for simultaneous voltammetric determination of acetaminophen and ascorbic acid. *Materials Science and Engineering: C*, **58**: 510-520.
- Shetti, N.P., Nayak, D.S., Reddy, K.R. and Aminabhvi, T.M., 2019. Graphene–clay-based hybrid nanostructures for electrochemical sensors and biosensors. *In Graphene-Based Electrochemical Sensors for Biomolecules* (pp. 235-274). Elsevier.
- Si, W., Lei, W., Han, Z., Zhang, Y., Hao, Q., Xia, M., 2014. Electrochemical sensing of acetaminophen based on poly (3, 4-ethylenedioxythiophene)/graphene oxide composites. *Sensors and Actuators B: Chemical*, **193**: 823-829.
- Simões, F. R., Xavier, M. G., 2016. Electrochemical Sensors. *Nanoscience and its Applications*: 155.
- Taleb, M., Ivanov, R., Bereznev, S., Kazemi, S. H., Hussainova, I., 2018. Alumina/graphene/Cu hybrids as highly selective sensor for simultaneous determination of epinephrine, acetaminophen and tryptophan in human urine. *Journal of Electroanalytical Chemistry*, **823**: 184-192.
- Tan, L., Zhou, K. G., Zhang, Y. H., Wang, H. X., Wang, X. D., Guo, Y. F., Zhang, H. L., 2010. Nanomolar detection of dopamine in the presence of ascorbic acid at  $\beta$ -cyclodextrin/graphene nanocomposite platform. *Electrochemistry Communications*, **12**(4): 557-560.
- Tang, H., Chen, J.H., Huang, Z.P., Wang, D.Z., Ren, Z.F., Nie, L.H., Kuang, Y.F. Yao, S.Z., 2004. High dispersion and electrocatalytic properties of platinum on well-aligned carbon nanotube arrays. *Carbon*, **42**(1): 191-197.
- Taylor Jr, R., Pergolizzi Jr, J. V., Raffa, R. B., 2012. Acetaminophen (paracetamol): properties, clinical uses, and adverse effects. *Properties, Clinical Uses And Adverse Effects*: 1.
- Teradale, A. B., Lamani, S. D., Ganesh, P. S., Swamy, B. E. K., Das, S. N., 2018. Electrochemical Sensor for the Determination of Paracetamol at Carbamazepine Film Coated Carbon Paste Electrode. *Zeitschrift für Physikalische Chemie*, **232**(3): 345-358.
- Thu, N. T. A., Duc, H. V., Hai Phong, N., Cuong, N. D., Hoan, N. T. V., Quang Khieu, D., 2018. Electrochemical determination of paracetamol using Fe<sub>3</sub>O<sub>4</sub>/reduced graphene-oxide-based electrode. *Journal of Nanomaterials*: 2018.
- Tyszczyk-Rotko, K., Jaworska, I., Jędruchiewicz, K., 2019. Application of unmodified boron-doped diamond electrode for determination of dopamine and paracetamol. *Microchemical Journal*, **146**: 664-672.
- Umemura, T., Sato, K., Kusaka, Y., Satoh, H., 2015. Palladium, in: G.F. Nordberg, B.A. Fowler, M. Nordberg (Eds.), *Handbook on the Toxicology of Metals*, Academic Press, New York, pp. 1113–1123.

- Wagner, C., Riggs, W. M., Davis, L. E., Moulder, J. F., Muilenberg, G. E., 1979. *Handbook of X-ray Photoelectron Spectroscopy, vol. 55. Physical Electronic Division, Perkin-Elmer, Eden Prairie, MN.*
- Wahlström, J., 2016. *Chemically Reduced Graphene Oxide in Electrochemical Sensing for Bio Applications*. Thesis of Master Degree. aalto university: 1-110
- Wang, H., Zhang, S., Li, S., Qu, J., 2018. Electrochemical sensor based on palladium-reduced graphene oxide modified with gold nanoparticles for simultaneous determination of acetaminophen and 4-aminophenol. *Talanta*, **178**: 188-194.
- Wang, J., 1999. Amperometric biosensors for clinical and therapeutic drug monitoring: a review. *Journal of Pharmaceutical and Biomedical Analysis*, **19(1-2)**, pp.47-53.
- Wangfuengkanagul, N., Chailapakul, O., 2002. Electrochemical analysis of acetaminophen using a boron-doped diamond thin film electrode applied to flow injection system. *Journal of Pharmaceutical and Biomedical Analysis*, **28(5)**: 841-847.
- White, S., Wong, S. H., 1998. Standards of laboratory practice: analgesic drug monitoring. *Clinical Chemistry*, **44(5)**: 1110-1123.
- Wu, W., Yang, Y., Zhou, H., Ye, T., Huang, Z., Liu, R. Kuang, Y., 2013. Highly efficient removal of Cu (II) from aqueous solution by using graphene oxide. *Water, Air, & Soil Pollution*, **224(1)**, p.1372.
- Yang, C. C., Wan, C. C., Lee, C. L., 2005. Palladium nanoparticles. *ChemInform*, **36(12)**: (397-413).
- Yang, H., Liu, B., Ding, Y., Li, L., Ouyang, X., 2015. Fabrication of cuprous oxide nanoparticles-graphene nanocomposite for determination of acetaminophen. *Journal of Electroanalytical Chemistry*, **757**: 88-93.
- Yu, L., Li, P., Ding, X., Zhang, Q., 2017. Graphene oxide and carboxylated graphene oxide: Viable two-dimensional nanolabels for lateral flow immunoassays. *Talanta*, **165**: 167-175.
- Yu, S., Li, H., Li, G., Niu, L., Liu, W., Di, X., 2018. Reduced graphene oxide-supported gold dendrite for electrochemical sensing of acetaminophen. *Talanta*, **184**: 244-250.
- Yusoff, N., 2019. Graphene-Polymer Modified Electrochemical Sensors. *In Graphene-Based Electrochemical Sensors for Biomolecules, Elsevier*: 155-186.
- Yusop, R.M., Unciti-Broceta, A., Johansson, E.M., Sánchez-Martín, R.M. Bradley, M. 2011. Palladium-mediated intracellular chemistry. *Nature Chemistry*, **3(3)**: 239.
- Zhang, X., Wang, K.P., Zhang, L.N., Zhang, Y.C. Shen, L., 2018. Phosphorus-doped graphene-based electrochemical sensor for sensitive detection of acetaminophen. *Analytica chimica acta*, **1036**: 26-32.
- Zhang, Y., Liu, X., Li, L., Guo, Z., Xue, Z., Lu, X., 2016. An electrochemical paracetamol sensor based on layer-by-layer covalent attachment of MWCNTs and a G4. 0 PAMAM modified GCE. *Analytical Methods*, **8(10)**: 2218-2225.
- Zhao, H. Zhao, T.S., 2013. Highly active carbon nanotube-supported Pd electrocatalyst for oxidation of formic acid prepared by etching copper template method. *International Journal of Hydrogen Energy*, **38(3)**: 1391-1396.
- Zhao, X., Liu, P., 2014. Biocompatible graphene oxide as a folate receptor-targeting drug delivery system for the controlled release of anti-cancer drugs. *RSC Advances*, **4(46)**: 24232-24239.

- Zheng, M., Gao, F., Wang, Q., Cai, X., Jiang, S., Huang, L., Gao, F., 2013. Electrocatalytical oxidation and sensitive determination of acetaminophen on glassy carbon electrode modified with graphene–chitosan composite. *Materials Science and Engineering: C*, **33**(3): 1514-1520.
- Zheng, Q., Kim, J. K., 2015. *Graphene for Transparent Conductors: Synthesis, Properties and Applications* (Vol. 23). Springer.
- Zhu, W., Huang, H., Gao, X., Ma, H., 2014. Electrochemical behavior and voltammetric determination of acetaminophen based on glassy carbon electrodes modified with poly (4-aminobenzoic acid)/electrochemically reduced graphene oxide composite films. *Materials Science and Engineering: C*, **45**: 21-28.
- Zobir, S.A.M., Rashid, S.A. Tan, T., 2019. Recent Development on the Synthesis Techniques and Properties of Graphene Derivatives. In *Synthesis, Technology and Applications of Carbon Nanomaterials*, Elsevier: pp 77-107.

## **APPENDIX: EXTENDED TURKISH SUMMARY (GENİŞLETİLMİŞ TÜRKÇE ÖZET)**

### **İNSAN SERUMUNDA PARASETAMOLÜN ELEKTROANALİTİK TAYİNİ İÇİN KARBOKSİLLENMİŞ GRAFEN OKSİT DESTEKLİ Pd NANOPARÇACIKLARIN SENTEZLENMESİ**

SALEEM, Shaimaa Jameel Saleem  
Yüksek Lisans Tezi, Kimya Bölümü  
Tez Danışmanı: Dr. Öğr. Üyesi Muhammet GÜLER  
Kasım 2019, 89 Sayfa

#### **1. GİRİŞ**

Parasetamol (N-asetil-p-aminophenol ya da asetaminofen), analjezik ve antipretik bir ilaç olup genellikle ateş düşürücü ve ameliyat sonrası ağrı, baş ağrısı, sırt ağrısı ve artrit gibi ağrıları dindirmek için kullanılmaktadır. Parasetamol, tedavi alanında önemli bir role sahiptir. Bu alanda parasetamol uygun dozajlarda kullanıldığı zaman, merkezi sinir sisteminde prostaglandin sentezini azaltır ve hipotalamik sıcaklık-düzenleyici merkezi sakinleştirir. Ancak, uzun süreli kullanımı vücutta parasetamolün toksik metabolitlerin birikmesine neden olabilir. Bunun sonucunda karaciğer hasarı, pankreas iltihabı, deri tahrişi ve hatta ölümcül hepatoksisite gibi bazı sağlık problemleri ortaya çıkmaktadır (Asghari et al., 2015; Fernandez et al., 2015). Bundan dolayı parasetamol, biyolojik sıvılarda hızlı ve etkili bir şekilde tayin edilmelidir.

Elektrokimyasal sensörler, vücutta bulunan elektrokimyasal olarak aktif olan molekülleri tayin etmek için kullanılan ucuz, basit ve etkili sensörlerdir. Sensörler

genellikle duyarlı olup hız bir şekilde cevap verme zamanlarına sahiptirler. Bu çalışmamızda parasetamolün elektrokimyasal olarak tayin edilmesi için destek maddesi olarak karboksillenmiş grafen oksit kompoziti kullanılarak Pd nanoparçacıkları destek üzerinde biriktirilerek GO-COOPd nanokompoziti elde edildi. Yaptığımız detaylı araştırmalar sonucunda parasetamolün elektroanalitik olarak tayin edilmesi için bu nanokompozit daha önce kullanılmamıştır. Çalışmada çalışma elektrodun kararlılığını ve seçiciliğini arttırmak için Nf kullanıldı. Hazırlanan kompozitler, yüksek çözünürlüklü transmisyon elektron mikroskobu (HRTEM), X-ışını difraksiyonu (XRD), X-ışını fotoelektrik spektroskopisi (XPS) ve Fourier transform infrared spektroskopisi (FTIR) kullanılarak karakterize edildi. Deney sonuçları, Nf/GO-COOPd nano kompozitin PA oksidasyonuna büyük elektrokatalitik cevap verdiğini göstermiştir.

## **2. MATERYAL ve YÖNTEM**

### **2.1. Materyal**

Grafit tozu, parasetamol, dopamin, Pd(NO<sub>3</sub>).2H<sub>2</sub>O, nafion (Nf) çözeltisi (%5 oranında alifatik alkoller ve su karışımı içinde), KCl, glukoz, askorbik asit, ürik asit, folik asit, mannoz, histidin Sigma-Aldrich®'den satın alındı. Etanol, ClCH<sub>2</sub>COOH, NaBH<sub>4</sub> ve kullanılan diğer bütün kimyasallar Merck®'den temin edildi. Elektrokimyasal çalışmalar, Autolab PGSTAT128N potansiyostat/galvanostat FRA 32M cihazı kullanılarak yapıldı. Camsı karbon elektrot (GCE), referans elektrot (Ag/AgCl), karşıt elektrot (Pt tel) Basi şirketinden satın alındı. Bidistile su, GFL 2108 double distillation water still marka saf su cihazı kullanılarak elde edildi ve bütün deneylerde bu su kullanıldı.

### **2.2. Yöntem**

Karboksillenmiş grafen oksitin (GO-COOH) sentezlenmesi için önce grafen oksit (GO) sentezlendi. Bunun için GO, Hummers metodu kısmen modifiye edilerek sentezlendi. Bunun için bir buz banyosu içinde 1 g grafit tozu ve 1 g NaNO<sub>3</sub>, 25 mL derişik H<sub>2</sub>SO<sub>4</sub> çözeltisi içeren bir behere eklenerek karışım 2 saat boyunca karıştırıldı. Daha sonra



karışıma 3 g  $\text{KMnO}_4$  eklenerek karışım 48 saat boyunca  $35\pm 3$  °C’da karıştırıldı. Karışıma 125 mL bidistile su eklenerek 98 °C’da 30 dakika boyunca karıştırıldı. Reaksiyonu sonlandırmak için karışıma 2.5 mL %30  $\text{H}_2\text{O}_2$  eklendi. Elde edilen karışım süzülerek çökelti elde edildi. Çökelti, 125 mL %10 HCl çözeltisine eklenerek ultrasonik banyo ile homojen karışım elde edilene kadar karıştırıldı. Bunun ardından karışım süzüldü. Elde edilen çökelti bidistile suda karıştırılarak santrifüj (20 dakika, 8000 rpm) edildi. Çözeltinin pH değeri 7 olana kadar santrifüj işlemine devam edildi. Son olarak, elde edilen GO vakum etüvünde 60 °C’da kurutuldu (Dikin ve ark., 2007; Guler ve ark., 2018)

GO-COOH’ın sentezlenmesi için 2 g GO ve 4 g KOH, 25 mL bidistile su içeren iki boyunlu bir balona eklendi. Karışım 2 saat reflux edildi. Daha sonra 6 ml bidistile suda çözünen 3g  $\text{ClCH}_2\text{COOH}$  çözeltisi karışıma eklenerek elde edilen son karışım 24 saat karıştırıldı. Karışım süzüldü ve sırasıyla bidistile su ( $3\times 20$  ml) ve saf etanol ( $3\times 20$  ml) ile yıkandı. Elde edilen GO-COOH vakum etüvünde 70 °C’da kurutuldu (Zhao ve Liu, 2014).

GO-COOPd nanokompozitini elde etmek için 60 mg GO-COOH, 5 mL bidistile su içeren 25 mL’lik bir balona eklendi. Homojen bir karışım elde etmek için karışım 30 dakika ultrasonik banyoda karıştırıldı. Daha sonra karışıma 26.52 mg (0.1 mmol)  $\text{Pd}(\text{NO}_3)_2\cdot 2\text{H}_2\text{O}$  eklenerek karışım 3 saat boyunca laboratuvar sıcaklığında karıştırıldı. Bunun ardından karışıma 56.46 mg (1.49 mmol)  $\text{NaBH}_4$  eklenerek karışım bir süre karıştırıldı. Son olarak karışım süzüldü ve sırasıyla bidistile su ( $3\times 20$  ml) ve saf etanol ( $3\times 20$  ml) ile yıkanarak vakum etüvünde 80 °C’da kurutuldu (Guler ve ark., 2017).

Camsı karbon elektrot (GCE) modifiye edilmeden önce alümina bulamacı ile temizlendi. Daha sonra ultrasonik banyoda sırasıyla nitrik asit/bidistile su (1:1) ve etanolde temizlenerek laboratuvar sıcaklığında kurutuldu. 2 mg GO-COOPd, 1 mL saf etanole eklenerek homojen karışım elde edilene kadar ultrasonik banyoda karıştırıldı. Elde edilen bu karışımdan 5  $\mu\text{L}$ , GCE üzerine damlatılarak kurutuldu. Son olarak %0.2 nafion çözeltisinden 3  $\mu\text{L}$  GO-COOPd/GCE üzerine damlatılarak laboratuvar sıcaklığında kurumaya bırakıldı. Bu şekilde Nf/GO-COOPd/GCE çalışma elektrodu elde edilmiş oldu. Diğer elektrotlar da bu şekilde hazırlandı.

### 3. BULGULAR

Çalışmamızda GO ve GO-COOH, FTIR kullanılarak yapısı tayin edildi. Şekil 4.1a'da görüldüğü gibi  $3344\text{ cm}^{-1}$  dalga boyunda elde edilen pik, -OH, grubunun karakteristik pikidir.  $1718\text{ cm}^{-1}$  dalga boyunda elde edilen pik, karboksilik asitte bulunan C=O grubunun gerilme titreşim pikidir.  $1053\text{ cm}^{-1}$  dalga boyunda gözlenen pik, C-O grubunun gerilme titreşiminden kaynaklanmaktadır. 1221, 1401, ve  $1620\text{ cm}^{-1}$  dalga boylarında elde edilen pikler sırasıyla epoksi C-O-C, C-OH ve C=C aromatik halkadan kaynaklanmaktadır (Bellamy, 2012). Şekil 4.1b'de görüldüğü gibi  $1230\text{ cm}^{-1}$  dalga boyunda elde edilen pik, O=C-OH grubundaki C-O'nun gerilme pikini göstermektedir.  $1581\text{ cm}^{-1}$  dalga boyundaki keskin pik, karboksillenmiş grafen oksidin C-O titreşim bandına aittir. Elde edilen bu sonuçlar, karboksillenmiş grafen oksitin sentezlendiğini göstermektedir.

GO, GO-COOH ve GO-COOPd kompozitlerin kristal yapısı XRD kullanılarak araştırıldı. Şekil 4.2a'da elde edilen XRD grafiğinde, GO'nun katmanlar arası aralığın,  $11.5^\circ$ 'de  $0.77\text{ nm}$  olduğu belirlenmiştir. Bu değer grafen oksit tabaların üzerindeki oksijen içeren fonksiyonel grupların varlığından dolayı grafitin değerinden ( $0.3\text{ nm}$ ) daha büyüktür. GO, karboksil gruplarıyla fonksiyonel hale getirildikten sonra  $24.89^\circ$  ve  $43.52^\circ$ 'de elde edilen pikler, GO-COOH kompozitin temel piklerini göstermektedir (Şekil 4.2b) (Park, 2014). Şekil 4.2c'de  $39.52^\circ$  ve  $67.05^\circ$  elde edilen pikler, sırasıyla (111) ve (220) yüzey merkezli kübik (FCC) Pd nanoparçacıklarına aittir (JCPDS No. 46–1043).

Nf/GCE, Nf/GO/GCE, Nf/Pd@GO/GCE, Nf/GO-COOH/GCE ve Nf/GO-COOPd/GCE elektrotların elektroaktif yüzey alanlarını belirlemek için elektrokimyasal empedans spektroskopisi (EIS) ve dönüşümlü voltametri (CV) yöntemleri kullanıldı. EIS, modifiye elektrodun aktif yüzey alanı hakkında önemli bilgiler vermektedir. Bir Nyquist grafiğinde yarım dairenin çapı yük transfer direncine (Rct) eşittir. Rct değeri arttıkça elektron transferi yavaşlamaktadır. Nf/GCE, Nf/GO/GCE, Nf/Pd@GO/GCE, Nf/GO-COOH/GCE ve Nf/GO-COOPd/GCE elektrotların Rct değerleri sırasıyla  $20.55\text{ k}\Omega$ ,  $10.47\text{ k}\Omega$ ,  $5.85\text{ k}\Omega$ ,  $1.3\text{ k}\Omega$  ve  $2.94\text{ k}\Omega$  olarak bulundu. Bu sonuçlara göre GO karboksillendikten sonra iletkenliği artmaktadır. CV kullanılarak her bir elektrodun aktif yüzey alanı hesaplanmıştır. Buna göre Nf/GCE, Nf/GO/GCE, Nf/Pd@GO/GCE, Nf/GO-COOH/GCE ve Nf/GO-COOPd/GCE elektrotların aktif yüzey alanları Randles-Sevcik eşitliği (Bard ve ark., 2000) yardımıyla sırasıyla  $0.0067$ ,  $0.009$ ,  $0.03$ ,  $0.229$  ve  $0.152\text{ cm}^2$  olduğu

görülmüştür (Şekil 4.9). Çalışma elektrotların parasetamola gösterdikleri elektrokimyasal davranışlar, CV kullanılarak değerlendirildi. Şekil 4.10 dikkatle incelendiğinde parasetamole en iyi cevabı veren elektrodun Nf/GO-COOPd/GCE olduğu görülmektedir. Bu durum Pd nanoparçacıkların parasetamolün elektron transferini hızlandırdığını göstermektedir. pH'nın sensör üzerindeki etkisini araştırmak için farklı pH değerlerine sahip 0.1 M fosfat tamponları (PBS) hazırlandı. Daha sonra her bir tamponun aynı derişimdeki parasetamole vermiş olduğu voltamogramlar elde edildi (Şekil 4.11). Elde edilen oksidasyon pik akımlarına karşı pH grafiği çizildi. Şekil 4.13'e göre maksimum oksidasyon pik akımı pH değeri 7.5 olan 0.1 M PBS tamponunda elde edilmiştir. Dolayısıyla sonraki elektrokimyasal çalışmalar için pH değeri 7.5 olan 0.1 M PBS tamponu kullanıldı.

Çalışmamızda yük transfer sabiti ( $\alpha$ ) ve elektrokimyasal reaksiyona katılan elektron sayısını ( $n$ ) belirlemek için Laviron eşitliği kullanıldı (Laviron, 1979). Laviron eşitliğinden elde edilen doğrusal grafiklerin eğimleri kullanılarak  $\alpha$  ve  $n$  değerleri sırasıyla 0.61 ve 1.88 olarak hesaplandı. Elde edilen bu değerler hem literatürde elde edilen değerler ile benzerlik gösterip hem de parasetamol için önerilen elektrokimyasal reaksiyon mekanizmasına uygun olduğunu göstermektedir (Razmi and Habibi, 2010; Raof et al., 2012).

Parasetamolün elektroanalitik olarak tayin edilmesi için amperometrik yöntem kullanıldı. Bu yöntem yardımıyla sensörün parasetamole olan duyarlılığı, parasetamolün gözlenebilme sınırı (LOD), tayin sınırı (LOQ), doğrusal tayin aralığı ve cevap zamanı belirlendi. Bu amaçla farklı derişimde parasetamol kullanılarak akım-zaman grafiği elde edildi (Şekil 4.16). Doğrusal regresyon denklemi  $i$  ( $\mu\text{A}$ ) = 0.0358c ( $\mu\text{M}$ ) + 0.4379 ( $R^2 = 0.9984$ ) olan grafik yardımıyla duyarlılık çalışma elektrodun aktif yüzey alanına bağlı olarak  $232.89 \mu\text{A mM}^{-1} \text{cm}^{-2}$  olarak hesaplandı. Sensörün LOD değeri sinyal/gürültü oranı 3 değerine bağlı olarak  $0.012 \mu\text{M}$  olarak hesaplandı. Sensörün LOQ değeri sinyal/gürültü oranı 10 değerine bağlı olarak  $0.04 \mu\text{M}$  olduğu görüldü. Parasetamolün cevap zamanı, oksidasyon pik akımının kararlı hale geçişinin %95'e ulaşması durumu dikkate alınarak belirlendi. Buna göre amperometrik grafikte, düşük konsantrasyonlarda cevap zamanı 0.65 s, yüksek konsantrasyonlarda ise 2 s olduğu belirlendi. Elde edilen bu değerler daha önceki çalışmalarla karşılaştırıldı. Tablo 4.1'e bakıldığında elde edilen sensör, parasetamole son

derece duyarlı, LOD değeri düşük ve doğrusal tayin aralığı son derece geniş olduğu görülmektedir.

Seçicilik sensor ve biyosensör uygulamalarında son derece hayati bir rol oynamaktadır. Bu amaçla askorbik asit, dopamin, ürik asit, glukoz, früktoz, mannoz, histidin ve folik asidin sensör üzerindeki girişim etkisi araştırıldı. Şekil 4.18’de görüldüğü gibi bu maddelerin kayda değer bir girişim yapmadıkları görülmüştür. Bununla birlikte sensörün tekrarlanabilirlik, tekrarolusturulabilirlik ve depolama karlılığı sonuçları tatmin edici olduğu sonucuna varıldı.

#### 4. TARTIŞMA ve SONUÇ

Yüksek lisans tezi olarak yapılan bu çalışmada karboksillenmiş grafen oksit (GO-COOH) desteğine Pd nanoparçacıkları tutturularak yeni bir parasetamol sensörü geliştirildi. Çalışma elektrodu olarak kullanılan GCE, GO-COOPd nanokompoziti ile modifiye edildi. Sensörün kararlılığını ve seçiciliğini arttırmak için nafion kullanıldı. Karboksil grupları bağlanan grafen oksitin çözünürlüğü, iletkenliği ve aktif yüzey alanında artış olduğu gözlemlendi. Bu sonuçlar, GO-COOH desteğin metal nanoparçacıkların destek üzerine bağlanması için uygun bir malzeme olduğunu göstermektedir. Bunlara ek olarak karboksil grupları, GCE ve Nf/GO/GCE ile karşılaştırıldığında sensörün elektrokatalitik aktivitesini arttırdığı görüldü. Elde edilen kompozit ve nanokompozitlerin yapısı FTIR, XPS, XRD ve TEM kullanılarak aydınlatıldı. Elektrokimyasal çalışmalar için dönüşümlü voltametri, amperometri ve elektrokimyasal empedans spektroskopisi kullanıldı. Elde edilen sonuçlara göre sensör, parasetamol için geniş bir doğrusal tayin aralığı, düşük bir LOD değeri, düşük cevap zamanı ve tatmin edici bir duyarlılık gösterdi. Bu destek üzerine farklı metal nanoparçacıkları tutturularak farklı elektroaktif maddelerin tayini için yeni sensör ve biyosensörler geliştirilebilecek çalışmalara iyi bir kaynak olacağını düşünüyoruz.

Son olarak yaptığımız bu çalışma “Electroanalytical determination of paracetamol using Pd nanoparticles deposited on carboxylated graphene oxide modified glassy carbon electrode (*Electroanalysis* 2019, 31(11) 2187, 2198)” başlık altında *Electroanalysis* dergisinde yayınlanmıştır.



## **CURRICULUM VITAE**

Shaimaa Jameel Saleem SALEEM was born in 1984, Duhok / Iraq. She finished secondary and high school education from Duhok in 2004. In the same year, she was accepted in Chemistry Department of College Education at Duhok University. In 2007, she graduated from Chemistry Department. At September, 2017 she started his graduate study in the department of Chemistry (Biochemistry), Institute of Science of Van Yüzüncü Yıl University.



UNIVERSITY OF VAN YUZUNCU YIL  
THE ISTITUTE OF NATURAL AND APPLIED SCIENCES  
THESIS ORIGINALITY REPORT

Date: 25/11/2019

Thesis Title: **Synthesis of Pd Nanoparticles Supported on Carboxylated Graphene Oxide for Electroanalytical Determination of Paracetamol in Human Serum**

The title of the mentioned thesis, above having total 89 pages with cover page, introduction, main parts and conclusion, has been checked for originality by Turnitin computer program on the date of 25.11.2019 and its detected similar rate was 15 % according to the following specified filtering

Originality report rules:

- Excluding the Cover page,
- Excluding the Thanks,
- Excluding the Contents,
- Excluding the Symbols and Abbreviations,
- Excluding the Materials and Methods
- Excluding the Bibliography,
- Excluding the Citations,
- Excluding the publications obtained from the thesis,
- Excluding the text parts less than 7 words (Limit match size to 7 words)

I read the Thesis Originality Report Guidelines of Yuzuncu Yil University for Obtaining and Using Similarity Rate for the thesis, and I declare the accuracy of the information I have given above and my thesis does not contain any plagiarism; otherwise I accept legal responsibility for any dispute arising in situations which are likely to be detected.

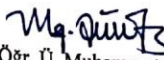
Sincerely yours,

25.11.2019  
Shaimaa Jameel Saleem SALEEM



Name and Surname: Shaimaa Jameel Saleem SALEEM  
Student ID#:  
Science: Chemistry  
Program: Biochemistry  
Statute: M. Sc.  Ph.D.

APPROVAL OF SUPERVISOR  
SUITABLE

  
Dr. Öğr. Ü. Muhammet GÜLER

(Title, Name-Surname, Signature)

APPROVAL OF THE INSTITUTE  
SUITABLE



(Title, Name-Surname, Signature)